FACILITY FORM 602
N70-32897
(ACCESSION NUMBER)
82
(PAGES)
CR-102787
(NASA CR OR TMX OR AD NUMBER)
(THRU)
1
(CODE)
33
(CATEGORY)
Reproduced by the
CLEARINGHOUSE
for Federal Scientific & Technical
Information Springfield Va. 22151

PHASE CHANGE SOLIDIFICATION PHENOMENA FOR THERMAL CONTROL

by

A. O. Ukanwa

F. J. Stermole

J. O. Golden

Annual Summary Report No. 1

21 November 1968 - 31 December 1969

Contract NAS 8-30511

for

National Aeronautics and Space Administration

George C. Marshall Space Flight Center

Marshall Space Flight Center, Alabama 35812

PREFACE

This report was prepared by Colorado School of Mines, Golden, Colorado, under Contract NAS 8-30511, "Research in Phase Change Thermal Control Technology" and under Colorado School of Mines Foundation Contracts F-6911 and F6915. The work was administered under the direction of the Space Sciences Laboratory, George C. Marshall Space Flight Center, with Mr. T. C. Bannister acting as the contracting officers' technical representative.

This report covers work from 21 November 1968 to 31 December 1969.

The work at Colorado School of Mines was carried out by Mr. A. O. Ukanwa under the direction of Dr. F. J. Stermole and Dr. J. O. Golden, Principal Investigators.

ABSTRACT

The goal of this investigation was to contribute to the understanding of solidification as it affects the performance and the suitability of phase-change materials in thermal control devices. A unidimensional mathematical model was established for the solidification of a liquid paraffin of finite geometry. The method was based on the numerical solution by computer of the two-phase heat-conduction equations with moving interface and variable boundary conditions. Constant properties were assumed for each phase although the properties varied from one phase to the other. The model assumed that internal convective effects could be neglected. Super-cooling and nucleation were also assumed to be insignificant.

An experimental system was set up to verify the theoretical analysis and results. The system consisted of a rectangular cell which was filled with a paraffin, n-hexadecane ($n\text{-}C_{16}H_{34}$). The cell itself was cooled from below by a coolant which was circulated by a refrigerator. The solidification process was studied by reading temperatures at different points in the cell by means of copper-constantan thermocouples.

A comparison has been made between results obtained from theoretical-analysis computer solutions and those obtained experimentally. Good agreement was obtained between the

experimental results and those from theory, although the numerical results of the mathematical model indicate a faster rate of solidification than that observed experimentally. Data for comparison between experimental and theoretical results are presented under each experimental run in the form of tables and graphs.

CONTENTS

	Page
LIST OF TABLES	vi
LIST OF FIGURES	vii
INTRODUCTION	1
LITERATURE SURVEY	4
THEORETICAL ANALYSIS	13
Formulation of the Problem	13
Finite Difference Formulation of Governing Equations	29
Stability Criteria for Governing Finite Difference Equations	66
EXPERIMENTAL EQUIPMENT AND PROCEDURE	70
Equipment	70
Experimental Procedure	89
COMPARISON OF EXPERIMENTAL AND THEORETICAL RESULTS	95
CONCLUSIONS	145
NOMENCLATURE	149
LITERATURE CITED	154
APPENDICES	
FORTRAN IV Computer Program for obtaining exponential fits to experimentally-measured temperatures of the bottom and the top plates	158
FORTRAN IV Computer Program for solving the pre-solidification problem	162
FORTRAN IV Computer Program for solving the solidification problem	165

LIST OF TABLES

Table		Page
1.	Temperature profiles obtained using 1-sec and 2-sec time steps	102
	Polynomial fits to bottom- and top-plate temperatures:	
2.	Run 1	103
3.	Run 2	110
4.	Run 3	117
5.	Run 4	124
6.	Run 5	131
7.	Run 6	138

LIST OF FIGURES

Figure		Page
1.	Axial section of test cell	14
2.	Moving interface from time t to time t + dt. . .	22
3.	Axial section of test cell showing space grids and nodes.	27
4.	Two-dimensional finite elements in time and space coordinates.	31
5.	Case A: Interface does not cross a space grid line.	40
6.	Case B: Interface crosses one space grid line. .	40
7.	Case C: Interface crosses two space grid lines .	44
8.	Case D: Interface crosses three or more space grid lines	44
9.	Test cell.	71
10.	Exploded view of test cell	73
11.	Cooling chamber.	75
12.	Plexi-glass chamber for test material.	78
13.	Diagram of top copper plate.	81
14.	Thermocouple arrangement	84
15.	Block diagram of assembly of main experimental equipment	87
16.	Temperature profiles for the pre-solidification problem: Run 1	104
17.	Temperature profiles for an entire run: Run 1.	106
18.	Height of solid n-hexadecane as a function of time: Run 1	108

Figure | Page

19. Temperature profiles for the pre-solidification problem: Run 2 111

20. Temperature profiles for an entire run: Run 2. 113

21. Height of solid n-hexadecane as a function of time: Run 2 115

22. Temperature profiles for the pre-solidification problem: Run 3 117

23. Temperature profiles for an entire run: Run 3. 120

24. Height of solid n-hexadecane as a function of time: Run 3 122

25. Temperature profiles for the pre-solidification problem: Run 4 125

26. Temperature profiles for an entire run: Run 4. 127

27. Height of solid n-hexadecane as a function of time: Run 4 129

28. Temperature profiles for the pre-solidification problem: Run 5 132

29. Temperature profiles for an entire run: Run 5. 134

30. Height of solid n-hexadecane as a function of time: Run 5 136

31. Temperature profiles for the pre-solidification problem: Run 6 139

32. Temperature profiles for an entire run: Run 6 141

33. Height of solid n-hexadecane as a function of time: Run 6 143

INTRODUCTION

Phase-change phenomena have received wide scientific attention for some time and are of significant importance in many technical problems such as solidification of a billet, formation of snow, solidification of an asphalt layer, formation of smog, melting of metals and alloys, and growth of crystals. However, it has been only in very recent years that phase-change materials have been seriously considered for spacecraft thermal control. In concept, such materials would be used in passive systems that employ the process of melting or solidification to remove or add thermal energy from or to a system. With the advent of spacecraft applications and space travel, the technology of phase-change phenomena is getting renewed scientific attention.

Presently, space vehicles lose heat to the environmental vacuum of space mainly by radiation. This may be an inefficient method of thermal control during high-energy dissipation periods, even if "heat-pipes" or other improved heat transfer systems are employed. Similarly, temperature-control systems based on liquid-vapor phase change may be inefficient, besides involving sophisticated irreversible fluid loop circuits. Systems based on solid-liquid phase change have many advantages which make them very useful for certain applications. They are light, easy to handle, and

easily used as wall-lining elements around electronic equipment. Moreover, they are essentially passive. One disadvantage that solid-liquid phase change materials have when compared to the liquid-vapor phase change materials is that the former have lower heat-elimination capacities. Fusible materials can be used to store the energy evolved during high-density dissipation periods. The stored energy can then be released continuously into space or to the system during low-temperature conditions. This cycle is pertinent in the case of space vehicles moving in extremes of temperature from the earth into space and from space to earth during re-entry.

The present solidification research program was mainly devoted to study of one-dimensional systems with time-dependent boundary conditions. It must be emphasized that the principal goal was not the study of the performance of fusible materials as actual phase-change temperature controllers, but the development of a reasonably accurate, simplified model for the solidification of a fusible material of finite rectangular dimensions under variable boundary conditions as would be the likely situation in an actual thermal controller.

Although from the theoretical standpoint almost any material would perform equally satisfactorily, it was preferred to select the fusible material from those generally accepted in current thermal-control research. Normal paraffins with even numbers of carbon atoms are those

materials most widely used because they satisfy most of the requirements of acceptable phase-change materials. They have melting or solidification points close to the acceptable range for the design media of electronic equipment, 40°F to 150°F, with phase-transition enthalpy changes higher than or, at least, equal to 100 Btu per pound. They are also non-corrosive, non-toxic, chemically inert and stable, as well as having low vapor pressures, small volume changes, and negligible sub-cooling. In the present research program, n-hexadecane ($n\text{-}C_{16}H_{34}$) was the material studied.

LITERATURE SURVEY

Much theoretical work has been done in the literature on problems which are directly or indirectly related to physical change of state. The basic feature of such problems of change of state is the existence of a moving boundary or surface between phases. Therefore, the problem that is most often considered is how to determine the way in which this surface or boundary moves. Heat may be liberated or absorbed on the surface; there may be volume change accompanying the change of state, and the thermal properties of the phases on either side of the interface may be different for the phases and may vary as the change of state proceeds. Therefore, the problem is essentially non-linear in nature and general analytical solutions for it may be wanting. Some exact solutions for models that mathematically approximate the real problems have been obtained, mostly for infinite or semi-infinite geometry.

Carslaw and Jaeger[1], who were among the first to give in-depth treatment of melting and solidification problems, comment on the need for numerical methods for solving these problems which are often rendered more complex by cylindrical, spherical, and other finite geometric configurations. Carslaw and Jaeger make no attempt to give any exact solutions for the phase change problem when finite geometries are involved. However, they do give a series solution for the

ordinary transient heat-transfer problem with no phase change. This is particularly useful in determining the temperature profile of a substance, which is subjected to heat change, for the interval beginning with the initiation of the heat change and ending with the initiation of change of state. Another good quality of the series solution that they give is that it takes into account time-dependent initial and boundary conditions.

Many of the solutions presented in the literature concerning phase change problems are valid only if the material under study is initially at its equilibrium temperature for change of state. These solutions ignore the more-frequently-encountered case in which the material under study may be initially at a temperature, say room temperature, that is quite different from its equilibrium phase-change temperature and may have to be brought to this equilibrium temperature from its initial temperature by some heat input, withdrawal, or generation.

Stefan[2] was the first to give a published discussion of a one-dimensional transient conduction problem with phase change, for a single component or eutectic composition with constant properties. Thus, the term "Stefan's Problem" came to be used to describe a one-dimensional conduction problem in which a semi-infinite slab initially at a constant temperature, T_o, has one face maintained at zero temperature for time greater than zero. For the solution to the problem

to satisfy the conditions for all times, the interface position as a function of time has to be proportional to the square root of the product of time and the thermal diffusivity of the material of the slab.

Saito[3] considered the problem of a semi-infinite solid in contact with a semi-infinite liquid. The resultant solidified liquid was regarded as having different properties from the initial solid. Saito tried to incorporate the latent heat as superheat. His results disagreed with later works. Pekeris and Slichter[4] obtained a series solution for the solidification of ice on an infinitely long cylinder.

Danckwerts[5] presented a system of equations in terms of arbitrary initial and boundary conditions for the temperature distribution in a semi-infinite solid. The equations were solved by trial and error. Booth[6], like Danckwerts, was more concerned with mass transfer problems, and the tarnishing reaction in particular. He approximated the position of the moving boundary by an infinite power series.

Kreith and Romie[7] presented solutions which applied to either solidification or melting and which gave the position of the phase front and the temperature profile for a sphere, cylinder or semi-infinite solid initially at the fusion temperature. They assumed constant temperature gradient and velocity at the interface. The temperature was determined in a dimensionless series form by a method of iterative approximations. The assumption of constant velocity was

valid only at the early stages of solidification.

Chambre[8] gave a complete solution for a Prandtl number equal to one for the growth of a solid starting from negligible initial dimensions with a plane, cylindrical or spherical boundary. Convection in the fluid was attributed to the unequal but assumed constant densities in the two phases and was studied with the incompressible Navier-Stokes equation. An ordinary differential equation which is a function of the quadrature of time was obtained for the solidification velocity and it was only partially solved.

Chao and Weiner[9] investigated the temperature in a solid and liquid while the liquid was being poured. The latent heat was treated as a "pseudo" specific heat and the solution, obtained by a Laplace transform technique was an integral that was solved numerically.

Many authors have applied the variational technique to heat conduction. The Onsager theorem[10], which was a reciprocity law of coupled phenomena, permitted certain irreversible processes to be expressed in terms of a variational principle. Chambers[11] was the first to show the applicability of the variational technique to heat conduction. Biot and Daughaday[12] used the variational technique to study heat conduction in a melting semi-infinite solid with constant properties. The heat input was assumed to be constant and the problem treated was an ablation problem in which the melt was removed as it was formed. It is characteristic of "re-entry" problems caused by aerodynamic heating

in hypersonic missile flight such as occurs during the re-entry of a space vehicle into the earth's atmosphere.

The heat-balance integral technique, an analytical method that gives approximate solutions to a wide variety of heat transfer problems, is used in many papers in the literature. It is mostly used for non-linear problems that must be solved either numerically or approximately. Its big advantage is that it changes the energy equation from a partial differential equation to an ordinary differential equation. This method as formulated by Goodman[13] is dependent upon the definition of a thermal layer, which is analogous to the hydrodynamic boundary layer in fluid flow. It assumes that, beyond the thermal layer, there is temperature equilibrium and no heat transfer. One disadvantage of this method is that the heat conduction equation is satisfied only on the average and this average equation is analogous to the von Karman and Pohlhausen[14] momentum integral equations for boundary-layer theory. Usually, a general polynomial form of the temperature profile is assumed and substituted into the governing equation of the heat transfer problem, which is integrated over the thermal layer. The result is a heat-balance integral. Goodman and Shea[15] used this technique in examining the melting of a finite slab initially below the melting temperature, one face of which is subjected to a constant heat input while the other face is insulated or at a constant temperature.

Poots[16] used the integral method to study a moving-boundary, two-dimensional problem in which he treated the inward solidification of a uniform prism, which had a square cross-section and was filled with a liquid initially at the fusion temperature. The integrals were solved by numerical methods.

In the literature, there are many other analytical approaches and techniques, many of which apply to special phase-change problems such as the study of phase change in alloys. In alloys, the complexity of finding the temperature distribution and the phase front velocity is increased by the fact that the latent heat effect no longer occurs at a single temperature, but over a range of temperatures.

Weiner[17], Rubinshtein[18], and Adams[19] are some of the men who have studied phase changes in alloys. For an alloy, the latent heat of fusion was mostly treated as an increase in the apparent specific heat of the metal between the liquidus and solidus temperatures. The curve of apparent specific heat versus temperature was approximated by two intersecting straight lines. The temperature corresponding to the point of intersection was used to divide the phase change region into two zones for analysis.

In order to obtain solutions for more general cases for phase change problems, numerical analysis may be the only feasible technique available. Dusinberre[20] has outlined an iteration method which involves laying out the region of

conduction in a grid system and considering the center of each grid element as a node point. By making the grid element small, only the temperatures of points adjacent to a node point and the temperature of the mode point itself need to be considered in calculating the change in temperature of the node point during a small time interval.

Miller[21] used the "surplus temperature" technique in an attempt to improve the predictions of the phase front. To account for the heat absorbed at the phase front using this method, the calculated temperature was permitted to exceed the actual melting temperature until an arbitrarily selected maximum value above the melting temperature was reached. When this maximum value was reached, the grid element containing this particular node point was considered to have melted, and the phase front was shifted to the next node.

Ehrlich[22] gave the implicit finite difference equations for the one-dimensional melting problem with a variable heat flux or heat input specified as a function of time. The implicit equations were then put into tridiagonal matrix forms for solution by Gauss elimination and by back substitution. Special modified equations were given for nodes near the freezing front. In the present study, the method used by Ehrlich to formulate finite difference equations to be solved implicitly was used to find the governing finite difference equations for the solidification of n-hexadecane.

Pujado[23] did theoretical and experimental studies on the melting of n-octadecane under adiabatic conditions. For the theoretical model, he used a unidimensional model and ignored convective effects in the liquid phase. He developed finite difference equations which were then solved by iterative methods.

The Northrop Corporation reports[24,25] presented a survey of the phase change problems involving selection of the proper compounds, evaluation of properties, experimental study of different test cells, and theoretical study by means of a hybrid system composed of a finite-difference electric analog and a digital computer. The study was concerned principally with thermal control in spacecraft by means of the phase change of fusible materials. Some of the physical property data given in the Northrop reports was used in the present study.

Considerations concerning the melting-solidification problem were summarized by Bannister[26] in a NASA Technical Memorandum. This memorandum gives emphasis on the study of nucleation theory as a basis for the study of sub-cooling phenomena in solidification problems. Bannister and Bentilla[27] presented an introductory paper which combined the basic results found in the Northrop reports and the NASA technical memorandum.

Sharma, Rotenberg, and Penner[28] also have studied analytically phase-change problems with variable surface

temperatures. They assumed different temperature profiles and assumed that physical properties were constant.

One of the most recent publications on phase-change phenomena is the interim report on space thermal control study which was presented by Grodzka[29] of Lockheed Missiles and Space Company and carried out under NASA sponsorship in a program directed by T. C. Bannister. It includes effects of gravity, magnetic and electric fields, and convective currents on solid-liquid phase change. The study points out that the pure conduction problem with phase change is valid as long as the liquid phase remains stable and that natural convection has to be considered after the Rayleigh number reaches a critical value of about 1720 for a layer of fluid either heated from below or cooled from above.

Many other papers besides those already mentioned are available on the subject of phase change. Some of them are of special analytical interest for they attempt to solve some specially defined problems of phase change. A full review of these papers can be found in many places in the literature and especially in a literature survey presented by Muehlbauer and Sunderland[30] on "Heat Conduction with Freezing or Melting."

THEORETICAL ANALYSIS

Formulation of the Problem

The problem to be studied is the solidification of n-hexadecane in a cell of height h and constant cross-sectional area in the plane perpendicular to the axis y of the cell (Fig. 1). The temperature profile and the rate of solidification of hexadecane are to be determined using a one-dimensional model along the y axis. Non-steady-state conditions with respect to time are assumed. Note that, for a one-dimensional model along the y axis, the shape of the cross-sectional area perpendicular to the y axis of the test cell is immaterial, provided this cross-sectional area remains constant throughout the height h of the cell. However, if the cross-sectional area varies with y, the shape of local cross-sections must be included in the theoretical analysis of the problem and two- or three-dimensional models would be much better in such cases. Even in a problem such as the one that is being considered here, in which the cross-sectional area of the cell remains constant for all h, a solution based on a one-dimensional model does not approximate the true solution as closely as a solution based on two- or three-dimensional model definitely would. However, the difficulty of solving this problem has dictated that the first attempts at solving it be made using the simpler

Figure 1. Axial section of test cell.

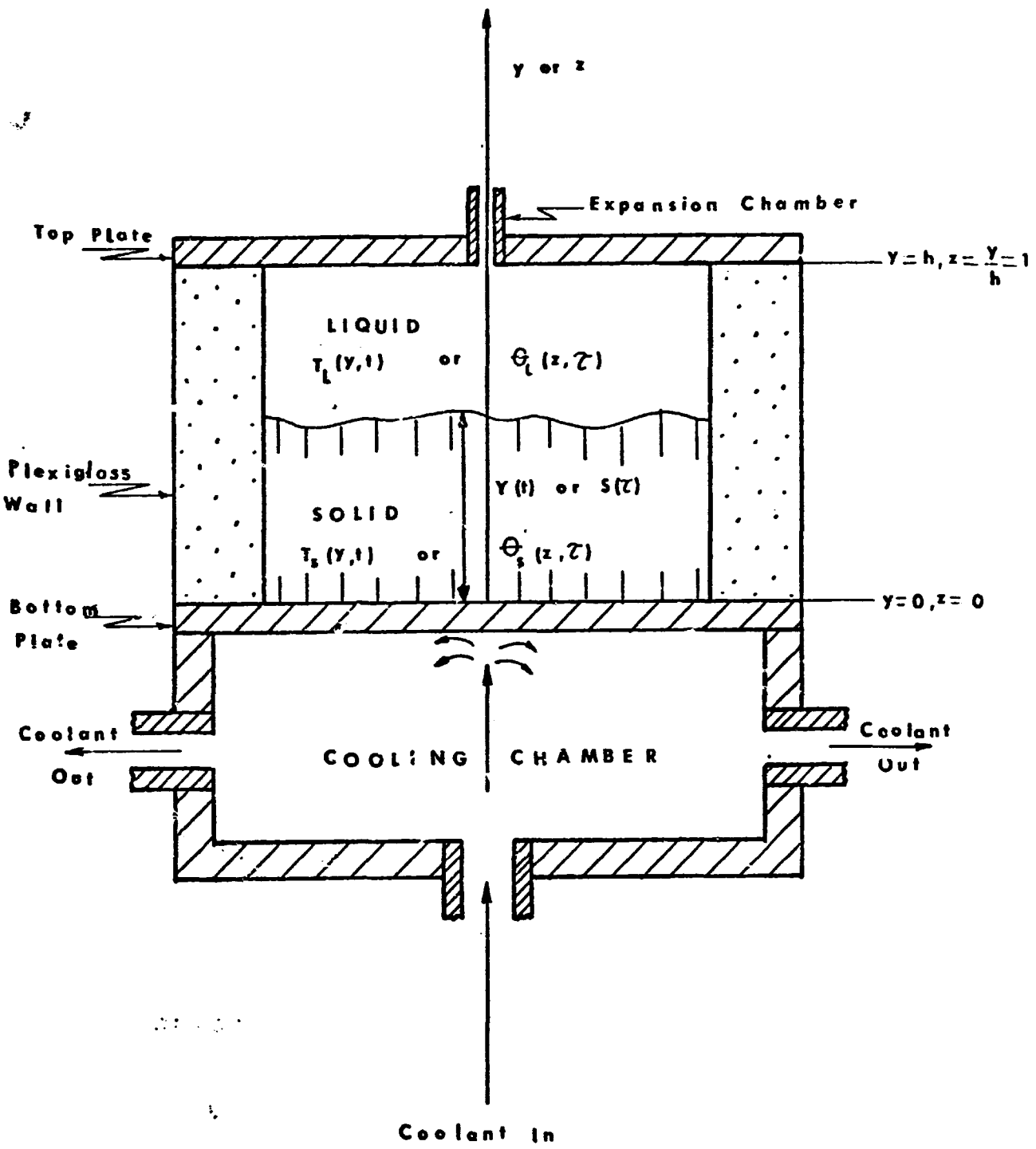

DIAGRAM OF AXIAL SECTION OF TEST CELL SHOWING ITS CONTENTS AT $t > t^*$ or $\tau_o > \tau_o^*$ or $\tau = \tau_o - \tau_o^* > 0$

one-dimensional model. Later studies may then be made using the more accurate two- or three-dimensional model and starting off from the valuable information which this one-dimensional study will furnish.

The cell which is completely filled with liquid n-hexadecane, is sealed at both ends by copper plates and has its bottom plate cooled by a coolant circulated by a refrigerator. A detailed description of the setup is given under "Experimental Equipment and Procedure." The effects of convection are assumed to be negligible. This is a reasonable assumption, since convective mixing that occurs when solidification is taking place is minimized by having the cell cooled from the bottom so that the solid formed at the bottom of the cell remains at the bottom. Another source of convection in the cell is the movement of the interface between the solid and liquid phases. When this interface advances a distance dY in the y direction, the mass of solid formed per unit cross-sectional area of cell, $\rho_s dY$, is derived from an equal mass of liquid which has disappeared. This corresponds to a thickness $(\rho_s/\rho_L)dY$ of liquid which has disappeared. Thus the liquid moves with a net velocity $u_y = (1 - \rho_s/\rho_L)\frac{dY}{dt}$ along the y axis. If there is no change in volume during solidification, $u_y = 0$, and convective effects may be neglected. Also, if the density ρ_s of solid is close to the density ρ_L of liquid, then u_y is approximately

equal to zero and convective effects may be neglected. This later case holds for n-hexadecane, and neglecting convective effects for this one-dimensional model should not introduce high errors into the solution.

It is further assumed that the cell and its contents are initially at ambient temperature and that as time increases, the temperatures of the inside faces of the bottom and top plates of the cell are functions, $f_1(t)$ and $f_2(t)$, of time respectively. The height h of the cell is defined as the distance along the y axis from the inside face of the bottom plate to the inside face of the top plate. The origin of the y axis is $y = 0$ at the inside face of the bottom plate and the positive y direction is towards the top plate. Note that, by these definitions, knowledge of the temperature profiles of the inside faces of the bottom and top plates of the cell, say by polynomial fits of experimentally-determined temperatures of these faces, makes it unnecessary to write energy balances on the copper plates themselves in order to solve the problem for n-hexadecane. The top plate is exposed to room temperature at all times.

The heat transfer problems for n-hexadecane are divided into two parts, arbitrarily, as follows:

1) "Pre-solidification" problem; it considers heat transfer in liquid n-hexadecane from the time ($t = 0$) when cooling of the bottom plate is initiated to the time ($t = t^*$) when the equilibrium temperature of solidification of n-hexadecane is reached at the bottom plate.

2) "Post-solidification" problem; it considers heat transfer in solid and liquid n-hexadecane and the rate of formation of solid n-hexadecane from the time ($t = t^*$) when the equilibrium temperature of solidification of n-hexadecane is reached at the bottom plate to a later time when the entire content of the cell is frozen.

Pre-solidification problem

Since convective effects are neglected and a one-dimensional model is considered, the governing equation, initial and boundary conditions are for $0 \leq t \leq t^*$,

$$\alpha_L \frac{\partial^2 T_{Lo}(y,t)}{\partial y^2} = \frac{\partial T_{Lo}(y,t)}{\partial t}, \quad (0 < y < h) \qquad (1)$$

(i) $T_{Lo}(0,t) = f_1(t)$ when $y = 0$

(ii) $T_{Lo}(h,t) = f_2(t)$ when $y = h$

(iii) $T_{Lo}(y,0) = T_a$ at $t = 0$, for $0 \leq y \leq h$.

T_a is ambient or room temperature which is assumed to be constant. α_L is thermal diffusivity of liquid n-hexadecane and is given by $\alpha_L = K_L/\rho_L c_{pL}$. Subscript L refers to liquid n-hexadecane, and subscript o refers to the pre-solidification problem. Thus T_{Lo} is the temperature of liquid n-hexadecane for the pre-solidification problem. K_L, ρ_L, and c_{pL} are the thermal conductivity, density, and specific heat, respectively, of liquid n-hexadecane.

Conditions (i) and (ii) state that the temperatures of the bottom and top plates are some functions of time. The initial condition (iii) states that, at the time that cooling of the bottom plate is just about to be initiated, i.e. at $t = 0$, the temperature of the liquid hexadecane in the cell is the same as the ambient (room) temperature for the entire height of the cell. Thus, the temperature profile $T_{Lo}(y,t)$ may be obtained for $0 \leq t \leq t^*$ and $0 \leq y \leq h$ by analytical or numerical integration, once T_a, $f_1(t)$ and $f_2(t)$ are known. Note that, at $t = 0$, $f_1(t) = f_2(t) = T_a$; at $t = t^*$, $f_1(t) = T_e$, where T_e is the equilibrium temperature of solidification of n-hexadecane. $f_1(t)$ and $f_2(t)$ may be obtained by doing least-squares-polynomial fits of temperatures of the inside faces of the bottom and top plates as measured with respect to time by copper-constantan thermocouples, with time set equal to zero at the start of cooling of the bottom plate. As will be shown when the results of the present study are discussed, $f_1(t)$ and $f_2(t)$ turn out, for this particular study, to be exponential functions of the type $A + Be^{-(c(t)t)}$, where A and B are constants that add up to the ambient temperature; A equals the steady state temperature of the coolant which is circulated by a refrigerator to cool the bottom plate. The function $c(t)$ is a polynomial of degree less than or equal to 5 which is determined by the fitting computer program.

<u>Post-solidification problem</u>

At time $t = t^*$, the temperature of the bottom plate is

equal to the equilibrium temperature of solidification of n-hexadecane, i.e., $f_1(t^*) = T_e$ and the n-hexadecane is still all liquid. Its temperature profile at this particular instant is $T_{Lo}(y,t^*)$. For $t>t^*$, the heat transfer problem becomes

$$\alpha_s \frac{\partial^2 T_s(y,t)}{\partial y^2} = \frac{\partial T_s(y,t)}{\partial t} \text{ for } 0 \leq y \leq Y(t) \tag{2a}$$

$$\alpha_L \frac{\partial^2 T_L(y,t)}{\partial y^2} = \frac{\partial T_L(y,t)}{\partial t} \text{ for } Y(t) \leq y \leq h \tag{2b}$$

subject to the following conditions:

(i) $T_s(Y,t) = T_L(Y,t) = T_e$ when $y = Y(t)$

(ii) $K_s \frac{\partial T_s}{\partial y} - K_L \frac{\partial T_L}{\partial y} = H_f \rho_s \frac{dY}{dt}$ when $y = Y(t)$

(iii) $T_L(y,t^*) = T_{Lo}(y,t^*)$ at $t = t^*$

(iv) $Y(t^*) = 0$ at $t = t^*$

(v) $T_s(0,t^*) = f_1(t^*) = T_{Lo}(0,t^*) = T_e$ at $t = t^*$, $y = 0$

(vi) $T_L(h,t^*) = T_{Lo}(h,t^*) = f_2(t^*)$ at $t = t^*$, $y = h$

(vii) $T_s(0,t) = f_1(t)$ at $y = 0$ for $t \geq t^*$

(viii) $T_L(h,t) = f_2(t)$ at $y = h$ for $t \geq t^*$

$Y(t)$ is the height of solid which has been formed from time $t = t^*$ to time $t = t$ and is measured from the inside face of the bottom plate up along the y axis to the interface separating liquid and solid hexadecane. Conditions (i), (ii) and (iv) describe the interface. Condition (i) says that, at

the interface, the temperature of the solid phase equals the temperature of the liquid phase for all t. Condition (ii) states that the rate of heat liberation at the interface by freezing must equal the net rate at which heat is conducted away into solid and liquid phases. H_f is the heat of fusion of solid hexadecane per unit mass. Subscripts s and L refer to the properties of solid and liquid phases respectively. Condition (iv) states that at time $t = t^*$ when the temperature of the cooled bottom plate first reaches the equilibrium freezing temperature of n-hexadecane, the amount of solid present is zero, i.e., the liquid hexadecane is still all liquid. Conditions (iii) to (vi) mean that the temperature profile in the liquid hexadecane during the pre-solidification problem still exists at time $t = t^*$. Conditions (vii) and (viii) state that the temperatures of the bottom and the top plates are functions of time which are also continuous with the temperature profiles that are obtained at these boundaries for the pre-solidification problem; in other words, the process of solidification does not introduce any discontinuity between the temperatures that are obtained for these boundaries for the pre-solidification problem and for the post-solidification problem.

Condition (ii) may be derived as follows. In a time dt let dL be thickness of liquid that has solidified to produce a solid of thickness dY. Let H_s and H_L be the enthalpies per unit mass of the solid and liquid phases respectively. Therefore $H_f = H_L - H_s$. A mass balance at the interface, (Fig. 2), gives $\rho_s dY = \rho_L dL$. Energy balance gives

Figure 2. Moving interface from time t to time t + dt.

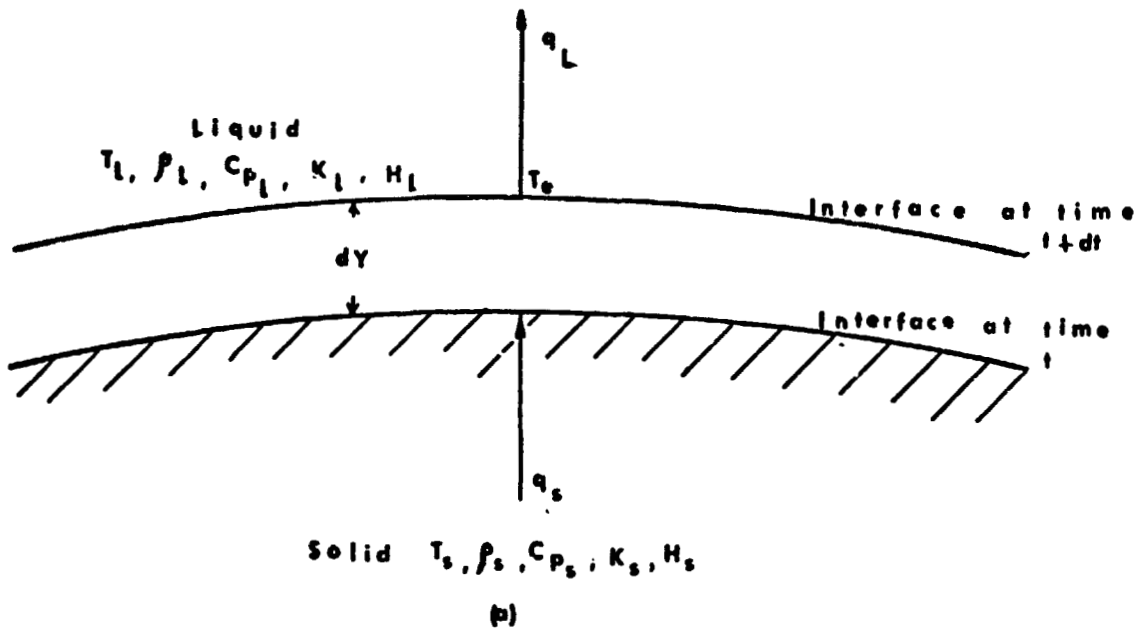

(a)

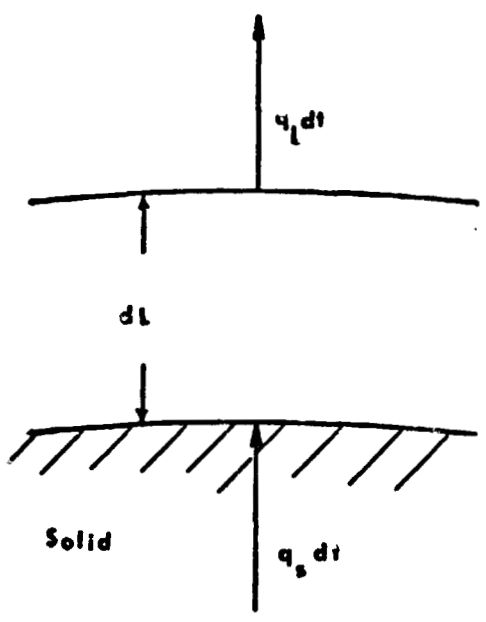

Initial State
(Liquid)

(b)

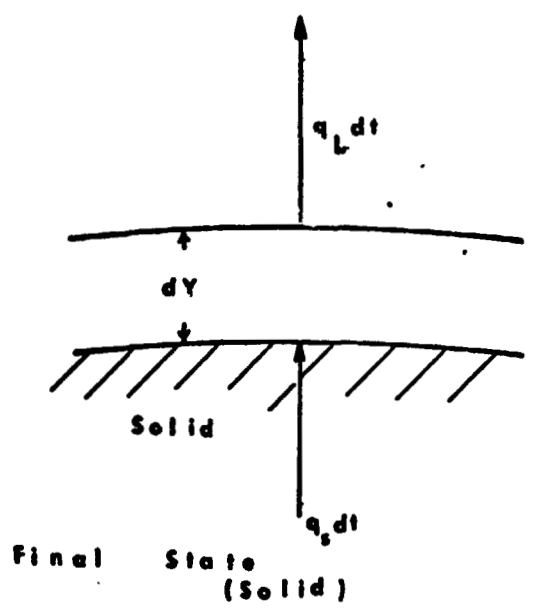

Final State
(Solid)

(c)

$\rho_s H_s dY - \rho_L H_L dL = q_s dt - q_L dt$, where q_s and q_L are heat fluxes per unit time per unit cross sectional area of solid and liquid phases respectively. All these equations have been written independent of the cross-sectional area because the cross sectional area of the cell is constant and is the same for both the solid and liquid phases. When the definition of H_f, and the mass-balance equation are introduced into the energy-balance equation, the following equation is obtained:

$$-\rho_s H_f \frac{dY}{dt} = q_s - q_L \tag{3}$$

By Fourier's law of conduction, $q_s = -K_s \frac{\partial T_s}{\partial y}$ and $q_L = -K_L \frac{\partial T_L}{\partial y}$. Putting these definitions for q_s and q_L into equation (3) and rearranging it, we get $K_s \frac{\partial T_s}{\partial y} - K_L \frac{\partial T_L}{\partial y} = H_f \rho_s \frac{dY}{dt}$, which is condition (ii).

The following dimensionless variables are defined.

$$\theta = T(y,t)/T_e$$

$$z = y/h$$

$$S = Y/h$$

$$\tau_o = (\alpha_L/h^2)t$$

$$\tau = (\alpha_L/h^2)(t - t^*) = \tau_o - \tau_o^*$$

$$\tau_o^* = (\alpha_L/h^2)t^*$$

The subscripts o, L, and s still apply as previously defined. In dimensionless form, the governing equations of the pre-solidification problem become, for $0 \leq \tau_o \leq \tau_o^*$

$$\frac{\partial^2 \theta_{Lo}(z,\tau_o)}{\partial z^2} = \frac{\partial \theta_{Lo}(z,\tau_o)}{\partial \tau_o} \text{ for } 0 \leq z \leq 1.0 \qquad (4)$$

(i) $\theta_{Lo}(0,\tau_o) = f_1(\tau_o)/T_e$ when $z = 0$

(ii) $\theta_{Lo}(1,\tau_o) = f_2(\tau_o)/T_e$ when $z = 1.0$

(iii) $\theta_{Lo}(z,0) = T_a/T_e$ at $\tau_o = 0$, for $0 \leq z \leq 1.0$

Also the governing equations for the post-solidification problem become, for $\tau > 0$ (or equivalently, for $\tau_o > \tau_o^*$),

$$\lambda \frac{\partial^2 \theta_s(z,\tau)}{\partial z^2} = \frac{\partial \theta_s(z,\tau)}{\partial \tau} \text{ for } 0 < z < S \qquad (5a)$$

$$\frac{\partial^2 \theta_L(z,\tau)}{\partial z^2} = \frac{\partial \theta_L(z,\tau)}{\partial \tau} \text{ for } S < z < 1.0 \qquad (5b)$$

subject to the following conditions:

(i) $\theta_s(S,\tau) = \theta_L(S,\tau) = 1.0$ at $z = S$ for $\tau \geq 0$

(ii) $M \frac{\partial \theta_s}{\partial z} - J \frac{\partial \theta_L}{\partial z} = \frac{dS}{d\tau}$ at $z = S$ for $\tau \geq 0$

(iii) $\theta_L(z,0) = \theta_{Lo}(z,\tau_o^*)$ at $\tau = 0$ (at $\tau_o = \tau_o^*$)

(iv) $S(0) = 0$ at $\tau = 0$

(v) $\theta_s(0,0) = f_1(\tau = 0)/T_e = 1.0$ when $\tau = 0$, at $z = 0$

(vi) $\theta_L(1,0) = f_2(\tau = 0)/T_e = \theta_{Lo}(1.0,0)$ when $\tau = 0$

where $\lambda = \alpha_s/\alpha_L$

$$M = \left(\frac{c_{p_s} T_e}{H_f}\right)\left(\frac{\alpha_s}{\alpha_L}\right)$$

$$J = \left(\frac{c_{pL} T_e}{H_f}\right)\left(\frac{\rho_L}{\rho_s}\right)$$

The dimensionless equations are now to be put into finite difference forms. The method of L. W. Ehrlich[22] is used to do this.

Figure 3. Axial section of test cell showing space grids and nodes.

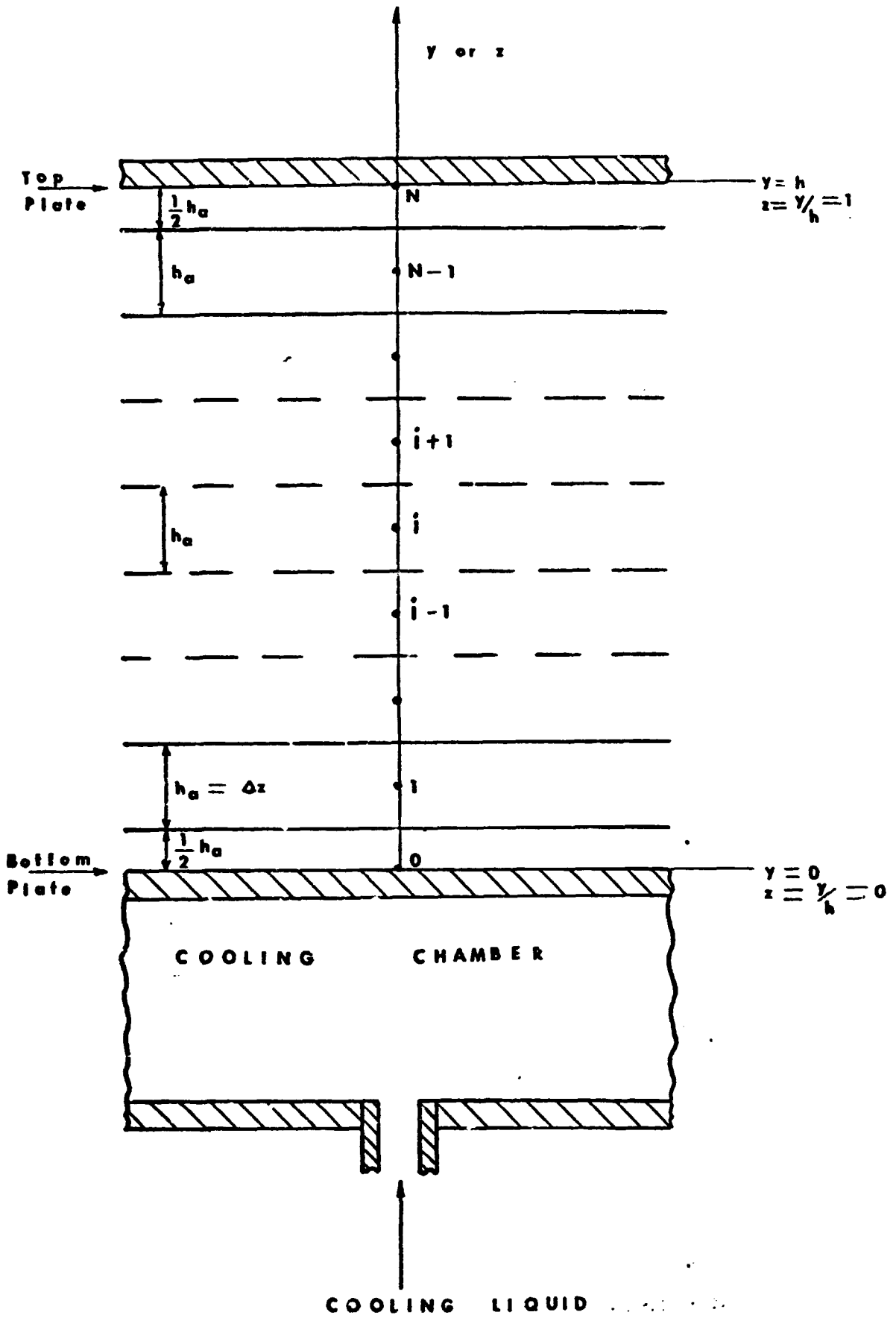

DIAGRAM OF AXIAL SECTION OF TEST CELL SHOWING SPACE GRIDS AND NODES

Finite Difference Formulation of Governing Equations

The Taylor series expansion of a function $f(x+a,y+b)$ about a point (x,y) is

$$f(x+a,y+b) = f(x,y) + \left(a\frac{\partial}{\partial x} + b\frac{\partial}{\partial y}\right)f(x,y) + \frac{1}{2!}\left(a\frac{\partial}{\partial x} + b\frac{\partial}{\partial y}\right)^2 f(x,y)$$

$$+ \frac{1}{3!}\left(a\frac{\partial}{\partial x} + b\frac{\partial}{\partial y}\right)^3 f(x,y) + \ldots + \frac{1}{(n-1)!}\left(a\frac{\partial}{\partial x} + b\frac{\partial}{\partial y}\right)^{n-1} f(x,y)$$

$$+ R_n \qquad (6)$$

where $R_n = \frac{1}{n!}\left(a\frac{\partial}{\partial x} + b\frac{\partial}{\partial y}\right)^n f(x+\zeta a, y+\gamma b)$, with $0 \leq \zeta \leq 1$ and $0 \leq \gamma \leq 1$, i.e. $R_n = 0(a+b)^n$. The symbol $0(\ )$ means "of the order of what is enclosed in the brackets." For this problem, we impose a mesh on the test cell, such that the space grid is vertical along the height of the cell and time grid is horizontal; that is, the time grid is perpendicular to the space grid. On the (z,τ_o) or the (z,τ) coordinates, the following are defined (see Fig. 3 and Fig. 4):

$h_a = \Delta z$ = mesh size in the space coordinate

$k_a = \Delta\tau_o = \Delta\tau$ = mesh size in the time coordinate

$p = k_a/(h_a^2)$

$(\theta_{Lo})_{i,j} = \theta_{Lo}(ih_a, jk_a)$

$(\theta_s)_{i,j} = \theta_s(ih_a, jk_a)$

$(\theta_L)_{i,j} = \theta_L(ih_a, jk_a)$

Pre-solidification Problem

The following approximations will be used for the partial derivatives.

$$\left(\frac{\partial^2\theta_{Lo}}{\partial z^2}\right)_{i,j+1} \simeq \frac{1}{h_a^2}\{(\theta_{Lo})_{i-1,j+1}$$

$$- 2(\theta_{Lo})_{i,j+1} + (\theta_{Lo})_{i+1,j+1}\} + O(h_a^2) \qquad (7)$$

$$\left(\frac{\partial\theta_{Lo}}{\partial\tau_o}\right)_{i,j} \simeq \frac{1}{k_a}\{(\theta_{Lo})_{i,j+1} - (\theta_{Lo})_{i,j}\}$$

$$- \frac{k_a}{2}\left(\frac{\partial^2\theta_{Lo}}{\partial\tau_o^2}\right)_{i,j} + O(k_a^2) \qquad (8)$$

$$\left(\frac{\partial^2\theta_{Lo}}{\partial z^2}\right)_{i,j} \simeq \frac{1}{h_a^2}\{(\theta_{Lo})_{i-1,j} - 2(\theta_{Lo})_{i,j} + (\theta_{Lo})_{i+1,j}\}$$

$$+ O(h_a^2) \qquad (9)$$

$$\left(\frac{\partial\theta_{Lo}}{\partial\tau_o}\right)_{i,j+1} \simeq \frac{1}{k_a}\{(\theta_{Lo})_{i,j+1} - (\theta_{Lo})_{i,j}\}$$

$$+ \frac{k_a}{2}\left(\frac{\partial^2\theta_{Lo}}{\partial\tau_o^2}\right)_{i,j+1} + O(k_a^2) \qquad (10)$$

The difference equations are to be derived in the implicit form so that they may be solved using tri-diagonal matrix, Gauss elimination and back-substitution. On substituting equations (7) and (10) into equation (4), we get

$$\frac{1}{k_a}\{(\theta_{Lo})_{i,j+1} - (\theta_{Lo})_{i,j}\}$$

$$= \frac{1}{h_a^2}\{(\theta_{Lo})_{i-1,j+1} - 2(\theta_{Lo})_{i,j+1} + (\theta_{Lo})_{i+1,j+1}\}$$

$$+ O(h_a^2) + O(k_a) \qquad (11)$$

Figure 4. Two-dimensional finite elements in time and space coordinates.

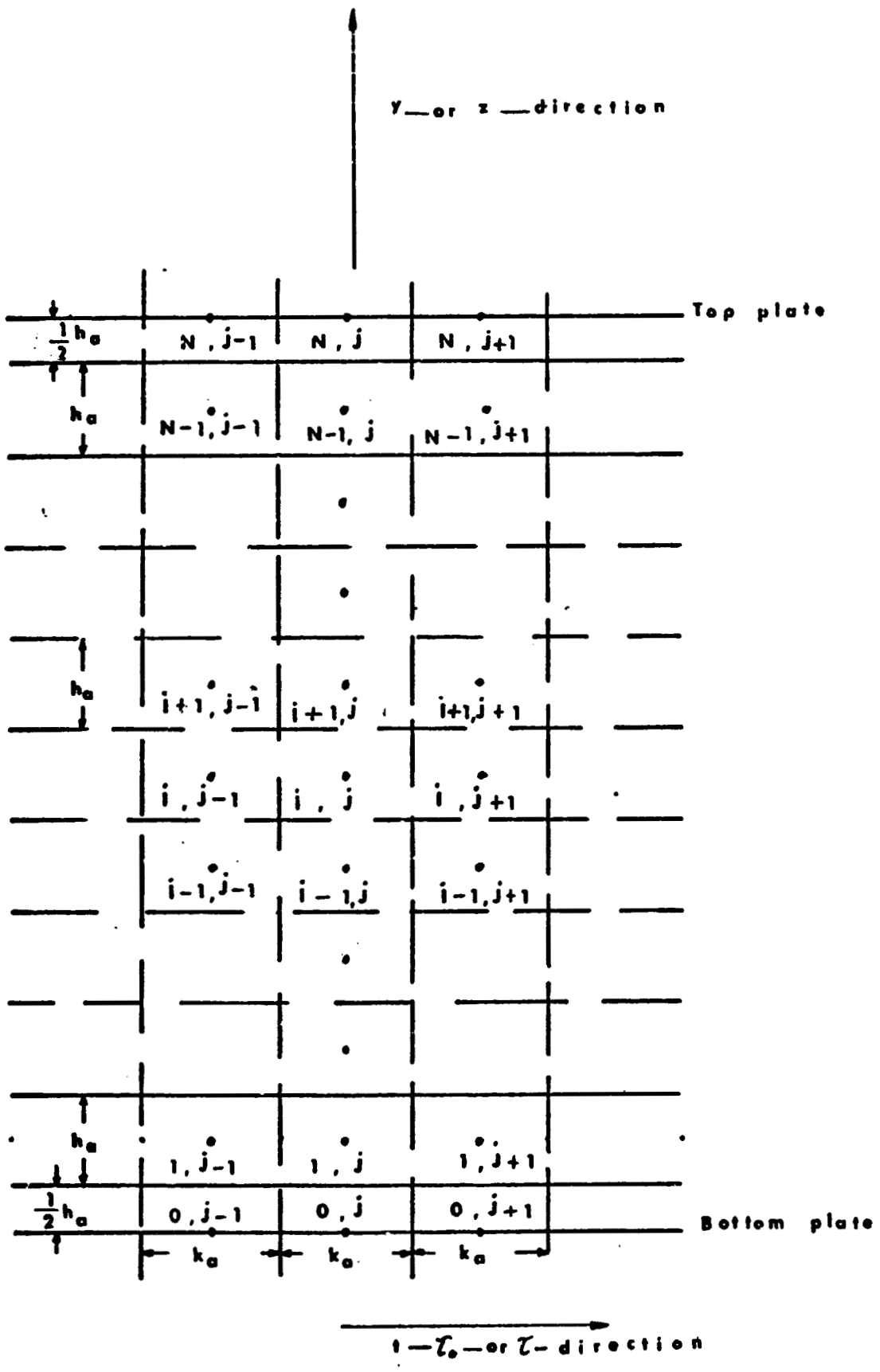
y — or z — direction
Top plate
$\frac{1}{2}h_a$
N , j-1
N , j
N , j+1
h_a
N-1, j-1
N-1, j
N-1, j+1
h_a
i+1, j-1
i+1, j
i+1, j+1
i , j-1
i , j
i , j+1
i-1, j-1
i-1, j
i-1, j+1
h_a
1, j-1
1 , j
1 , j+1
$\frac{1}{2}h_a$
0 , j-1
0 , j
0 , j+1
Bottom plate
k_a
k_a
k_a
t — τ_o — or τ - direction

On substituting equations (8) and (9) into equation (4), we get

$$\frac{1}{k_a}\{(\theta_{Lo})_{i,j+1} - (\theta_{Lo})_{i,j}\} = \frac{1}{h_a^2}\{(\theta_{Lo})_{i-1,j} - 2(\theta_{Lo})_{i,j}$$

$$+ (\theta_{Lo})_{i+1,j}\} + O(h_a^2) + O(k_a) \qquad (12)$$

Addition of equations (11) and (12) yields

$$\frac{2}{k_a}\{(\theta_{Lo})_{i,j+1} - (\theta_{Lo})_{i,j}\} = \frac{1}{h_a^2}\{(\theta_{Lo})_{i-1,j+1}$$

$$- 2(\theta_{Lo})_{i,j+1} + (\theta_{Lo})_{i+1,j+1} + (\theta_{Lo})_{i-1,j}$$

$$-2(\theta_{Lo})_{i,j} + (\theta_{Lo})_{i+1,j}\} + O(k_a^2) + O(h_a^2) \qquad (13)$$

Using the definition for p in equation (13), we get

$$-\frac{p}{2}(\theta_{Lo})_{i-1,j+1} + (1+p)(\theta_{Lo})_{i,j+1} - \frac{p}{2}(\theta_{Lo})_{i+1,j+1}$$

$$= \frac{p}{2}(\theta_{Lo})_{i-1,j} + (1-p)(\theta_{Lo})_{i,j} + (\frac{p}{2})(\theta_{Lo})_{i+1,j}$$

$$+ O(k_a^3) + O(k_a h_a^2) \qquad (14)$$

The local error term in equation (14) is $O(k_a^3) + O(k_a h_a^2)$. Therefore the governing pre-solidification equations become, for $0 \leq \tau_o \leq \tau_o^*$,

$$-\frac{p}{2}(\theta_{Lo})_{i-1,j+1} + (1+p)(\theta_{Lo})_{i,j+1} - (\frac{p}{2})(\theta_{Lo})_{i+1,j+1}$$

$$= \frac{p}{2}(\theta_{Lo})_{i-1,j} + (1-p)(\theta_{Lo})_{i,j} + \frac{p}{2}(\theta_{Lo})_{i+1,j} + O(k_a^3)$$

$$+ O(k_a h_a^2), \qquad 1 \leq i \leq N-1 \qquad (15)$$

subject to the following conditions:

(i) $(\theta_{Lo})_{o,j} = \frac{(f_1)_j}{T_e}$; $(\theta_{Lo})_{o,j+1} = \frac{(f_1)_{j+1}}{T_e}$, at $i = 0$

(ii) $(\theta_{Lo})_{N,j} = \frac{(f_2)_j}{T_e}$; $(\theta_{Lo})_{N,j+1} = \frac{(f_2)_{j+1}}{T_e}$, at $i = N$

(iii) $(\theta_{Lo})_{i,o} = T_a/T_e$ at $j = 0$ for $0 \leq i \leq N$

where N is the total number of nodes in the space direction with the first node on the bottom plate and the Nth node on the top plate.

<u>Post-solidification Problem</u>

$$\left(\frac{\partial^2\theta_s}{\partial z^2}\right)_{i,j+1} \simeq \frac{1}{h_a^2}\{\theta_{s_{i-1,j+1}} - 2\theta_{s_{i,j+1}} + \theta_{s_{i+1,j+1}}\} + O(h_a^2) \tag{16}$$

$$\left(\frac{\partial\theta_s}{\partial\tau}\right)_{i,j+1} \simeq \frac{1}{k_a}\{\theta_{s_{i,j+1}} - \theta_{s_{i,j}}\} + \frac{k_a}{2}\left(\frac{\partial^2\theta_s}{\partial\tau^2}\right)_{i,j+1} + O(k_a^2) \tag{17}$$

$$\left(\frac{\partial^2\theta_s}{\partial z^2}\right)_{i,j} \simeq \frac{1}{h_a^2}\{\theta_{s_{i-1,j}} - 2\theta_{s_{i,j}} + \theta_{s_{i+1,j}}\} + O(h_a^2) \tag{18}$$

$$\left(\frac{\partial\theta_s}{\partial\tau}\right)_{i,j} \simeq \frac{1}{k_a}\{\theta_{s_{i,j+1}} - \theta_{s_{i,j}}\} - \frac{k_a}{2}\left(\frac{\partial^2\theta_s}{\partial\tau^2}\right)_{i,j} + O(k_a^2) \tag{19}$$

$$\left(\frac{\partial^2\theta_L}{\partial z^2}\right)_{i,j+1} \simeq \frac{1}{h_a^2}\{\theta_{L_{i-1,j+1}} - 2\theta_{L_{i,j+1}} + \theta_{L_{i+1,j+1}}\} + O(h_a^2) \tag{20}$$

$$\left(\frac{\partial\theta_L}{\partial\tau}\right)_{i,j} \simeq \frac{1}{k_a}\{\theta_{L_{i,j+1}}-\theta_{L_{i,j}}\} - \frac{k_a}{2}\left(\frac{\partial^2\theta_L}{\partial\tau^2}\right)_{i,j}+0(k_a^2) \tag{21}$$

$$\left(\frac{\partial^2\theta_L}{\partial z^2}\right)_{i,j} \simeq \frac{1}{h_a^2}\{\theta_{L_{i-1,j}}-2\theta_{L_{i,j}}+\theta_{L_{i+1,j}}\} + 0(h_a^2) \tag{22}$$

$$\left(\frac{\partial\theta_L}{\partial\tau}\right)_{i,j+1} \simeq \frac{1}{k_a}\{\theta_{L_{i,j+1}}-\theta_{L_{i,j}}\}+\frac{k_a}{2}\left(\frac{\partial^2\theta_L}{\partial\tau^2}\right)_{i,j+1}+0(k_a^2) \tag{23}$$

$$\left(\frac{\partial^2\theta_s}{\partial z^2}\right)_{R,j+1} \simeq \left\{\frac{2}{h_a^2(1+x_{j+1})x_{j+1}}\right\}\{1-\theta_{sR,j+1}+x_{j+1}\theta_{s_{R-1,j+1}}$$

$$- x_{j+1}\theta_{s_{R,j+1}}\} + 0(h_a) \tag{24}$$

$$\left(\frac{\partial\theta_s}{\partial\tau}\right)_{R,j+1} \simeq \frac{1}{k_a}\{\theta_{s_{R,j+1}}-\theta_{s_{R,j}}\} + 0(k_a) \tag{25}$$

$$\left(\frac{\partial^2\theta_L}{\partial z^2}\right)_{R+1,j+1} \simeq \frac{2}{h_a^2(2-x_{j+1})}\left\{\frac{1-\theta_{L_{R+1,j+1}}}{1-x_{j+1}} + \theta_{L_{R+2,j+1}}\right.$$

$$\left. - \theta_{L_{R+1,j+1}}\right\} + 0(h_a) \tag{26}$$

$$\left(\frac{\partial\theta_L}{\partial\tau}\right)_{R+1,j+1} \simeq \frac{1}{k_a}\{\theta_{L_{R+1,j+1}}-\theta_{L_{R+1,j}}\} + 0(k_a) \tag{27}$$

$$\left(\frac{\partial^2\theta_s}{\partial z^2}\right)_{R-1,j+1} \simeq \frac{1}{h_a^2}\{\theta_{s_{R-2,j+1}}-2\theta_{R-1,j+1}+\theta_{R,j+1}\}$$

$$+ 0(h_a^2) \tag{28}$$

$$\left(\frac{\partial\theta_s}{\partial\tau}\right)_{R-1,j+1} \approx \frac{1}{k_a}\{\theta_{s_{R-1,j+1}} - \theta_{s_{R-1,j}}\} + O(k_a) \tag{29}$$

$$\left(\frac{\partial\theta_s}{\partial\tau}\right)_{R,j+1} \approx \frac{x_{j+1}\theta_{R,j+1}^{-1}}{a_R k_a} + O(k_a) \tag{30}$$

$$\left(\frac{\partial\theta_s}{\partial\tau}\right)_{R-1,j+1} \approx \frac{\theta_{R-1,j+1}^{-1}}{a_{R-1}k_a} + O(k_a) \tag{31}$$

$$\left(\frac{\partial\theta_L}{\partial z}\right)_{\text{interface},j+1} \approx \frac{1}{h_a}\left\{\frac{2-x_{j+1}}{1-x_{j+1}}\theta_{L_{R+1,j+1}} - \frac{1-x_{j+1}}{2-x_{j+1}}\theta_{L_{R+2,j+1}} - \frac{3-2x_{j+1}}{(1-x_{j+1})(2-x_{j+1})}\right\}$$

$$= \sigma_L/h_a + O(h_a^2) \tag{32}$$

$$\left(\frac{\partial\theta_s}{\partial z}\right)_{\text{interface},j+1} \approx \frac{1}{h_a}\left\{\frac{x_{j+1}}{1+x_{j+1}}\theta_{s_{R-1,j+1}} - \frac{1+x_{j+1}}{x_{j+1}}\theta_{s_{R,j+1}} + \frac{1+2x_{j+1}}{x_{j+1}(1+x_{j+1})}\right\} + O(h_a^2) = \sigma_s/h_a + O(h_a^2) \tag{33}$$

$$\left(\frac{\partial\theta_L}{\partial z}\right)_{\text{interface},\ j+1} \approx \frac{1}{2h_a}\{-(5-2x_{j+1})\theta_{L_{R+1,j+1}} + 4(2-x_{j+1})\theta_{L_{R+2,j+1}} - (3-2x_{j+1})\theta_{L_{R+3,j+1}}\} = \sigma_L'/h_a + O(h_a^2) \tag{34}$$

$$\left(\frac{\partial\theta_s}{\partial z}\right)_{\text{interface},j+1} \approx \frac{1}{2h_a}\{(1+2x_{j+1})\theta_{s_{R-2,j+1}} - 4(1+x_{j+1})\theta_{s_{R-1,j+1}} + (3+2x_{j+1})\theta_{s_{R,j+1}}\} + O(h_a^2)$$

$$= \sigma_s'/h_a + O(h_a^2) \tag{35}$$

$$\left(\frac{\partial\theta_s}{\partial z}\right)_{\text{interface},j+1} \approx \frac{1-\theta_{s_{0,j+1}}}{h_a x_{j+1}} = \frac{1-(f_1)_{j+1}/T_e}{h_a x_{j+1}} + O(h_a) \quad (36)$$

$$\left(\frac{\partial\theta_L}{\partial z}\right)_{\text{interface},\ j+1} \approx \frac{\theta_{L_{N,j+1}}-1}{h_a(1-x_{j+1})}$$

$$+ O(h_a) = \frac{\frac{1}{T_e}(f_2)_{j+1}-1}{h_a(1-x_{j+1})} + O(h_a) \quad (37)$$

$$\left(\frac{\partial\theta_L}{\partial z}\right)_{\text{interface},\ j+1} \approx \frac{\theta_{L_{N,j+1}}-1}{h_a(2-x_{j+1})} + O(h_a)$$

$$= \frac{\frac{1}{T_e}(f_2)_{j+1}-1}{h_a(2-x_{j+1})} + O(h_a) \quad (38)$$

$$\left(\frac{dS}{d\tau}\right)_{j+1} \approx \frac{S_{j+1}-S_j}{k_a} = \frac{h_a}{k_a}\{(R_{j+1}+x_{j+1})-(R_j+x_j)\} + O(k_a) \quad (39)$$

The governing equations for the post-solidification problem apply for $\tau_o \geq \tau_o^*$ or for $\tau \geq 0$. Equations (16) through (39) are obtained by Taylor series expansion around the points where the derivatives are to be found. Equations (16) through (23) apply to the solid and liquid phases for nodes not near the solid-liquid interface. For regions near and on the interface, these equations have to be modified. Equations (24) through (31) are such modified equations that apply near the interface. Equations (32) to (38) apply at the solid-liquid interface itself. Equation (39) describes the rate at which solid of dimensionless height S is formed. Equations (16) to (23) are obtained by exactly the same

operation that yielded equations (7) to (10) and when they are substituted into equations (5a) and (5b) in the same way that equations (7) to (10) were substituted into equation (4) the following equations result:

$$-p/2\theta_{L_{i-1,j+1}}+(1+p)\theta_{L_{i,j+1}}-p/2\theta_{L_{i+1,j+1}}$$
$$= p/2\theta_{L_{i-1,j}}+(1-p)\theta_{L_{i,j}}+p/2\theta_{L_{i+1,j}}$$
$$+ O(k_a^3) + O(k_a h_a^2) \tag{40}$$

$$-\lambda p/2\theta_{s_{i-1,j+1}}+(1+\lambda p)\theta_{L_{i,j+1}}-\lambda p/2\theta_{L_{i+1,j+1}}$$
$$= \lambda p/2\theta_{s_{i-1,j}}+(1-\lambda p)\theta_{s_{i,j}}+\lambda p/2\theta_{s_{i+1,j}}$$
$$+ O(k_a^3) + O(k_a h_a^2\lambda) \tag{41}$$

It is to be emphasized again that these equations are good for nodes not near the interface.

For nodes near the solid-liquid interface, we proceed as follows. Suppose that the distribution of temperature and the position of the freezing front are known for the jth time step. Suppose also that the position of the freezing front for the (j + 1)st time step has been estimated; the section under "Solutions of Governing Finite Difference Equations" will indicate how this estimation is done. Define R as that space node on the moving interface or just below it, for a given time step. R varies with time step. Thus R may be better labelled as R_j for the jth time step or R_{j+1}

f . ne (j+1)st time tep. R corresponds to the number of full space nodes that have solidified for a given time step. The following cases, each of which is illustrated by figures (5) to (8), can occur.

A) The freezing front does not cross a space grid line, that is, the freezing front lies entirely between two space grid lines

B) The freezing front crosses one space grid line

C) The freezing front crosses two space grid lines

D) The freezing front crosses three or more space grid lines.

Each case requires special equations for the points near the interface, that is, for the points marked with "*" in figures (5) to (8). Let x_j be the fractional part of the space mesh between the freezing front and the node i=R during the jth time step. As was stated earlier, R may vary with the time step since it is always the node at or nearest the freezing front in the solid phase during a given time step. Let a_R be the fractional part of time grid that lies between the point (R, j+1) and the intersection of the freezing front with the space grid line at i=R during the (j+1)st time step.

<u>Case A</u>: Figure (5) illustrates this case. Equations (24) and (25) obtain at (R, j+1). On substituting equations (24) and (25) into equation (5a), we obtain

Figure 5. Case A: Interface does not cross a space grid line.

Figure 6. Case B: Interface crosses one space grid line.

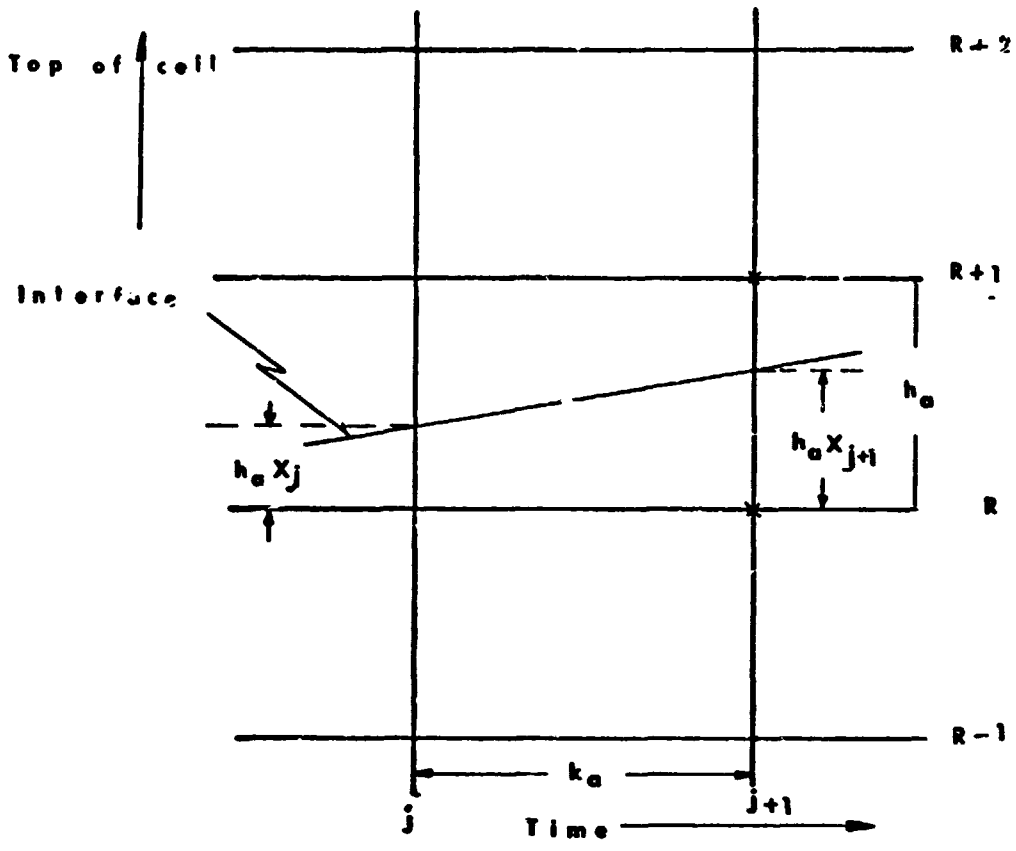
Top of cell
R+2
Interface
R+1
h_a
$h_a X_{j+1}$
$h_a X_j$
R
R-1
k_a
j
j+1
Time

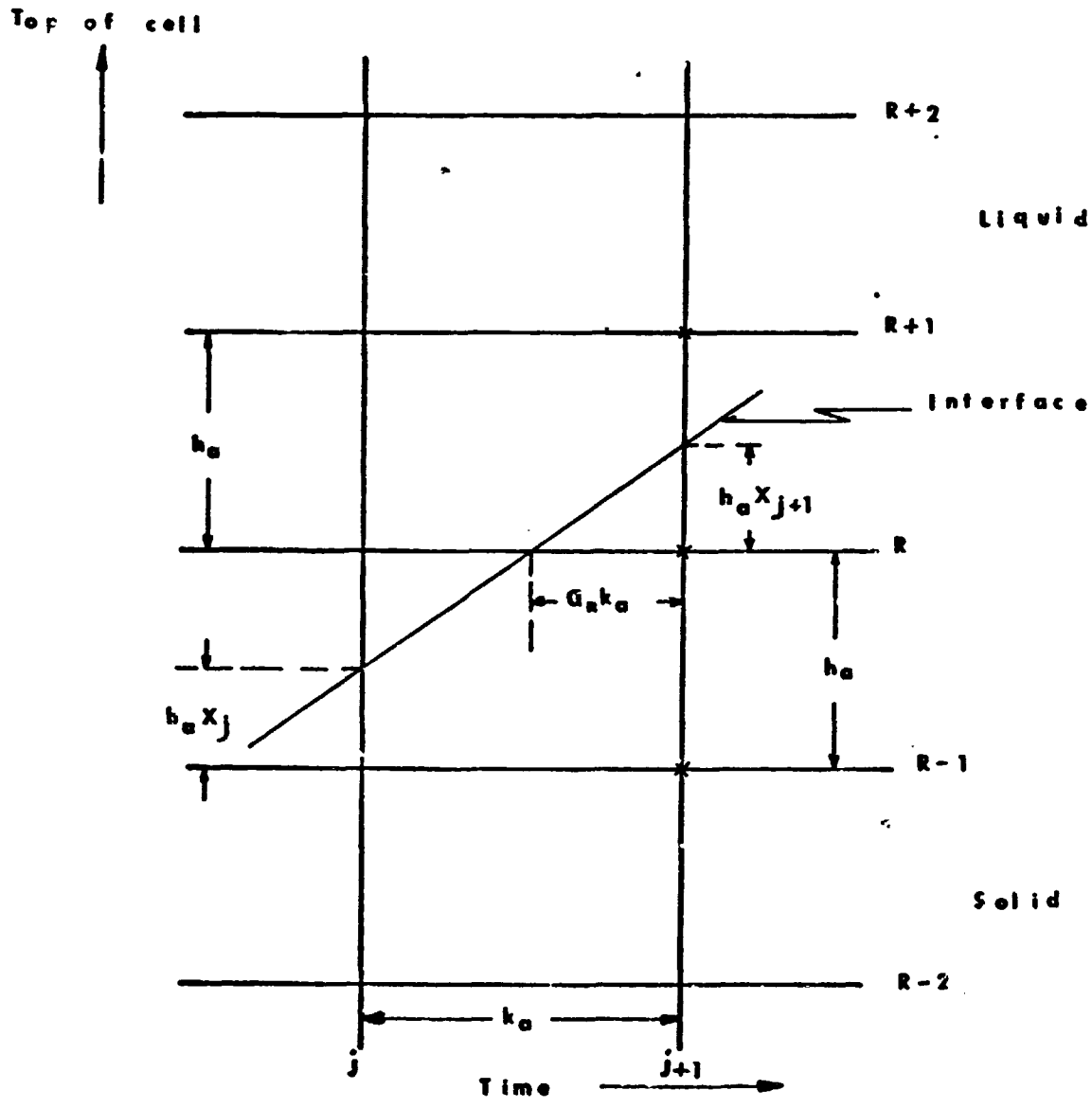
Top of cell
R+2
Liquid
R+1
Interface
h_a
$h_a X_{j+1}$
R
$G_s k_a$
h_a
$h_a X_j$
R-1
Solid
R-2
k_a
j
j+1
Time

$$-\frac{2\lambda p x_{j+1}}{1+x_{j+1}}\theta_{s_{R-1,j+1}}+(2\lambda p+x_{j+1})\theta_{s_{R,j+1}}=x_{j+1}\theta_{s_{R,j}}$$

$$+\frac{2\lambda I}{1+x_{j+1}} \tag{42}$$

$$\text{Error} \approx O(k_a^2)+O(\lambda k_a h_a)$$

which is the modified equation for the solid phase for nodes near the interface and it holds good for $R \geq 1$. On substituting equations (26) and (27) into equation (5b), we obtain

$$(2-x_{j+1})(1+2p-x_{j+1})\theta_{L_{R+1,j+1}}-2p(1-x_{j+1})\theta_{L_{R+2,j+1}}$$

$$=(2-x_{j+1})(1-x_{j+1})\theta_{L_{R+1,j}}+2p \tag{43}$$

$$\text{Error} \approx O(k_a^2)+O(h_a k_a)$$

which is the modified equation for the liquid phase for nodes near the freezing front and it holds good for $0 \leq R \leq N-2$.

<u>Case B</u>: Figure (6) illustrates Case B. On substituting equations (28) and (29) into eq tion (5a), we get

$$-\lambda p\theta_{s_{R-2,j+1}}+(1+2\lambda p)\theta_{s_{R-1,j+1}}-\lambda p\theta_{s_{R,j+1}}=\theta_{s_{R-1,j}} \tag{44}$$

$$\text{Error} \approx O(k_a^2)+O(\lambda k_a h_a^2)$$

On substituting equations (24) and (30) into equation (5a), we get

$$-\frac{2\lambda p x_{j+1}}{1+x_{j+1}}\theta_{s_{R-1,j+1}}+(2\lambda p+\frac{x_{j+1}}{a_R})\theta_{s_{R,j+1}}=\frac{x_{j+1}}{a_R}+\frac{2\lambda p}{1+x_{j+1}} \tag{45}$$

$$\text{Error} \approx O(k_a^{\,2}) + O(\lambda k_a h_a)$$

where a_R has the definition that has already been given and for this case it has a magnitude

$$a_R = x_{j+1}/(1-x_j + x_{j+1})$$

obtained by the theorem of similar triangles and the geometry of figure (6). Equations (44) and (45) apply to the solid phase near the interface. Equation (43) still holds for the liquid phase in this case.

<u>Case C</u>: Figure (7) illustrates Case C. On substituting equations (28) and (31) into equation (5a), we get

$$-\lambda a_{R-1} p\theta_{s_{R-2,j+1}} + (2\lambda a_{R-1} p+1)\theta_{s_{R-1,j+1}} - \lambda p a_{R-1}\theta_{s_{R,j+1}} = 1 \quad (46)$$

$$\text{Error} \approx O(k_a^{\,2}) + O(k_a h_a^{\,2}\lambda)$$

On substituting i=R-2 into equation (16), we get an equation for $(\frac{\partial^2\theta_s}{\partial z^2})_{R-2,j+1}$. Also on replacing R by R-2 in equation (25) we get an equation for $(\frac{\partial\theta_s}{\partial\tau})_{R-2,j+1}$. When these two equations are substituted into equation (5a), we get

$$-\lambda p\theta_{s_{R-3,j+1}} + (1+2\lambda p)\theta_{s_{R-2,j+1}} - \lambda p\theta_{s_{R-1,j+1}} = \theta_{s_{R-2,j}} \quad (47)$$

$$\text{Error} \approx O(k_a^{\,2}) + O(\lambda k_a h_a^{\,2})$$

Equations (43) and (45) still apply to the liquid and solid phases, respectively. For Case C, $a_R = x_{j+1}/(2-x_j + x_{j+1})$ and $a_{R-1} = (1+x_{j+1})/(2-x_j + x_{j+1})$ = fractional part of the

Figure 7. Case C: Interface crosses two space grid lines.

Figure 8. Case D: Interface crosses three or more space grid lines.

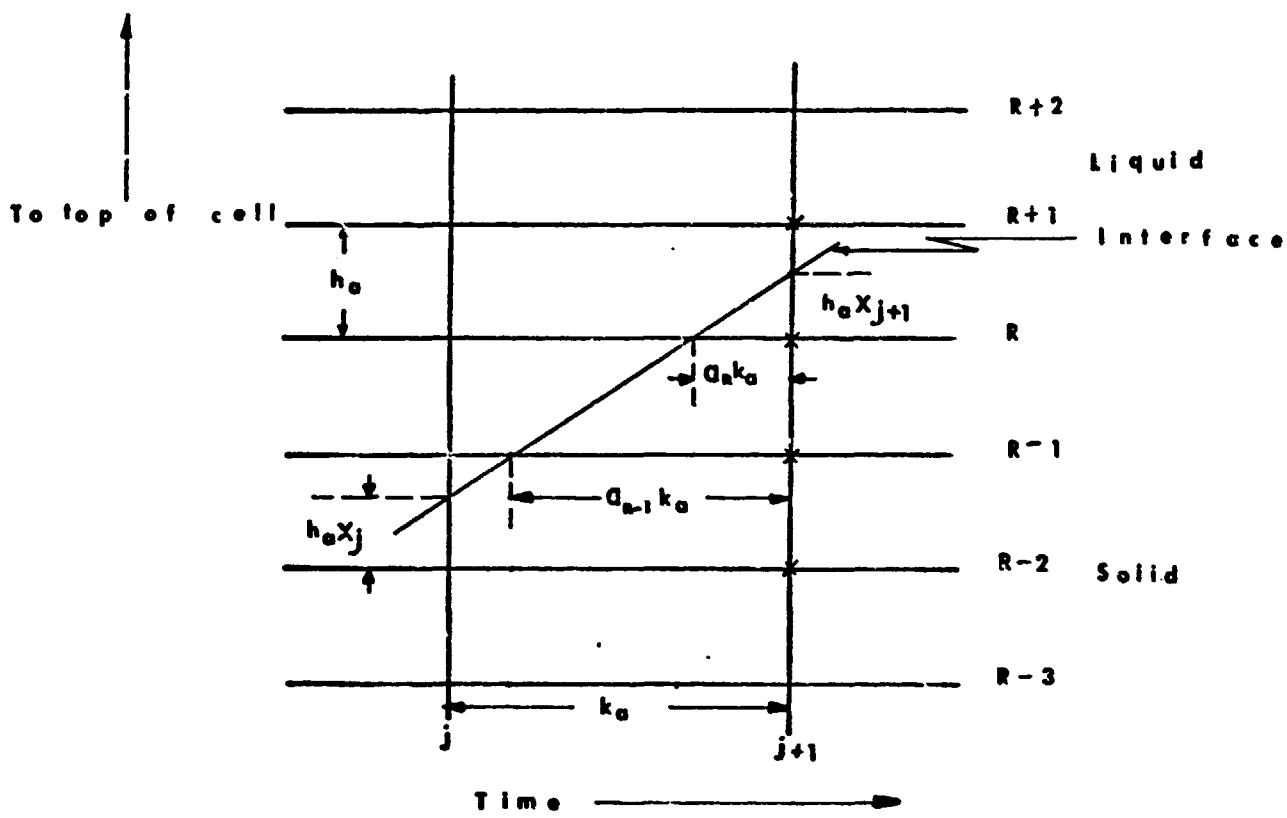
To top of cell
R+2
Liquid
R+1
Interface
h_a
$h_a X_{j+1}$
R
$a_R k_a$
R-1
$a_{R-1} k_a$
$h_a X_j$
R-2
Solid
R-3
k_a
j
j+1
Time

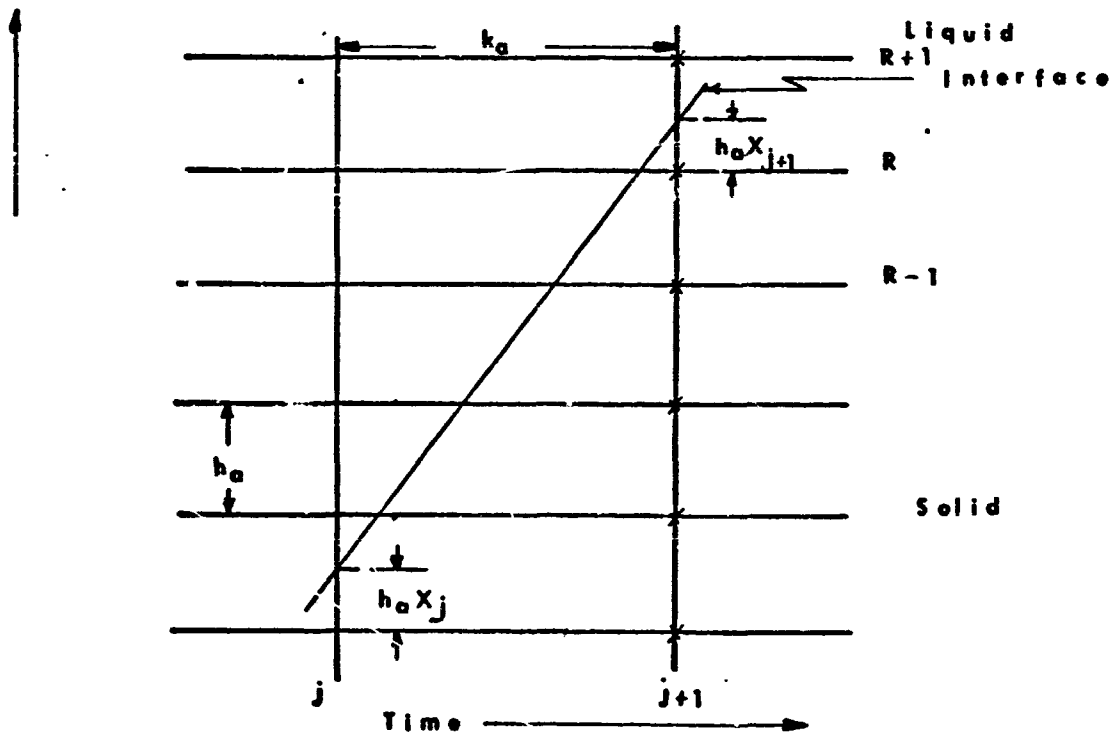
k_a
Liquid
R+1
Interface
$h_a X_{j+1}$
R
R-1
h_a
Solid
$h_a X_j$
j
j+1
Time

time grid between the point (R-1, j+1) and the intersection of the freezing front with the space grid line through R-1, during the (j+1)st time step. R is an integer such that $0 \leq R \leq N$.

Case D: Figure (8) illustrates this case. When this occurs, the time step is first reduced to half its normal value and the estimated position of the freezing front is now checked to see if any of cases A to C occurs, in which case the appropriate equations under cases A to C are used. If the interface still crosses three or more grid lines, the time step is still reduced further by a half. The new freezing front is checked against cases A to C. This process is repeated until one of cases A to C is obtained, after which the regular full time step is returned to again.

Special approximations must be used to obtain the derivatives to be used in the interface condition of equation (5) (ii) which is satisfied at the interface. Equations (32) to (39) are these special approximations. They are obtained by appropriate combinations of Taylor series expansions of temperatures at the interface for the (j+1)st time step. When they are applied to equation 5(ii), under conditions dictated by the values of R and x_{j+1}, the height S_{j+1} of solid formed at any given (j+1)st time step may be obtained.

The foregoing finite difference equations which have been obtained for the post-solidification problem will now

be arranged according to the groups in which they are used to obtain the post-solidification temperature profiles of solid and liquid n-hexadecane: For the solid phase the following grouping holds good:

(i) If $R(j+1)-R(j) = 0$, (this corresponds to Case A),

(a) if $R(j+1) = 1$, the governing equation is

$$-\frac{2\lambda p x_{j+1}}{1+x_{j+1}}\theta_{s_{R-1,j+1}}+(2\lambda p+x_{j+1})\theta_{s_{R,j+1}}$$

$$= x_{j+1}\theta_{s_{R,j}} + \frac{2\lambda p}{1+x_{j+1}} , \tag{48}$$

(b) if $R(j+1) \geq 2$, the governing equations are

$$-\frac{\lambda p}{2}\theta_{s_{i-1,j+1}}+(1+\lambda p)\theta_{s_{i,j+1}}-(\lambda p/2)\theta_{s_{i+1,j+1}}$$

$$= \tfrac{1}{2}\lambda p\theta_{s_{i-1,j}}+(1-\lambda p)\theta_{s_{i,j}}+\tfrac{1}{2}\lambda p\theta_{s_{i+1,j}} \quad \text{for } 1\leq i\leq R-1 \tag{49}$$

$$-\frac{2\lambda p x_{j+1}}{1+x_{j+1}}\theta_{s_{R-1,j+1}}+(2\lambda p+x_{j+1})\theta_{s_{R,j+1}}$$

$$= x_{j+1}\theta_{s_{R,j}} + \frac{2\lambda p}{1+x_{j+1}} . \tag{50}$$

(ii) If $R(j+1)-R(j) = 1$, (this corresponds to Case B), then

(a) if $R(j+1) = 1$, the governing equation is

$$-\frac{2\lambda p x_{j+1}}{1+x_{j+1}}\theta_{s_{R-1,j+1}}+(2\lambda p+\frac{x_{j+1}}{a_R})\theta_{s_{R,j+1}}$$

$$= \frac{x_{j+1}}{a_R} + \frac{2\lambda p}{1+x_{j+1}} \tag{51}$$

where $a_R = x_{j+1}/(1-x_j + x_{j+1})$,

(b) if $R(j+1) = 2$, the governing equations are

$$-\lambda p\theta_{s_{R-2,j+1}} + (1+2\lambda p)\theta_{s_{R-1,j+1}} - \lambda p\theta_{s_{R,j+1}} = \theta_{s_{R-1,j}} \tag{52}$$

$$-\frac{2\lambda p x_{j+1}}{1+x_{j+1}}\theta_{s_{R-1,j+1}} + (2\lambda p + \frac{x_{j+1}}{a_R})\theta_{s_{R,j+1}}$$

$$= \frac{x_{j+1}}{a_R} + \frac{2\lambda p}{1+x_{j+1}} \tag{53}$$

where a_R still has the same value as in part (a) above.

(c) if $R(j+1) \geq 3$, the governing equations are

$$-\tfrac{1}{2}\lambda p\theta_{s_{i-1,j+1}} + (1+\lambda p)\theta_{s_{i,j+1}} - \tfrac{1}{2}\lambda p\theta_{s_{i+1,j+1}}$$

$$= \tfrac{1}{2}\lambda p\theta_{s_{i-1,j}} + (1-\lambda p)\theta_{s_{i,j}} + \tfrac{1}{2}\lambda p\theta_{s_{i+1,j}}$$

$$\text{for } 1 \leq i \leq R-2 \tag{54}$$

$$-\lambda p\theta_{s_{R-2,j+1}} + (1+2\lambda p)\theta_{s_{R-1,j+1}} - \lambda p\theta_{s_{R,j+1}}$$

$$= \theta_{s_{R-1,j}} \tag{55}$$

$$-\frac{2\lambda p x_{j+1}}{1+x_{j+1}}\theta_{s_{R-1,j+1}} + (2\lambda p + \frac{x_{j+1}}{a_R})\theta_{s_{R,j+1}}$$

$$= \frac{x_{j+1}}{a_R} + \frac{2\lambda p}{1+x_{j+1}} \tag{56}$$

a_R still has the same value as in parts (a) and (b) above.

(iii) if $R(j+1)-R(j) = 2$, (this corresponds to Case C), then $R(j+1) \geq 2$.

(a) If $R(j+1) = 2$, then the governing equations are

$$-\lambda p a_{R-1}\theta_{s_{R-2,j+1}} + (2\lambda p a_{R-1}+1)\theta_{s_{R-1,j+1}} - \lambda p a_{R-1}\theta_{s_{R,j+1}} = 1 \tag{57}$$

$$-\frac{2\lambda p x_{j+1}}{1+x_{j+1}}\theta_{s_{R-1,j+1}} + (2\lambda p + \frac{x_{j+1}}{a_R})\theta_{s_{R,j+1}} = \frac{x_{j+1}}{a_R} + \frac{2\lambda p}{1+x_{j+1}} \tag{58}$$

where $a_{R-1} = (1+x_{j+1})/(2-x_j+x_{j+1})$ and

$$a_R = x_{j+1}/(2-x_j + x_{j+1})$$

(b) if $R(j+1) = 3$, the governing equations are

$$-\lambda p\theta_{s_{R-3,j+1}} + (1+2\lambda p)\theta_{s_{R-2,j+1}} - \lambda p\theta_{s_{R-1,j+1}} = \theta_{s_{R-2,j}} \tag{59}$$

$$-\lambda a_{R-1}p\theta_{s_{R-2,j+1}} + (2\lambda p a_{R-1}+1)\theta_{s_{R-1,j+1}} - \lambda p a_{R-1}\theta_{s_{R,j+1}} = 1 \tag{60}$$

$$\frac{-2\lambda p x_{j+1}}{1+x_{j+1}}\,\theta_{s_{R-1,j+1}}+\left(2\lambda p+\frac{x_{j+1}}{a_R}\right)\theta_{s_{R,j+1}}$$

$$=\frac{x_{j+1}}{a_R}+\frac{2\lambda p}{1+x_{j+1}} \tag{61}$$

where a_{R-1} and a_R have the same values as in part (a) above.

(c) if $R(j+1) \geq 4$, the governing equations are

$$-\tfrac{1}{2}\lambda p\theta_{s_{i-1,j+1}}+(1+\lambda p)\theta_{s_{i,j+1}}-\tfrac{1}{2}\lambda p\theta_{s_{i+1,j+1}}$$

$$=\tfrac{1}{2}\lambda p\theta_{s_{i-1,j}}+(1-\lambda p)\theta_{s_{i,j}}+\tfrac{1}{2}\lambda p\theta_{s_{i+1,j}} \quad \text{for } 1\leq i\leq R-3 \tag{62}$$

$$-\lambda p\theta_{s_{R-3,j+1}}+(1+2\lambda p)\theta_{s_{R-2,j+1}}-\lambda p\theta_{s_{R-1,j+1}}=\theta_{s_{R-2,j}} \tag{63}$$

$$-\lambda p a_{R-1}\theta_{s_{R-2,j+1}}+(2\lambda p a_{R-1}+1)\theta_{s_{R-1,j+1}}$$

$$-\lambda p a_{R-1}\theta_{s_{R,j+1}}=1 \tag{64}$$

$$-\frac{2\lambda p x_{j+1}}{1+x_{j+1}}\,\theta_{s_{R-1,j+1}}+\left(2\lambda p+\frac{x_{j+1}}{a_R}\right)\theta_{s_{R,j+1}}$$

$$=\frac{x_{j+1}}{a_R}+\frac{2\lambda p}{1+x_{j+1}} \tag{65}$$

where a_{R-1} and a_R still have the same values as in parts (a) and (b) above.

(iv) If $R(j+1) - R(j) \geq 3$ (this corresponds to Case D), we halve the time step, make a new estimate of $R(j+1)$ and check if $R(j+1) - R(j)$ has a value that will satisfy one of cases (A) to (C) which we have already treated. If one of these cases applies, we use the corresponding group of

equations for it. If none of the cases has occurred yet, we again halve the new time increment and continue doing this until one of cases A to C has occurred. After using the appropriate equations to calculate temperature profiles, we return to the regular time increment for the next time step.

For each of the groups of equations above, the following boundary and initial conditions apply:

$$\theta_{s_{o,j+1}} = (f_1)_{j+1}/T_e \tag{66}$$

$$\text{For } i = 0,\ \theta_{s_{o,o}} = \theta_s(o,o) = 1 \text{ when } \tau=0 \text{ or } \tau_o=\tau_o^* \tag{67}$$

$$\text{For } i > 0,\ \theta_s(ih_a,o) = \theta_{s_{i,o}} = 0 \text{ at } \tau=0 \text{ or } \tau_o=\tau_o^* \tag{68}$$

For the liquid phase, no matter the value of $R(j+1) - R(j)$, the following groupings hold.

(a) If $0 \leq R(j+1) \leq N-3$ where N is the total number of space nodes (from 0 at the bottom plate to N at the top plate), then the governing equations are

$$(2-x_{j+1})(1+2p-x_{j+1})\theta_{L_{R+1,j+1}} - 2p(1-x_{j+1})\theta_{L_{R+2,j+1}}$$
$$= (2-x_{j+1})(1-x_{j+1})\theta_{L_{R+1,j}} + 2p \tag{69}$$

$$-\tfrac{1}{2}p\theta_{L_{i-1,j+1}} + (1+p)\theta_{L_{i,j+1}} - \tfrac{1}{2}p\theta_{L_{i+1,j+1}}$$
$$= \tfrac{1}{2}p\theta_{L_{i-1,j}} + (1-p)\theta_{L_{i,j}} + \tfrac{1}{2}p\theta_{L_{i+1,j}}$$
$$\text{for } R+2 \leq i \leq N-1 \tag{70}$$

$$\theta_{L_{N,j+1}} = (f_2)_{j+1}/T_e \tag{71}$$

Equation (71) is a boundary condition which is satisfied at the top plate.

(b) If $R(j+1) = N-2$, the governing equations are

$$(2-x_{j+1})(1+2p-x_{j+1})\theta_{L_{R+1,j+1}} - 2p(1-x_{j+1})\theta_{L_{R+2,j+1}}$$

$$= (2-x_{j+1})(1-x_{j+1})\theta_{L_{R+1,j}} + 2p \tag{72}$$

$$\theta_{L_{N,j+1}} = (f_2)_{j+1}/T_e \tag{73}$$

(c) If $R(j+1) = N-1$, the governing equation is

$$\theta_{L_{N,j+1}} = (f_2)_{j+1}/T_e \tag{74}$$

(d) If $R(j+1) = N$, then the entire content of the cell has solidified with the top plate just at the equilibrium temperature of solidification. The initial condition for all the foregoing groups of equations is

$$\theta_{L_{i,o}} = \theta_{Lo}(ih_a, \tau_o^*) \quad \text{for} \quad 0 \leq i \leq N \tag{75}$$

$$\theta_{L_{o,o}} = \theta_{Lo}(o, \tau_o^*) = 1 \text{ at the bottom plate.} \tag{76}$$

For the calculation of S_{j+1}, the height of solid which has formed at the (j+1)st time step, the following equations apply:

For $0 \leq x_{j+1} \leq 1$ and $0 \leq R \leq N$, equation (77) applies

$$S_{j+1} = h_a\{R(j+1) + x_{j+1}\} \tag{77}$$

Also when the appropriate derivatives from equation (32) through equation (39) are substituted into condition (51i) of the post-solidification problem, equations which apply

for certain values of $R(j+1)$ and x_{j+1} are obtained for S_{j+1}. Thus

(a) if $1/4 < x_{j+1} \leq 3/4$, we get

$$S_{j+1} = S_j + h_a p(M\sigma_s - J\sigma_L), \text{ for } 1 \leq R \leq N-2 \tag{78}$$

and $$S_{j+1} = S_j + h_a p\{(M/x_{j+1})(1-\theta_{s_{o,j+1}}) - J\sigma_L\}, \text{ for } R=0 \tag{79}$$

and $$S_{j+1} = S_j + h_a p\{M\sigma_s - J(\theta_{L_{N,j+1}}-1)/(1-x_{j+1})\}, \text{ for } R=N-1 \tag{80}$$

The limits of $1/4 \leq x_{j+1} \leq 3/4$ were set so as to avoid dividing by numbers close to or equal to zero which would make the results blow up.

(b) If $0 \leq x_{j+1} \leq 1/4$, we use

$$S_{j+1} = S_j + h_a p(M\sigma_s' - J\sigma_L), \text{ for } 2 \leq R \leq N-3 \tag{81}$$

or $$S_{j+1} = S_j + h_a p\{(M/b)(1-\theta_{s_{o,j+1}}) - J\sigma_L\}, \text{ for } R=0$$

$$\text{where } b = 1/4 \tag{82}$$

or when $R = 1$, $$\left(\frac{\partial\theta_s}{dz}\right)_{\text{interface},j+1} = (1-\theta_{s_{o,j+1}})/(1+x_{j+1}) \tag{83}$$

so that

$$S_{j+1} = S_j + h_a p\{M(1-\theta_{s_{o,j+1}})/(1+x_{j+1}) - J\sigma_L\}, \text{ for } R=1 \tag{84}$$

or

$$S_{j+1} = S_j + h_a p\{M\sigma_s' - J(\theta_{L_{N,j+1}}-1)/(2-x_{j+1})\}, \text{ for } R=N-2 \tag{85}$$

or

$$S_{j+1} = S_j + h_a p\{M\sigma_s' - J(\theta_{L_{N,j+1}}-1)/(1-x_{j+1})\}, \text{ for } R=N-1 \tag{86}$$

(c) If $3/4 < x_{j+1} \leq 1$, we use

$$S_{j+1} = S_j + h_a p\{M\sigma_s - J\sigma_L'\}, \text{ for } 2 \leq R \leq N-3 \tag{87}$$

or

$$S_{j+1} = S_j + h_a p\{(M/x_{j+1})(1-\theta_{s_{o,j+1}}) - J\sigma_L'\}, \text{ for } R=0 \tag{88}$$

or

$$S_{j+1} = S_j + h_a p\{M(1-\theta_{s_{o,j+1}})/(1+x_{j+1}) - J\sigma_L'\}, \text{ for } R=1 \tag{89}$$

or

$$S_{j+1} = S_j + h_a p\{M\sigma_s - J(\theta_{L_{N,j+1}}-1)/(2-x_{j+1})\}, \text{ for } R=N-2 \tag{90}$$

or

$$S_{j+1} = S_j + h_a p\{M\sigma_s - J(\theta_{L_{N,j+1}}-1)/b\}, \text{ for } R=N-1 \tag{91}$$

where $b = 1/4$

<u>Tridiagonal Matrix or Jacobi Forms of Finite Difference Equations for Temperature</u>

Each of the groups of finite difference equations for temperature that describe both the pre-solidification and the post-solidification problems can be arranged in Jacobi or tridiagonal matrix equations of the form

$$\begin{aligned} B_o\theta_{o,j+1}+C_o\theta_{1,j+1} &= d_o \\ A_i\theta_{i-1,j+1}+B_i\theta_{i,j+1}+C_i\theta_{i+1,j+1} &= d_i, \text{ for } 1 \leq i \leq N-1 \\ A_N\theta_{N-1,j+1}+B_N\theta_{N,j+1} &= d_N \end{aligned} \tag{92}$$

where A_i, B_i, C_i, and d_i are constants obtainable from the difference equations themselves. Note that in using equation (92), we are calculating $\theta_{i,j+1}$ for the (j+1)st time step with the assumption that $\theta_{i,j}$ for the jth time step is known for every i. Thus, for the pre-solidification problem,

equation (15) and its boundary and initial conditions 15(i) to 15(iii) can be rearranged into equation (93)

$$(\theta_{Lo})_{o,j+1} = (f_1)_{j+1}/T_e$$

$$-\tfrac{1}{2}p(\theta_{Lo})_{i-1,j+1}+(1+p)(\theta_{Lo})_{i,j+1}-\tfrac{1}{2}p(\theta_{Lo})_{i+1,j+1}$$

$$= \tfrac{1}{2}p(\theta_{Lo})_{i-1,j}+(1-p)(\theta_{Lo})_{i,j}+p/2(\theta_{Lo})_{i+1,j}$$

$$\text{for } 1 \leq i \leq N-1 \qquad (93)$$

$$(\theta_{Lo})_{N,j+1} = (f_2)_{j+1}/T_e$$

so that for the (j+1)st time step, the coefficients of equation (92) take on the values in equation (93) of

$$B_o = 1$$

$$C_o = 0 \; ; \; d_o = (f_1)_{j+1}/T_e$$

$$A_i = -\tfrac{1}{2}p \;, \text{ for } 1 \leq i \leq N-1$$

$$B_i = 1+p, \quad \text{for } 1 \leq i \leq N-1$$

$$C_i = -\tfrac{1}{2}p, \quad \text{for } 1 \leq i \leq N-1$$

$$d_i = \tfrac{1}{2}p(\theta_{Lo})_{i-1,j} + (1-p)(\theta_{Lo})_{i,j}$$

$$+ \tfrac{1}{2}p(\theta_{Lo})_{i+1,j} \quad \text{for } 1 \leq i \leq N-1$$

d_i is easily obtained since $(\theta_{Lo})_{i,j}$ is known for every i for the jth time step. The above equations apply for $0 \leq \tau < \tau_o^*$.

For the post-solidification problem, we consider the equations according to the way in which they were grouped in the previous section. Thus for the solid phase, for $\tau_o \geq \tau_o^*$ or $\tau \geq 0$,(i) if $R(j+1) - R(j) = 0$, then

(a) if $R(j+1) = 1$, equation (48) and the boundary condition (66) give

$$B_o\theta_{s_{o,j+1}} = d_o$$

$$A_R\theta_{s_{R-1,j+1}} + B_R\theta_{s_{R,j+1}} = d_R \tag{94}$$

where $B_o = 1$

$C_o = 0$

$d_o = (f_1)_{j+1}/T_e$

$A_R = -\dfrac{2\lambda p x_{j+1}}{1+x_{j+1}}$; $B_R = 2\lambda p + x_{j+1}$

and

$$d_R = x_{j+1}\theta_{s_{R,j}} + \frac{2\lambda p}{1+x_{j+1}}.$$

(b) if $R(j+1) \geq 2$, the boundary condition (66) and equations (49) and (50) give

$$B_o\theta_{s_{o,j+1}} = d_o$$

$$A_i\theta_{s_{i-1,j+1}} + B_i\theta_{s_{i,j+1}} + C_i\theta_{s_{i+1,j+1}} = d_i, \text{ for } 1 \leq i \leq R-1 \tag{95}$$

$$A_R\theta_{s_{R-1,j+1}} + B_R\theta_{s_{R,j+1}} = d_R$$

where $B_o = 1$, $C_o = 0$, $d_o = (f_1)_{j+1}/T_e$

$A_i = -\lambda p/2$ for $1 \leq i \leq R-1$

$B_i = 1 + \lambda p$ for $1 \leq i \leq R-1$

$C_i = -\lambda p/2$ for $1 \leq i \leq R-1$

$d_i = \frac{1}{2}\lambda p\theta_{s_{i-1,j}} + (1-\lambda p)\theta_{s_{i,j}} + \frac{1}{2}\lambda p\theta_{s_{i+1,j}}$

for $1 \leq i \leq R-1$

$$A_R = \frac{-2\lambda p x_{j+1}}{1+x_{j+1}}$$

$$B_R = 2\lambda p + x_{j+1} \; ; \; d_R = x_{j+1}\theta_{s_{R,j}} + 2\lambda p/(1+x_{j+1})$$

(ii) if $R(j+1) - R(j) = 1$, then

(a) if $R(j+1) = 1$, boundary condition equation (66) and equation (51) give

$$B_o\theta_{s_{o,j+1}} = d_o$$

$$A_R\theta_{s_{R-1,j+1}} + B_R\theta_{s_{R,j+1}} = d_R$$

where $B_o = 1, \; d_o = (f_1)_{j+1}/T_e, \quad C_o = 0$ (96)

$$A_R = \frac{-2\lambda p x_{j+1}}{1+x_{j+1}}, \; B_R = 2\lambda p + \frac{x_{j+1}}{a_R} = 2\lambda p + 1 - x_j + x_{j+1}$$

$$d_R = \frac{2\lambda p}{1+x_{j+1}} + \frac{x_{j+1}}{a_R} = \frac{2\lambda p}{1+x_{j+1}} + 1 - x_j + x_{j+1}$$

(b) if $R(j+1) = 2$, equations (52) and (53) together with the boundary condition give

$$B_o\theta_{s_{o,j+1}} = d_o$$

$$A_{R-1}\theta_{s_{R-2,j+1}} + B_{R-1}\theta_{s_{R-1,j+1}} + C_{R-1}\theta_{s_{R,j+1}} = d_{R-1}$$

$$A_R\theta_{s_{R-1,j+1}} + B_R\theta_{s_{R,j+1}} = d_R$$

where $B_o = 1; \; d_o = (f_1)_{j+1}/T_e; \; C_o = 0$ (97)

$$A_{R-1} = -\lambda p; \quad B_{R-1} = 1 + 2\lambda p; \quad C_{R-1} = -\lambda p; \quad d_{R-1} = \theta_{s_{R-1,j}}$$

$$A_R = \frac{-2\lambda p x_{j+1}}{1+x_{j+1}} \; ; \quad B_R = 2\lambda p + \frac{x_{j+1}}{a_R} = 2\lambda p + 1 - x_j + x_{j+1}$$

$$d_R = \frac{2\lambda p}{1+x_{j+1}} + \frac{x_{j+1}}{a_R} = \frac{2\lambda p}{1+x_{j+1}} + 1 - x_j + x_{j+1}$$

(c) if $R(j+1) \geq 3$, equations (54), (55), and (56) together with the boundary condition give

$$\begin{aligned}
B_o\theta_{s_{o,j+1}} &= d_o \\
A_i\theta_{s_{i-1,j+1}} + B_i\theta_{s_{i,j+1}} + C_i\theta_{s_{i+1,j+1}} &= d_i \text{ for } 1 \leq i \leq R-2 \\
A_{R-1}\theta_{s_{R-2,j+1}} + B_{R-1}\theta_{s_{R-1,j+1}} + C_{R-1}\theta_{s_{R,j+1}} &= d_{R-1} \qquad (98) \\
A_R\theta_{s_{R-1,j+1}} + B_R\theta_{s_{R,j+1}} &= d_R
\end{aligned}$$

where B_o, C_o, d_o, A_{R-1}, B_{R-1}, C_{R-1}, d_{R-1}, A_R, B_R and d_R have the same values as in part (b) above and

$$\begin{aligned}
A_i &= -\tfrac{1}{2}\lambda p \quad \text{for} \quad 1 \leq i \leq R-2 \\
B_i &= 1+\lambda p \quad \text{for} \quad 1 \leq i \leq R-2 \\
C_i &= -\tfrac{1}{2}\lambda p \quad \text{for} \quad 1 \leq i \leq R-2 \\
d_i &= \tfrac{1}{2}\lambda p\theta_{s_{i-1,j}} + (1-\lambda p)\theta_{s_{i,j}} + \tfrac{1}{2}\lambda p\theta_{s_{i+1,j}} \text{ for } 1 \leq i \leq R-2
\end{aligned}$$

(iii) If $R(j+1) - R(j) = 2$, then

(a) if $R(j+1) = 2$, equations (57), (58), and (66) give

$$\begin{aligned}
B_o\theta_{s_{o,j+1}} &= d_o \\
A_{R-1}\theta_{s_{R-2,j+1}} + B_{R-1}\theta_{s_{R-1,j+1}} + C_{R-1}\theta_{s_{R,j+1}} &= d_{R-1} \qquad (99) \\
A_R\theta_{s_{R-1,j+1}} + B_R\theta_{s_{R,j+1}} &= d_R
\end{aligned}$$

where B_o, d_o, and C_o have the same values as in part (ii) above;

$$A_{R-1} = -a_{R-1}\lambda p = -\lambda p(1+x_{j+1})/(2-x_j+x_{j+1})$$

$$B_{R-1} = 1+2\lambda p a_{R-1} = 1+2\lambda p(1+x_{j+1})/(2-x_j+x_{j+1})$$

$$C_{R-1} = -\lambda p a_{R-1} = -\lambda p(1+x_{j+1})/(2-x_j+x_{j+1})$$

$$d_{R-1} = 1;\ A_R = \frac{-2\lambda p x_{j+1}}{1+x_{j+1}};\ B_R = 2\lambda p + \frac{x_{j+1}}{a_R} = 2\lambda p+2-x_j+x_{j+1}$$

$$d_R = \frac{2\lambda p}{1+x_{j+1}} + \frac{x_{j+1}}{a_R} = \frac{2\lambda p}{1+x_{j+1}} + 2 - x_j + x_{j+1}$$

(b) if $R(j+1) = 3$, equations (59) to (60) plus the boundary condition equation (66) give

$$\begin{aligned} B_o\theta_{s_{o,j+1}} &= d_o \\ A_{R-2}\theta_{s_{R-3,j+1}}+B_{R-2}\theta_{s_{R-2,j+1}}+C_{R-2}\theta_{s_{R-1,j+1}} &= d_{R-2} \qquad (100) \\ A_{R-1}\theta_{s_{R-2,j+1}}+B_{R-1}\theta_{s_{R-1,j+1}}+C_{R-1}\theta_{s_{R,j+1}} &= d_{R-1} \\ A_R\theta_{s_{R-1,j+1}}+B_R\theta_{s_{R,j+1}} &= d_R \end{aligned}$$

where B_o, C_o, d_o, A_{R-1}, B_{R-1}, C_{R-1}, d_{R-1}, A_R, B_R, d_R have the same values as in part (a) above.

$$A_{R-2} = -\lambda p;\ B_{R-2} = 1+2\lambda p;\ C_{R-2} = -\lambda p;\ d_{R-2} = \theta_{s_{R-2,j}}$$

(c) if $R(j+1) \geq 4$, equations (62) to (65) and equation (66) give

$$\begin{aligned} B_o\theta_{s_{o,j+1}} &= d_o \\ A_i\theta_{s_{i-1,j+1}}+B_i\theta_{s_{i,j+1}}+C_i\theta_{s_{i+1,j+1}} &= d_i \qquad 1 \leq i \leq R-3 \\ A_{R-2}\theta_{s_{R-3,j+1}}+B_{R-2}\theta_{s_{R-2,j+1}}+C_{R-2}\theta_{s_{R-1,j+1}} &= d_{R-2} \qquad (101) \end{aligned}$$

$$A_{R-1}\theta_{s_{R-2,j+1}}+B_{R-1}\theta_{s_{R-1,j+1}}+C_{R-1}\theta_{s_{R-1,j+1}} = d_{R-1}$$

$$A_R\theta_{s_{R-1,j+1}} + B_R\theta_{s_{R,j+1}} = d_R$$

where B_o, C_o, d_o, A_{R-2}, B_{R-2}, C_{R-2}, d_{R-2}, A_{R-1}, B_{R-1}, C_{R-1}, d_{R-1}, A_R, d_R have the same values as in part (b) above, and

$A_i = -\frac{1}{2}\lambda p$ for $1 \leq i \leq R-3$

$B_i = 1+2\lambda p$ for $1 \leq i \leq R-3$

$C_i = -\frac{1}{2}\lambda p$ for $1 \leq i \leq R-3$

$d_i = \frac{1}{2}\lambda p\theta_{s_{i-1,j}}+(1-\lambda p)\theta_{s_{i,j}}+\frac{1}{2}\lambda p\theta_{s_{i+1,j}}$ for $1 \leq i \leq R-3$

For the liquid phase, if

(a) $0 \leq R(j+1) \leq N-3$, then equations (69) to (71) give

$$B_{R+1}\theta_{L_{R+1,j+1}}+C_{R+1}\theta_{L_{R+2,j+1}} = d_{R+1}$$

$$A_i\theta_{L_{i-1,j+1}}+B_i\theta_{L_{i,j+1}}+C_i\theta_{L_{i+1,j+1}} = d_i \text{ for } R+2 \leq i \leq N-1 \tag{102}$$

where

$B_{R+1} = (2-x_{j+1})(1+2p-x_j)$

$C_{R+1} = -2p(1-x_{j+1})$

$d_{R+1} = (2-x_{j+1})(1-x_{j+1})\theta_{L_{R+1,j}}+2p$

$A_i = -\frac{1}{2}p$ for $R+2 \leq i \leq N-1$

$B_i = 1+p$ for $R+2 \leq i \leq N-1$

$C_i = -\frac{1}{2}p$ for $R+2 \leq i \leq N-1$

$B_N = 1$

$d_N = (f_2)_{j+1}/T_e$

(b) if $R(j+1) = N-2$, equations (72) and (73) give

$$B_{R+1}\theta_{L_{R+1,j+1}} + C_{R+1}\theta_{L_{R+2,j+1}} = d_{R+1}$$
$$B_N\theta_{L_{N,j+1}} = d_N \qquad (103)$$

where B_{R+1}, C_{R+1}, d_{R+1}, B_N and d_N have the same values as in part (a) above.

(c) if $R(j+1) = N-1$, then

$$\theta_{L_{N,j+1}} = (f_2)_{j+1}/T_e \qquad (104)$$

and the temperature profile for $0 \leq i \leq N-1$ is obtained from the solid phase.

Solutions of Governing Finite Difference Equations

Each of the tridiagonal matrix equations (93) to (103) has a solution given by the solution of equation (92) as follows:

$$\theta_{N,j+1} = q_N$$
$$\theta_{i,j+1} = q_i - b_i\theta_{i+1,j+1} \text{ for } 0 \leq i \leq N-1 \qquad (105)$$

where $q_o = \frac{d_o}{B_o}$; $b_o = C_o/B_o$

$$q_i = (d_i - A_i q_{i-1})/(B_i - A_i b_{i-1}) \text{ for } 1 \leq i \leq N$$

and $b_i = C_i/(B_i - A_i b_{i-1})$ for $1 \leq i \leq N-1$

Equation (105) applies as it is to the pre-solidification problem for $0 \leq \tau_o \leq \tau_o^*$. For the post-solidification problem, equation (105) becomes for the solid phase

$$\theta_{s_{R,j+1}} = q_R$$
$$\theta_{s_{i,j+1}} = q_i - b_i\theta_{s_{i+1,j+1}}, \text{ for } 0 \leq i \leq R-1 \qquad (106)$$

where $q_o = \frac{d_o}{B_o} = d_o$; $b_o = C_o/B_o = 0$

$$q_i = (d_i - A_i q_{i-1})/(B_i - A_i b_{i-1}) \quad \text{for } 1 \leq i \leq R$$

and $$b_i = C_i/(B_i - A_i b_{i-1}) \quad \text{for } 1 \leq i \leq R-1$$

and for the liquid phase, it becomes

$$\theta_{L_{N,j+1}} = q_N \tag{107}$$

$$\theta_{L_{i,j+1}} = q_i - b_i \theta_{L_{i+1,j+1}} \quad \text{for } R+1 \leq i \leq N-1$$

where $q_N = (f_2)_{j+1}/T_e$

$$q_i = (d_i - A_i q_{i-1})/(B_i - A_i b_{i-1}) \quad \text{for } R+2 \leq i \leq N$$

$$b_i = C_i/(B_i - A_i b_{i-1}) \quad \text{for } R+2 \leq i \leq N-1$$

$$q_{R+1} = d_{R+1}/B_{R+1} \quad \text{and} \quad b_{R+1} = C_{R+1}/B_{R+1}$$

We start at time $\tau_o = 0$ to solve the pre-solidification problem. Thus, for $j=0$, $(\theta_{Lo})_{i,o} = T_a/T_e$ for $0 \leq i \leq N$. Thus we can find the temperature profile, $(\theta_{Lo})_{i,1}$, for every i by using equation (105) since all the constants are now known. For the next time step (i.e. $j=1$), we calculate $(\theta_{Lo})_{i,2}$ by using the values of $(\theta_{Lo})_{i,1}$, which we have found, to calculate the constants to be used in equation (105). Thus we continue calculating $(\theta_{Lo})_{i,j+1}$, (for $0 \leq i \leq N$), for each given j until $j = j^*$ such that, at the bottom plate, $(\theta_{Lo})_{o,j^*} \geq 1.0$ and $(\theta_{Lo})_{o,j^*+1} < 1$. At such a time we have reached τ_o^*. After j^* is located, we calculate τ_o^* by the equation

$$\tau_o^* = k_a(j^* + r) \tag{108}$$

where $r = \dfrac{(\theta_{Lo})_{o,j^*} - 1.0}{(\theta_{Lo})_{o,j^*} - (\theta_{Lo})_{o,j^*+1}}$ approximates the fraction of full time increment, which is needed to cool the temperature of the bottom plate from $(\theta_{Lo})_{o,j^*}$ to 1.0. Note that the dimensionless equilibrium temperature of solidification of n-hexadecane is equal to 1.0. To find the temperature profile of the liquid at τ_o^*, we take the temperature of the bottom plate to be 1.0 at τ_o^*, i.e. $\theta_{Lo}(0,\tau_o^*) = 1.0$ and instead of taking time increment to be k_a, we take the fraction $k_a new = k_a r < k_a$ to be our new time step, and therefore the new value for p for this step is $p_{new} = pr$. The value for r and the known temperature profiles $(\theta_{Lo})_{i,j^*}$ are now used in equation (109) to calculate $\theta_{Lo}(ih_a, \tau_o^*)$:

$$(\theta_{Lo})_{i,j+1} = rp(\theta_{Lo})_{i-1,j^*} + (1-2rp)(\theta_{Lo})_{i,j^*} + rp(\theta_{Lo})_{i+1,j^*} \tag{109}$$

We now know τ_o^* and the temperature profile $\theta_{Lo}(ih_a,\tau_o)$ for the pre-solidification problem for $0 \leq i \leq N$ and $0 \leq \tau_o \leq \tau_o^*$. We now start the calculations for the post-solidification problem.

To start, set $\tau=0$. This corresponds to $\tau = \tau_o - \tau_o^* = 0$ at $\tau_o = \tau_o^*$. We start off again at $j = 0$ corresponding to $\Delta\tau$ increments. The first time step for the post-solidification problem is a full time step. Also the first value used for p corresponds to a full time step. These values, together with $\theta_{Lo}(ih_a,\tau_o^*)$ which we have calculated are used in the first

calculations. The temperature of the bottom plate is taken as the temperature of the solid phase at $i = 0$. We thus have the first estimates of temperature profiles in the liquid and solid phases at $i = 0$. We now proceed to estimate $R(j+1)$ and x_{j+1} and to calculate S_{j+1} as follows.

<u>Estimation of R_{j+1}, x_{j+1} and Calculation of S_{j+1}.</u>

First of all, we set $S_j = 0$, $R(j) = 0$, $x_j = 0$, at $j = 0$. Next we assume,

$$S'_{j+1} = \tfrac{1}{2} h_a \tag{110}$$

S'_{j+1} is the first approximation of S_{j+1}. Since $R(j+1)$ is an integer and $0.0 \leq x_{j+1} \leq 1.0$, we can find $R(j+1)$ and x_{j+1} from S'_{j+1} since $S'_{j+1} = h_a(R_{j+1} + x_{j+1})$. (77)

We now have $R(j+1)$ and x_{j+1} to use in starting our more accurate calculations. We may now rename S'_{j+1} as $S_{j+1}(\text{old})$. Using the values of $R(j+1)$ and x_{j+1} which we now have, we can go back to calculate new temperature profiles employing whichever of equations (94) to (102) applies, as determined by the values of $R(j+1)-R(j)$, x_{j+1}, and $R(j+1)$. We also calculate a new value for S_{j+1}, (which we will call $S_{j+1}(\text{new})$), by using whichever of equations (78) to (91) that applies as determined by values of $R(j+1)$, x_{j+1}, and of $R(j+1)-R(j)$. We check $S_{j+1}(\text{new})$ against $S_{j+1}(\text{old})$ and if the absolute value of their difference exceeds a certain number, ε, determined by error analysis, we set $S'_{j+1} = \tfrac{1}{2}\{S_{j+1}(\text{old})+S_{j+1}(\text{new})\}$. Again we use

S'_{j+1} in equation (77) to find R(j+1) and x_{j+1} which are to be used to find new temperature profiles and new S_{j+1}. Thus in summary, the steps are outlined below.

(1) Use equation (110) to find S'_{j+1} for the first full time step.

(2) Set S'_{j+1} equal to S_{j+1}(old).

(3) Use equation (77) to calculate R(j+1) and x_{j+1} noting that R is an integer between 0 and N and that $0 \leq x_{j+1} \leq 1$.

(4) Use values which have been found for R and x_{j+1} in the appropriate equations to calculate new temperature profiles.

(5) Calculate S_{j+1}(new) using whichever of equations (78) to (91) that applies.

(6) If $\text{abs}\{S_{j+1}(\text{old}) - S_{j+1}(\text{new})\} > \varepsilon$, set S'_{j+1} equal to $\frac{1}{2}\{S_{j+1}(\text{new}) + S_{j+1}(\text{old})\}$ and repeat steps (2) to (6) until $\text{abs}\{S_{j+1}(\text{old}) - S_{j+1}(\text{new})\} \leq \varepsilon$. S_{j+1} is now known for this time step and $S_{j+1} = S_{j+1}(\text{new})$, and $\Delta S_{j+1} = S_{j+1} - S_j$. The first time step is now taken as fully calculated. We return to more time steps. ε is calculated from analysis of truncation errors of the finite difference equations.

For the second time step, set ΔS_{j+1}, found from the previous time step, equal to ΔS_j, and let the new ΔS_{j+1} to be used for our new time step be $\Delta S_{j+1} = (\frac{\Delta S}{k_a})_j k_a$. Also set the S_{j+1}, x_{j+1}, R_{j+1} from the first time step equal to S_j, x_j, and R_j, respectively. Therefore, for the second time

step, the first approximation for S_{j+1} is $S'_{j+1} = S_j + \Delta S_{j+1}$. S'_{j+1} is now used to repeat steps (2) to (6) stated previously until the second time step is fully calculated. For more time steps, we proceed as before by setting the S_{j+1}, x_{j+1}, and R_{j+1} from our previous time step equal to S_j, x_j, and R_j, respectively, and by obtaining our new ΔS_{j+1} from the relation

$$\Delta S_{j+1} = (\Delta S_j)\left(\frac{\text{magnitude of new time increment}}{\text{magnitude of previous time increment}}\right).$$

Then $S'_{j+1} = S_j + \Delta S_{j+1}$, which we then use in steps (2) to (6) outlined previously. We continue this sort of calculation until the entire content of the cell is frozen, when $S_{j+1} = 1.0$. Thus S_{j+1} is calculated by iteration. S_{j+1} and the temperature profiles are dimensionless, but are easily converted into dimensioned values.

Stability Criteria for Governing Finite Difference Equations

By definition $R(j+1)$ is a non-negative integer between 0 and N where N is the total number of nodes in the space direction along z. Thus $R(j+1)$ is an integer such that $0 \leq R \leq N$. Also x_{j+1} is by definition a fraction between 0 and 1. It is also non-negative. Therefore, x_{j+1} must lie in the region $0 \leq x_{j+1} \leq 1$. $R(j+1)$ and x_{j+1} must satisfy these conditions lest there arise instability in the solution of the difference equations. $R(j)$ and x_j must also satisfy the same conditions as $R(j+1)$ and x_{j+1}. If the coefficient of any temperature $\theta_{i,j}$ or $\theta_{i,j+1}$ were to oscillate freely

between positive and negative values, the solutions to the difference equations would become unstable. Thus, for stability, we insist that the coefficients of $\theta_{i,j}$ or $\theta_{i,j+1}$ retain the same sign throughout the solution. Thus if the coefficient of $\theta_{i,j}$ is positive for any i,j, it must stay greater than or equal to zero for any other i,j. If it is negative for any i,j, it must stay less than or equal to zero for any other i,j. These conditions must be particularly so since the temperatures T and Te which give θ by the equation $\theta = T/Te$ are defined on the absolute temperature scale and must therefore each be non-negative for any i,j. Thus $\theta_{i,j}$ must be non-negative. With these points in mind, we check each of the equations that give the temperature profiles $\theta_{i,j+1}$ and impose on it the condition that none of the coefficients may change sign. On checking equations (48) through (91) we find that for stable solutions the following conditions must be satisfied:

$$0 \leq x_j \leq 1 \qquad (111(a))$$

$$0 \leq x_{j+1} \leq 1 \qquad (111(b))$$

R must be an integer such that $0 \leq R(j) \leq N$ (112(a))

and $0 \leq R(j+1) \leq N$ (112(b))

$$0 \leq \theta_{i,j} \leq 1 \qquad (113)$$

$$1 - \lambda p \geq 0 \qquad (114)$$

$$1 - p \geq 0 \qquad (115)$$

$$S_{j+1} - S_j \geq 0 \qquad (116)$$

Equation (116) merely states that if a position node, i, has solidified at the jth time step, it should stay solidified during the (j+1)st time step since net heat is being removed all the time from the system. $p = k_a/h_a^2$ and p is positive for positive time step. From equation (109), $1 - 2rp \geq 0$ (117) for stable solutions. Since $0 \leq r \leq 1$, the maximum value is $r = 1$. Therefore, equation (117) is satisfied if

$$1 - 2p \geq 0 \tag{118}$$

Therefore, the maximum value of p above which the solutions become unstable and below which the solutions are stable is given by equating the left hand side of either equation (114) or equating (118) to zero. Which of the two values of p to accept as the acceptable maximum depends on the value of λ. λ is non-negative since $\lambda = \alpha_s/\alpha_L$. Thus,

$$p_{max,1} = 1/\lambda \tag{119(a)}$$

and

$$p_{max,2} = 1/2 \tag{119(b)}$$

Thus, if λ is less than 2, then $p_{max,1}$ is greater than ½ and $p_{max,2}$ is the acceptable p_{max} since it satisfies both equation (114) and (118). If λ is greater than 2, then $p_{max,1}$ is the acceptable p_{max} since it satisfies both equations (114) and (118) in this case. Having selected p_{max}, we now know that any value of p that satisfies the inequality equation $0 < p \leq p_{max}$ will give stable solutions. Thus if h_a has been chosen and fixed, the k_a's that will give stable solutions are given by the inequality equation,

$0 < k_a \leq k_{a_{max}}$ where $k_{a_{max}}$ is given by $k_{a_{max}} = h_a^2/\lambda$ or $k_{a_{max}} = \frac{1}{2}h_a^2$, depending on whether λ is greater than 2 or less than 2.

EXPERIMENTAL EQUIPMENT AND PROCEDURE

A short description of the main components of the experimental equipment and an account of the experimental procedure are given in this section.

Equipment

The principal element of the equipment was the test cell. The auxiliary elements were thermocouple assembly, one 4-channel-continuous-temperature recorder, a power-driven pump and a refrigerator. Each element is given a concise description below.

Test Cell: The test cell (Fig. 9) had a constant square cross-section of external dimensions 5 in. and overall height of 3-15/32 in. It was composed of a cooling chamber which was sealed with soft solder to one face of an 1/8-in.-thick copper plate (the bottom plate or cold plate); a plexi-glass frame 1-15/32 in. high which was sealed with epoxy to the bottom plate to form the chamber in which the test material, n-hexadecane, would be contained; and another 1/8-in.-thick copper plate (the top plate) which was in turn attached to the other end of the plexi-glass frame by means of bolts and screws. Figure (10) shows the exploded view of the test cell.

The cooling chamber (Fig. 11) was constructed from ¼-in.-thick copper plates. The void of the cooling chamber had a square base of 4½-in. sides and a height of 1½ in.

Figure 9. Test cell.

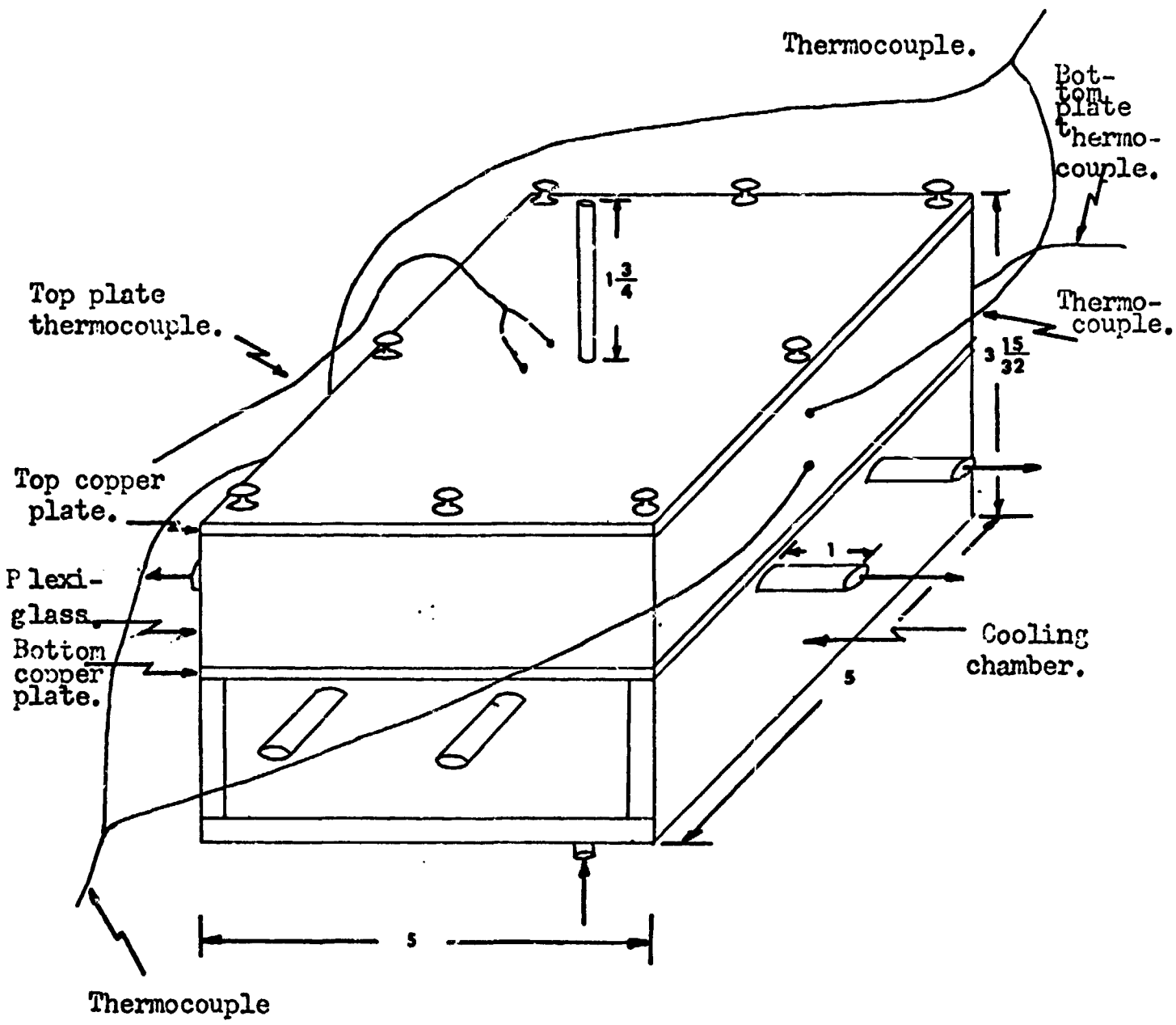

TEST CELL

Dimensions in inches
Scale 1:2

Figure 10. Exploded view of test cell.

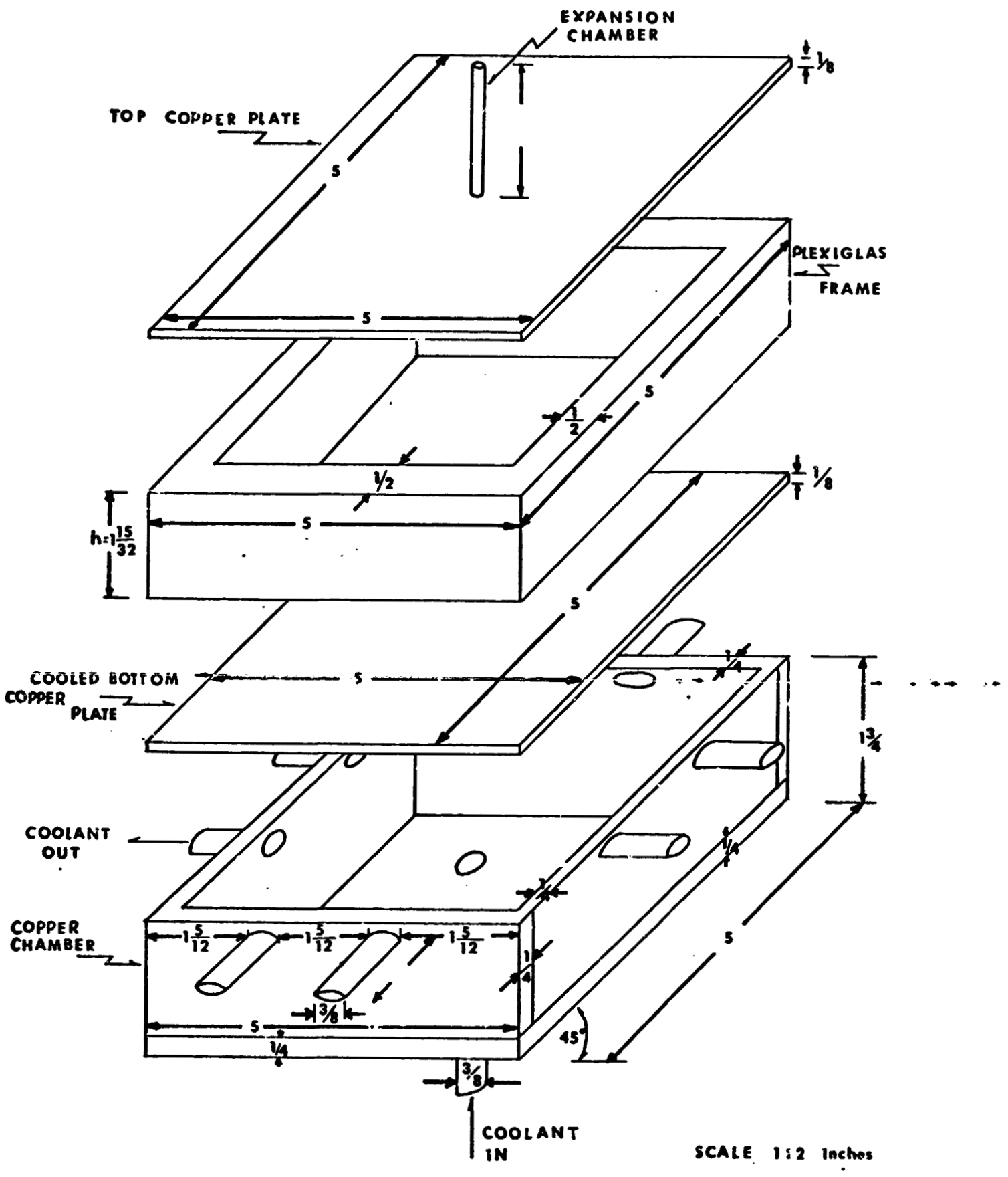
EXPANSION CHAMBER
TOP COPPER PLATE
PLEXIGLAS FRAME
COOLED BOTTOM COPPER PLATE
COOLANT OUT
COPPER CHAMBER
COOLANT IN
SCALE 1:2 Inches

Figure 11. Cooling chamber.

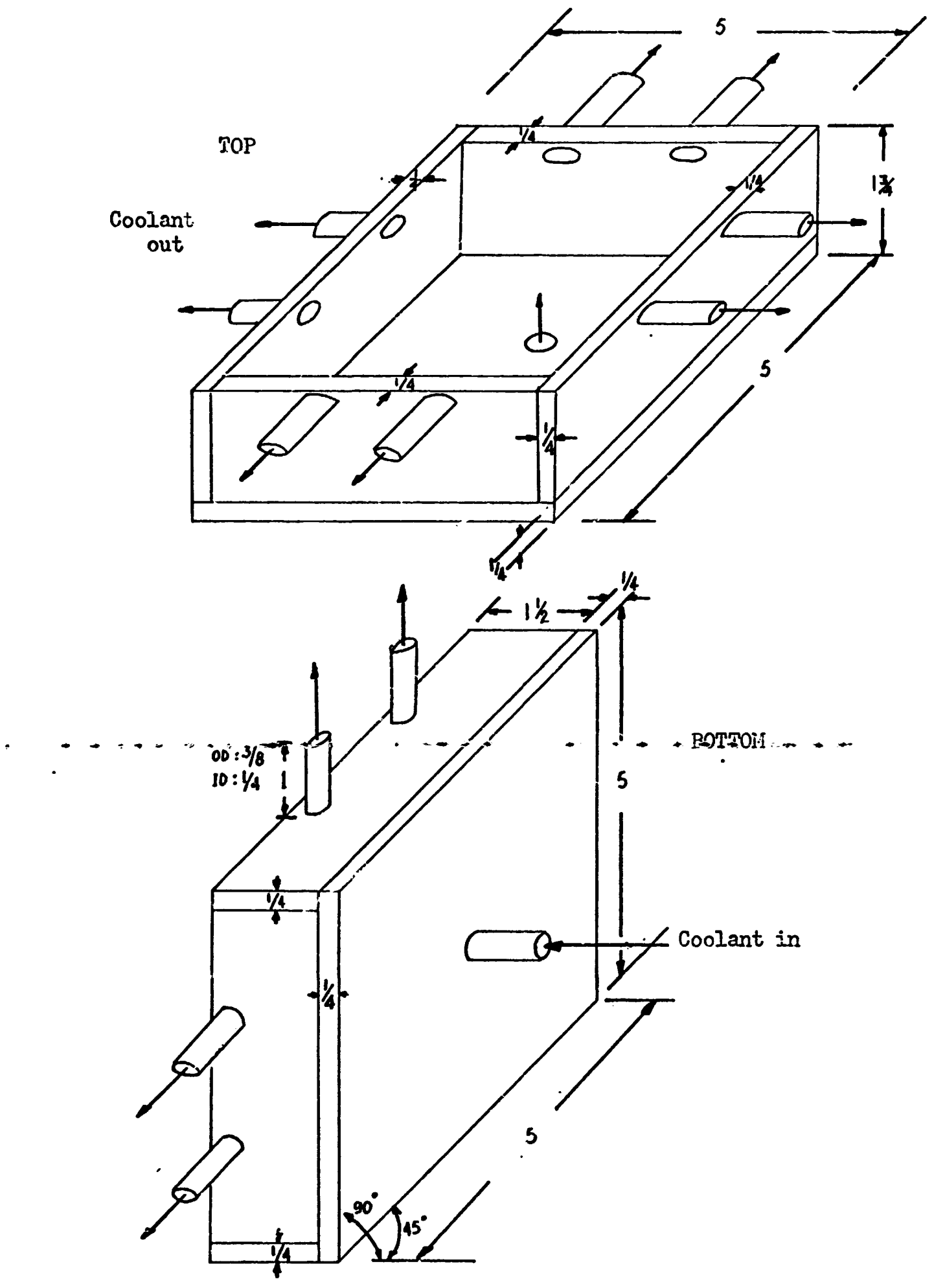

COOLING CHAMBER

Scale 1:2
Dimensions in inches

Externally, the cooling chamber had a square base of 5-in. sides and a height of 1-3/4 in. On each of its vertical sides and very close to the bottom plate, the cooling chamber carried two equally spaced 3/8-in.-external-diameter copper tubes which served as outlets for the coolant. Each tube was 1 in. long. Thus, there were eight of these side tubes in all. Also, at the center of its base, the cooling chamber had one 3/8-in.-external-diameter copper tube which served as inlet for the coolant. This last tube was also 1 in. long. Thus, the chamber made it possible for a coolant for the bottom plate to flow in through the base tube and flow out through the eight side tubes. The coolant used was liquid methanol.

The bottom plate (Fig. 12) was simply a 5-in.-square copper plate of 1/8-in. thickness. It was soldered to the cooling chamber on one face and glued to the plexi-glass frame on the other. On the center of the face which was soldered to the plexi-glass frame it carried a copper-constantan thermocouple. The thermocouple was admitted through a hole which had been drilled on a side of the plexi-glass frame and which was thereafter sealed with epoxy resin.

The plexi-glass frame (Fig. 12) was machined out of a thick plexi-glass slab. The frame was ½-in. thick, 1-15/32-in. high and had a 5-in.-square outside cross-section. It was glued at one end to the side of the bottom plate that carried a thermocouple, with the resulting formation of

Figure 12. Plexi-glass chamber for test material.

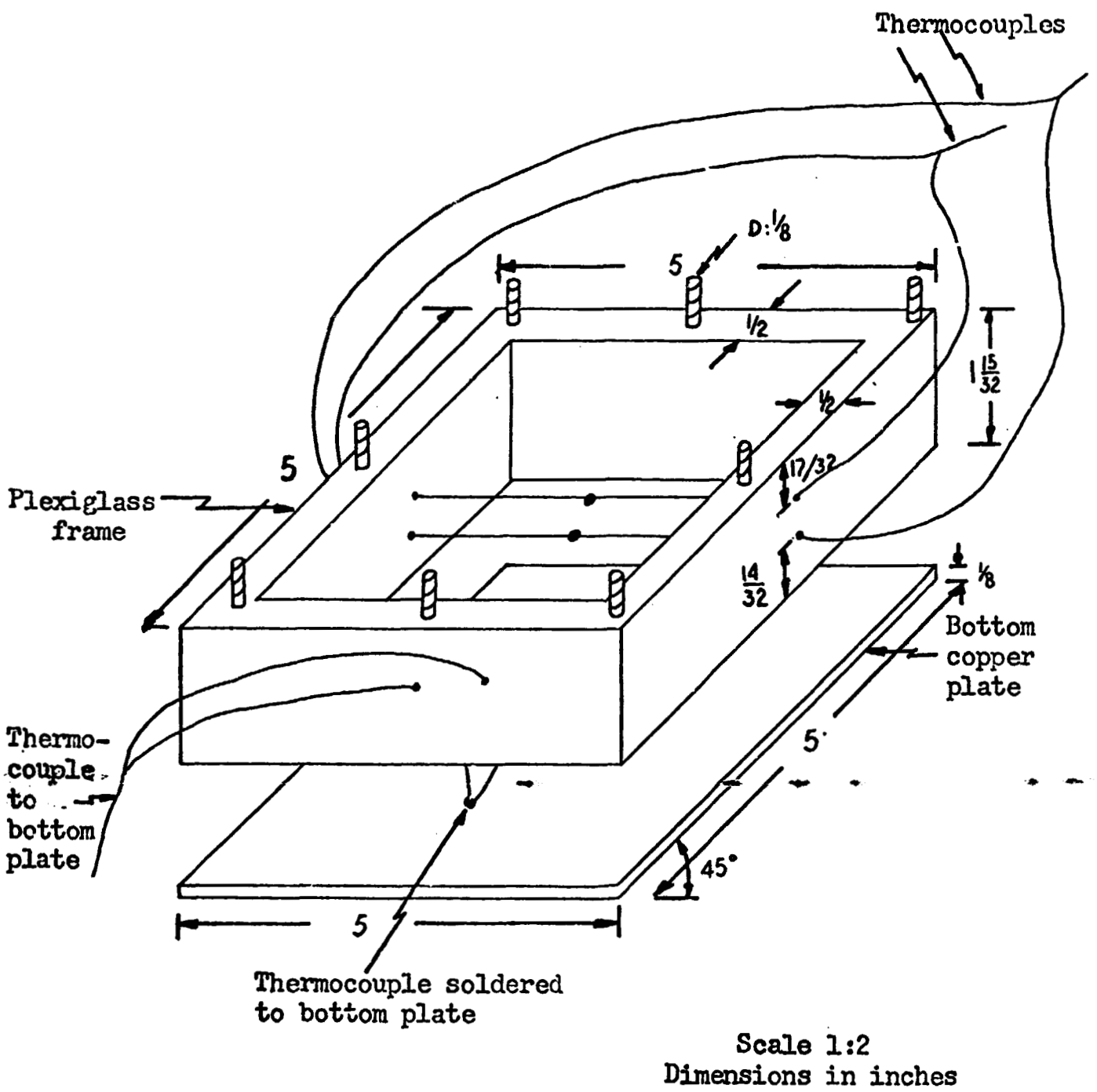

Scale 1:2
Dimensions in inches

PLEXIGLASS CHAMBER FOR TEST MATERIAL

a chamber of 4-in.-square cross-section and 1-15/32-in. height. This chamber would contain the test material and its height of 1-15/32 in. would be the height referred to as h in the present study. At the other end, the plexi-glass frame had eight screwed-in bolts with one at each corner and one at the middle of each edge. The top copper plate would be attached to the test cell by means of these bolts. The frame carried two copper-constantan thermocouples on its side at distances of 14/32 in. (or 14h/47) and 30/32 in. (or 30h/47) from the bottom plate.

The top plate (Fig. 13) was another 5-in.-square copper plate of 1/8-in. thickness. At the corners and the centers of each of its four edges, holes were drilled to receive the bolts from the plexi-glass frame. Screws would then be used to bolt the plate down on the plexi-glass frame. There were two main reasons for using bolts and screws here instead of solder seal. The first reason was that trying to seal a copper plate on to the plexi-glass frame was very difficult since the plexi-glass tended to melt before the copper plate could be hot enough to give a good seal. Although it was relatively easy to attach a copper frame by soldering on to a hot copper plate, it was not as easy to attach a copper plate by soldering it on to a hot plexi-glass frame. The second reason for using screws and bolts was to facilitate the filling and emptying of the test cell. The top plate also carried, at the center of its face, a 1-3/4-in. long copper tube of 1/16-in. internal diameter and 1/8-in. external

Figure 13. Diagram of top copper plate.

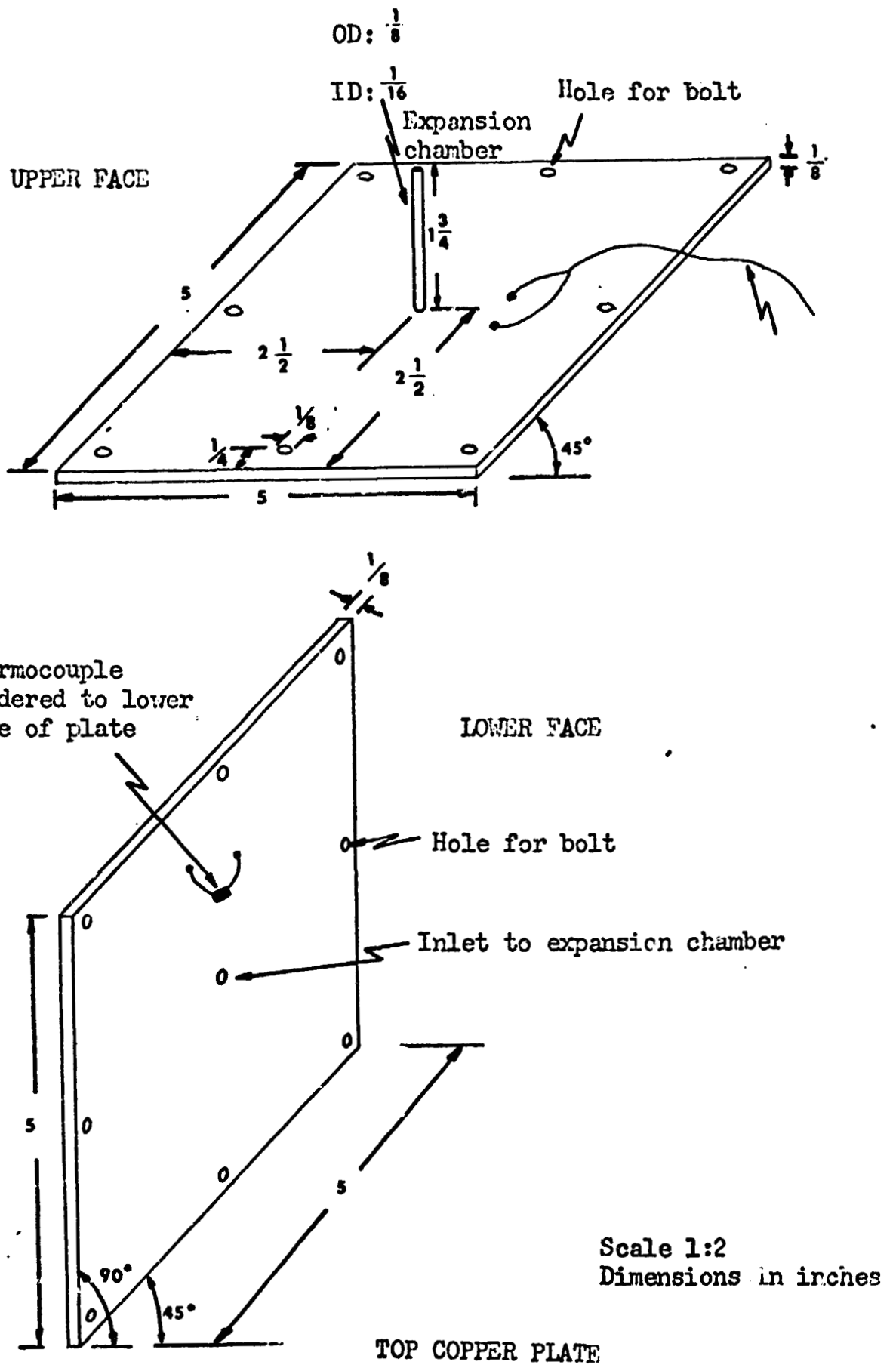
OD: 1/8
ID: 1/16
Expansion chamber
Hole for bolt
UPPER FACE
1/8
1 3/4
5
2 1/2
2 1/2
1/8
1/4
45°
5
1/8
Thermocouple soldered to lower face of plate
LOWER FACE
Hole for bolt
Inlet to expansion chamber
5
5
90°
45°
Scale 1:2
Dimensions in inches
TOP COPPER PLATE

diameter. This acted as an expansion chamber in case there was a volume increase of the test material during phase change. A copper-constantan thermocouple was passed through a hole drilled into the top plate and its junction was affixed to the inside face of the plate by soldering.

Thermocouple assembly: As was shown in the description of the test cell, the cell carried four copper-constantan thermocouples located as follows: one each at the inside faces of the bottom and top plates, a third at 14/32 in. or 14h/47 from the bottom plate, through the plexi-glass walls and the fourth at 30/32 in. or 30h/47 from the bottom plate, also through the plexi-glass walls. The other ends of the thermocouples were appropriately joined by soldering and the junctions were immersed in a mixture of ice and water in a Dewar flask to form cold junctions at 0.0°C (Fig. 14). The free ends were then connected to plugs that led into a four-channel recorder. Each of the four channels was connected to a single thermocouple.

Temperature recorder: The recorder was a 4-channel Sanborn[31] continuous recorder, Model 150-1500. Thus, each channel could record the temperature profile sensed by one thermocouple continuously on a chart as a function of time. Thus the four channels allowed the use of four thermocouples only. The Sanborn Low Level Preamplifier, Model 150-1500, which formed each channel of the recorder, was a chopper type of amplifier for measuring slowly varying direct voltages or measuring slowly varying currents by adding an external shunt

Figure 14. Thermocouple arrangement:

(a) Assemblage showing cold junction and plug for a single thermocouple.

(b) The panel of one channel of the recorder showing a socket for receiving thermocouple plug.

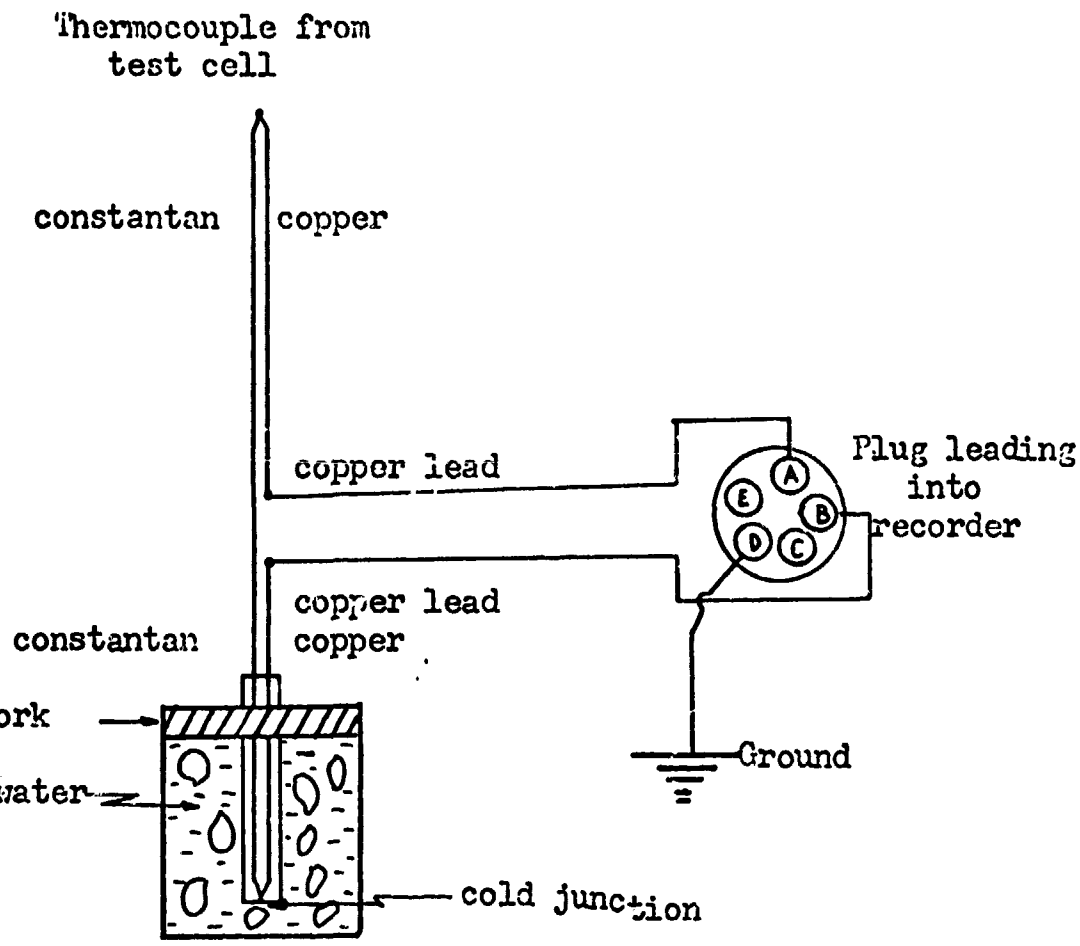

(a) THERMOCOUPLE ASSEMBLAGE

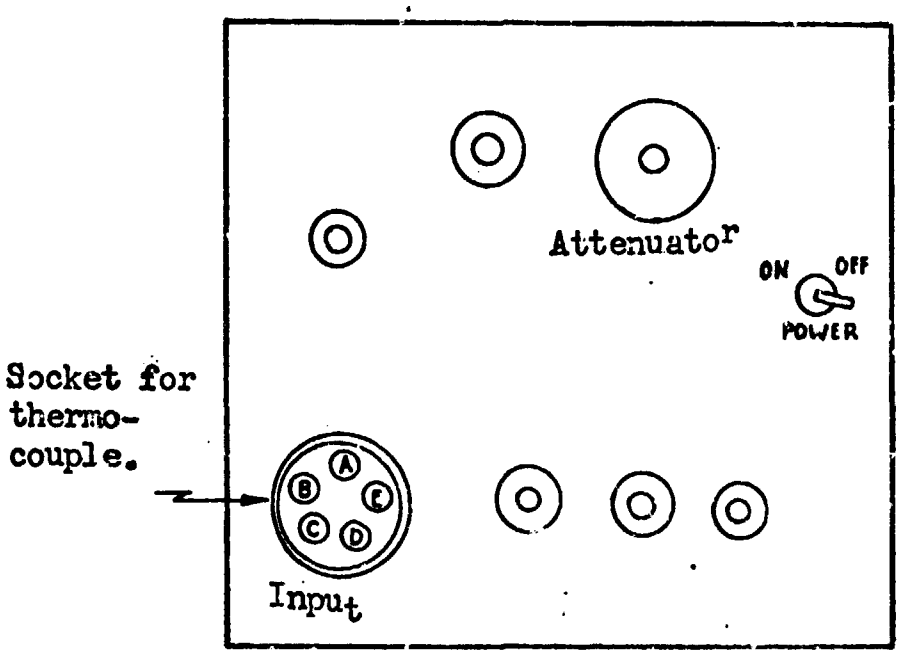

(b) THE PANNEL OF ONE CHANNEL OF THE RECORDER

resistor. The signals could be read in circuits removed from the ground by as much as 300 volts DC. It had a sensitivity of 100 microvolts per centimeter to 0.1 volt per centimeter of chart in ten steps. For instance, when calibrated at 500 microvolts per centimeter, the accuracy in reading the chart was ±0.025 millivolts. For a copper-constantan thermocouple, this corresponded to an accuracy of ±0.7°C. The speed of the chart was in the range of 0.025 millimeters per second to 10 millimeters per second arranged as follows (all units being millimeters per second):

0.025, 0.05, 0.1, 0.25, 0.5, 1, 2.5, 5, 10.

Thus, time intervals could be obtained from the speed of the charting paper.

Pump: The pump used to circulate the coolant (methanol) from the refrigerator to the test cell was a Chemical Rubber Company[32] "No-Seal" centrifugal pump, Model ABIP005N#. It operated on 115-volts, 60 cycles, alternating current only. It could attain 3000 revolutions per minute and pump from 420 gallons per hour at a head of 1 ft to 250 gallons per hour at a head of 9 ft under normal atmospheric conditions.

Refrigerator: The refrigerator for the coolant was a Bar Ray of Brooklyn, New York, Model 557T refrigerator that operated on a 60-cycle, 115-volt alternating current. It had a regulator that could be used to adjust the steady state temperature to which the refrigerant is cooled. A schematic picture of the assembled equipment is shown in Figure (15).

Figure 15. Block diagram of assembly of main experimental equipment.

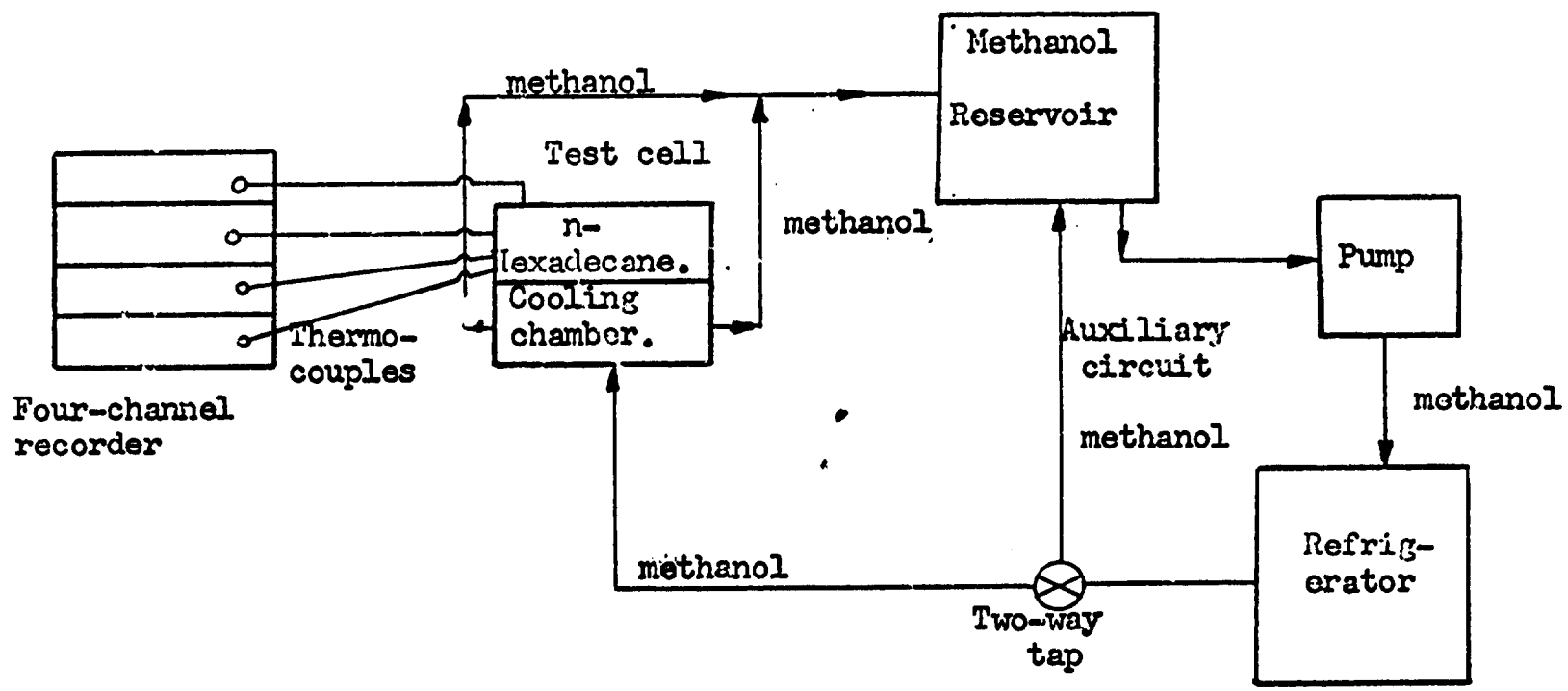

BLOCK DIAGRAM OF ASSEMBLY OF MAIN EXPERIMENTAL EQUIPMENT

Experimental Procedure

The top plate was removed from the cell, the test cell was completely filled with the test material, n-hexadecane and the top plate was replaced and bolted down by screws to seal the cell. The cell was supported on an open cardboard box. The inlet and outlet tubes of the cooling chamber were connected by tygon tubings to the pump and to a methanol reservoir filled with methanol. The methanol reservoir was also connected to the refrigerator by a tygon tubing. The thermocouples were plugged in and the appropriate scales were set on the chart for continuously recording temperatures in the form of voltages. Initially, a two-way tap between the test cell and the refrigerator was used to shut off the flow of methanol from the refrigerator to the test cell and the pump was turned on to circulate methanol only within the rest of the equipment for a few minutes. In this way the temperature of the methanol in the system was made approximately uniform before being led into the cooling chamber of the test cell. It also became possible to start recording temperatures at the same time that the coolant (methanol) started flowing into the cooling chamber of the test cell. Thus when it was certain that the system was ready, the recorder chart was set in motion, the two-way tap was used to allow enough flow rate of the coolant to ensure turbulent flow into the cooling chamber of the test cell, and the time was noted as t=0 at the start of the experiment. The room temperature was also

read with a mercury thermometer at the beginning of the experiment and at regular intervals during the experiment.

When all of the n-hexadecane or enough of it had solidified (sometimes it took more than 90 minutes to solidify about three quarters of the amount of n-hexadecane), the experiment was terminated. The thermocouple readings were then translated from the voltage recordings of the chart to degrees Centigrade by using a table of emf's and temperatures for a copper-constantan thermocouple.

Polynomial fits for $f_1(t)$ and $f_2(t)$: As was stated in the theoretical analysis, the experimentally-determined temperature profiles of the bottom and the top plates were to be used to obtain polynomial fits, $f_1(t)$ and $f_2(t)$, respectively, that would act as time-dependent boundary conditions for the theoretical problem of this study. $f_1(t)$ and $f_2(t)$ were obtained for each experiment by using exponential fits of the type

$T(t) = A + B \exp(-c(t)t)$ where $c(t)$ was a polynomial of degree 5 or less found by the least-squares fit. "A" corresponded to the final steady state temperature of the cold bottom plate and the sum of A and B equalled the initial temperature at $t=0$, i.e., the room temperature T_a which was fairly constant throughout the particular experimental run. Thus, if the final steady state temperature of the cold bottom plate was T_{cpf}, then

$$A = T_{cpf}, \text{ and } A+B = T_a \text{ or } B = T_a - T_{cpf}.$$

Thus, for a particular run, the fit to the temperature of the bottom plate was

$$f_1(t) = T_{cpf} + (T_a - T_{cpf}) \exp(-c_1(t)t) = T(t)_{\text{bottom plate}} \tag{120}$$

and the fit to the temperature of the top plate was

$$f_2(t) = T_{cpf} + (T_a - T_{cpf}) \exp(-c_2(t)t) = T(t)_{\text{top plate}} \tag{121}$$

The use of an exponential fit of this form was prompted by the following reasons. The first reason was that a polynomial fit of degree 5 or less still gave a standard deviation between fitted temperature and experimental temperature that was too large compared to the error in reading the actual temperatures experimentally. A polynomial of degree more than 5 was thought to be unwieldy. Also, the round-off errors from the computing program became significant for degrees greater than 5. A different fit had to be found. The second reason was that the experimentally measured temperature of the bottom plate approached the profile of a decaying exponential. It started off from room temperature and fell to a constant steady state temperature that depended only on the setting of the refrigerator current. Since no part of the cell could be colder than the coolant being circulated by the refrigerator and since at the beginning of the experiment the cell and its entire contents were at a constant room temperature, it was decided that at the final steady state of the entire cell, the temperature would be equal to the steady

state temperature of the bottom plate, which, in turn, equalled the steady state temperature of the coolant as regulated by the refrigerator. Thus, the temperature profiles of the bottom and the top plates would only differ by the values of the exponents, particularly c_1 and c_2.

A computer program was written that would read in T_a, T_{cpf}, T(t) and t, and also calculate c(t) from the equation

$$c'(t) = \frac{1}{t}\ln\{(T(t)-T_{cpf})/(T_a-T_{cpf})\} \text{ for } t > 0 \qquad (122)$$

where c(t) is a polynomial fit of c'(t) and c'(t) is calculated from experimental values by Equation 122. If T(t) was the experimentally determined temperature for the bottom plate, then c'(t) was $c_1'(t)$; if it was for the top plate, then c'(t) was $c_2'(t)$. At t=0, $T(t)=T_a$ and $\{c'(t)\}t=0$. When $T(t) = T_{cpf}$, then $e^{-\{c'(t)\}t}=0$. Thus c'(t) was calculated by equation (122) only for t > 0 and for t such that $T(t)<T_{cpf}$. The computer program then would obtain a polynomial fit c(t) for c'(t) of degree 5 or less using the least-squared method. The values for c(t) were then put into equation (120) or equation (121) to obtain $T(t)_{(fit)}=f(t)$. The sum of the squares of the differences between $T(t)_{(fit)}$ and $T(t)_{(experiment)}$ was then calculated for each degree of c(t). That degree of $c_1(t)$ or $c_2(t)$, which gave a standard deviation of $T(t)_{(fit)}$ from $T(t)_{(experimental)}$ such that the standard deviation was minimum and also less than or equal to the error in reading T(t) experimentally, was taken as the best one to use in equation (120) or equation (121). The computer program has

been included in the appendix. Computer programs for the pre- and the post-solidification problems have also been included in the appendix.

Estimation of ε: The convergence criteria used in calculating S_{j+1} was that if $|S_{j+1}(\text{old}) - S_{j+1}(\text{new})| \leq \varepsilon$, then S_{j+1} was taken to have been calculated within the limits allowable by the truncation errors of the finite difference equations which were used. Then $S_{j+1} = S_{j+1}(\text{new})$ for the (j+1)st time step. ε was calculated by considering the largest absolute value of the truncation errors in each of equations (78) to (91). The largest truncation errors were

$$0(k_a h_a{}^2 M) + 0(k_a h_a{}^2 J) \tag{123a}$$

$$0(k_a h_a M) + 0(k_a h_a{}^2 J) \tag{123b}$$

$$0(k_a h_a{}^2 M) + 0(k_a h_a J) \tag{123c}$$

The orders of magnitude were replaced by the absolute values of each term in equation (123). Since k_a and h_a were fractions between 0 and 1, the largest absolute value of the truncation error in calculating S_{j+1} was obtained from either equation (123b) or equation (123c) as

$$\varepsilon = \text{abs}(k_a h_a M) + \text{abs}(k_a h_a{}^2 J) \tag{124a}$$

or $$\varepsilon = \text{abs}(k_a h_a{}^2 M) + \text{abs}(k_a h_a J) \tag{124b}$$

depending on the actual magnitudes of M, J, k_a, and h_a.

However, a value for ε which was larger than that given by either equation (124a) or equation (124b) had to be used so

as to account for round-off errors from the computer program for calculating S_{j+1}. The actual value of ε to be used was found by fixing M, J, k_a and h_a, and assuming smaller and smaller values of ε until such a value that either did not affect the accuracy of the calculated S_{j+1} significantly or caused the computer to go into an indefinite loop. In the event that the computer went into a loop, the next higher value of ε was used. The value, $\varepsilon = 0.0004$, which was used in the computer program for the present study was obtained in this manner. This value corresponded to 1.88% of the magnitude of the space increment h_a and to 0.04% of the total height of n-hexadecane in the test cell. Thus, when the entire content of the test cell was frozen, the calculated height of solid varied from that predicted by an exact solution of equations (2a) and (2b) by about ±0.04% of the actual height of solid in the test cell.

COMPARISON OF THEORETICAL AND EXPERIMENTAL RESULTS

The experimental results given in this section were obtained for the test cell that was described previously. The test material was practical n-hexadecane ($n\text{-}C_{16}H_{34}$) of molecular weight 226.45 and it was distributed by the Eastman Kodak Company for chemical purposes. It had small impurities that did not change its properties appreciably. It completely filled a void of the test cell of 4-in.-square cross-section and 1-15/32-in. height. The values of the parameters used to obtain the theoretical results were obtained from Northrop's final report[25]. Data from Northrop's report were:

Density

Solid n-hexadecane $\rho_s = 1.0772 - 8.41 \times 10^{-4} T$ gm/cm^3

for $T \leq 289.9^\circ K$

Liquid n-hexadecane $\rho_L = 0.9726 - 6.813 \times 10^{-4} T$ gm/cm^3

for $289.9^\circ K \leq T \leq 400.0^\circ K$

Specific Heat

Solid n-hexadecane $c_{ps} = 0.5$ cal/(gm-$^\circ$K)

for $250^\circ K \leq T \leq 289.9^\circ K$

Liquid n-hexadecane $c_{pL} = 0.1626 + 1.164 \times 10^{-3} T$ cal/(gm-$^\circ$K)

for $289.9^\circ K \leq T \leq 480.0^\circ K$

Conductivity

Solid n-hexadecane $K_s = 2.390 \times 10^{-3} - 3.047 \times 10^{-6} T$ watt/(cm-$^\circ$K)

for $250.0^\circ K \leq T \leq 289.9^\circ K$

Liquid n-hexadecane $K_L = 2.390 \times 10^{-3} - 3.047 \times 10^{-6} T$ watt/(cm-°K)

for $289.9^{\circ}K \leq T \leq 425.0^{\circ}K$

Solidification temperature

$T_e = 289.9^{\circ}K = 16.7^{\circ}C$

Latent heat of solidification

$H_f = 102.0$ Btu/lb $= 56.67$ cal/gm

Since the theoretical model of the present study assumed constant but different properties for the solid and the liquid phases, constant values were calculated from Northrop's report using average temperatures for those properties that were temperature dependent. Since the solidification temperature was 289.9°K and the lowest temperature found in the test cell during a run was approximately 262.2°K, the average of these temperatures, $T_{av} = \frac{1}{2}(289.9+262.2)^{\circ}K = 276.1^{\circ}K$, was substituted into the equations for the temperature dependent properties of the solid phase to obtain average values that were used as constant properties for the solid phase. Similarly, since the highest temperature encountered in the experiment was approximately 302.0°K, the average temperature, $T_{L_{av}} = \frac{1}{2}(302+289.9)^{\circ}K = 295.9^{\circ}K$, was used to calculate properties for the liquid phase. Thus the values of the properties used for the present study were:

Density

Solid n-hexadecane $\rho_s = 0.845$ gm/cm^3

Liquid n-hexadecane $\rho_L = 0.771$ gm/cm^3

Specific heat

Solid n-hexadecane $c_{ps} = 0.5$ cal/(gm-^{o}K)

Liquid n-hexadecane $c_{PL} = 0.507$ cal/(gm-^{o}K)

Conductivity

Solid n-hexadecane $K_s = 1.549 \times 10^{-3}$ watt/(cm-^{o}K)

$= 2.22 \times 10^{-2}$ cal/(cm-min-^{o}K)

Liquid n-hexadecane $K_L = 1.488 \times 10^{-3}$ watt/(cm-^{o}K)

$= 2.13 \times 10^{-2}$ cal/(cm-min-^{o}K)

Thermal diffusivity

Solid n-hexadecane $\alpha_s = K_s/(\rho_s c_{Ps}) = 5.254 \times 10^{-2}$ cm^2/min

Liquid n-hexadecane $\alpha_L = K_L/(\rho_L c_{PL}) = 5.457 \times 10^{-2}$ cm^2/min

Solidification temperature

$T_e = 289.9^{o}$K

Latent heat of solidification

$H_f = 56.67$ cal/gm

<u>Dimensionless variables</u>

$\lambda = \alpha_s/\alpha_L = 0.9627$

$M = (\frac{\alpha_s}{\alpha_L})(c_{Ps}T_e/H_f) = 2.463$

$J = (\rho_L/\rho_s)(c_{PL}T_e/H_f) = 2.367$

$\tau_o = (\alpha_L/h^2)t = 3.921 \times 10^{-3}t$ where t is in min.

$h_a = \Delta z = 1/47$

Other values used were

$h = 1\text{-}15/32$ in. $= 47/32$ in. $= 3.73$ cm

$\Delta y = (\Delta z)h = (h_a)h = 1/32$ in. $= 7.9 \times 10^{-2}$ cm

$t = 255\ \tau_o$ minutes

$t = 15,300\ \tau_o$ seconds

Following the argument in the theoretical analysis of the conditions for stability, equation (119b) was used to find p_{max} since λ was less than 2. Thus

$$p_{max} = 0.5 \text{ and } p \leq 0.5$$

$$k_{a,max} = p_{max} h_a^2 = 0.5/(47)^2 = 2.26 \times 10^{-4}$$

$$\Delta t_{max} = 3.5 \text{ sec} = 0.058 \text{ min.}$$

Thus, for the chosen $h_a = 1/47$, any Δt less than 3.5 sec satisfied the stability criteria. Δt of 1.0 second and 2.0 seconds were used. They corresponded to values of k_a of 1/15 300 and 2/15,300, respectively. It was found (as a glance at Table 1 would show) that there was no significant difference between the temperature profiles calculated using a 1-second time step and those calculated using a 2-second time step. The two-second time step reduced the computer time required for the calculations without affecting the accuracy of the results. Tables (1) to (7) and Figures (16) to (33) show the experimental results and the results of the theoretical analysis corresponding to each experimental run.

The only manner in which the experimental runs were different from one another was in the values of one or both of the following two physical conditions: ambient temperature, T_a, and the steady state temperature, T_{cpf}, to which the bottom plate was cooled. The earlier termination of some experimental runs compared to other runs was mostly arbitrary and it had nothing to do with operational requirements

or experimental limitations. For instance, the first three experimental runs (Runs 1, 2, and 3) were terminated soon after about one-third of the content of the test cell had solidified, while the remaining three experimental runs (Runs 4, 5, and 6) were terminated after about two-thirds of the content of the cell had solidified and before the entire content of the cell had solidified. The maximum number of points that could be recorded on a graph of experimentally-observed height of solid formed versus time was 4 since only four thermocouples were used.

In general, the experimental results of the tests performed show good agreement with the theoretical results obtained from the numerical analysis. There was much better agreement of experimental results with theoretical results for the pre-solidification problem than for the post-solidification problem. As time elapsed, the experimental results indicated a much slower decrease in temperature than that predicted by the theoretical results. The height of solid formed, as indicated by the experiment, agreed well initially with that predicted by the theoretical calculations, but it became smaller than that predicted theoretically as time elapsed and as the solidification front approached the top plate of the cell. Thus, the theoretical analysis predicted, in the early parts of the experiments, about the same rate of solidification as was observed experimentally, but it predicted a faster rate of solidification than that

observed experimentally as the freezing front approached the top of the test cell.

The polynomial fits of the experimentally-observed temperature profiles of the bottom plate or the top plate agreed closely with the experimentally-determined temperature profiles themselves. The maximum standard deviation which was found between any experimentally-observed temperature profile and its polynomial fit was much less than the $\pm 1.0^{\circ}K$ which was the estimated error in observing the temperature profile experimentally. Similarly, the maximum observed difference between t^* as found experimentally and t^* as found by numerical analysis was less than ± 2.0 seconds. It should be recalled that t^* was defined as the time interval between the start of cooling of the bottom plate and the initiation of solidification of n-hexadecane on the bottom plate. In each of the graphs of the height of solid formed versus time, t^* represents the interval between $t=0$ and the point where the curve intersects the time coordinate.

One reason why the experimental and theoretical results agreed during the early stages of solidification, but differed during the latter stages was perhaps that the heat gained from the surroundings during the early period of solidification, when the freezing front was still near the cold plate, was not yet sufficient to cause any appreciable change in the rate at which heat was being withdrawn from the

cold plate by the refrigerated coolant. But as time passed and as the amount of the liquid phase which was left became smaller the heat gained from the surroundings began to have appreciable effects on the cooling process and therefore slowed down the rate of solidification. However, the one-dimensional model which was used to obtain the theoretical results essentially ignored heat gains or losses in all directions but that direction in which the one-dimensional model was formulated. Consequently, the theoretical result predicted a much faster rate of solidification than that observed experimentally.

Table 1

Comparison of temperature profiles obtained theoretically (at t = 48.0 sec) using 1.0-sec and 2.0-sec time steps. Run 1: Pre-solidification problem.

Distance from bottom plate y cm	Temperature, °K (1.0-sec time step)	Temperature, °K (2.0-sec time step)
0.00	290.6	290.6
0.16	296.4	296.4
0.32	298.7	298.7
0.48	299.4	299.4
0.63	299.6	299.6
0.79	299.6	299.6
0.95	299.7	299.7
1.11	299.7	299.7
1.27	299.7	299.7
1.43	299.7	299.7
1.59	299.7	299.7
1.75	299.7	299.7
1.91	299.7	299.7
2.06	299.7	299.7
2.22	299.7	299.7
2.38	299.7	299.7
2.54	299.7	299.7
2.70	299.7	299.7
2.86	299.7	299.7
3.02	299.7	299.7
3.18	299.7	299.7
3.33	299.7	299.7
3.49	299.7	299.7
3.65	299.7	299.7
3.73	299.7	299.7
	t* = 51.0	t* = 51.0

Run 1

Table 2

Least-squares polynomial fits, $f_1(t)$ and $f_2(t)$, to experimentally-measured temperatures of the bottom and the top plates respectively: Run 1.

T_a = Ambient temperature = $299.7^{\circ}K$

T_{cpf} = Final steady-state temperature of the bottom plate = $262.7^{\circ}K$

$f_1(t)$ = Polynomial obtained from a least-squares fit of experimentally-measured temperatures of the bottom plate

$$= 262.7 + 37.0e^{-c_1 t} \pm 0.4^{\circ}K$$

where $c_1 = 0.14620836 + 0.34113500t - 0.11745415t^2 + 1.7961587 \times 10^{-2}t^3 - 1.3204283 \times 10^{-3}t^4 + 3.8116175 \times 10^{-5}t^5$,

and t is measured in minutes: $0.0 \leq t \leq 17.9$

$f_2(t)$ = Polynomial obtained from a least-squares fit of experimentally measured temperatures of the top plate

$$= 262.7 + 37.0e^{-c_2 t} \pm 0.1^{\circ}K$$

where $c_2(t) = -7.1034089 \times 10^{-4} + 8.5043082 \times 10^{-4}t - 6.4550809 \times 10^{-5}t^2 + 1.7082712 \times 10^{-6}t^3$,

and t is measured in minutes: $0.0 \leq t \leq 17.9$

Run 1 (cont.)

Figure 16. Temperature profiles (experimental and theoretical) for the pre-solidification problem (Run 1).

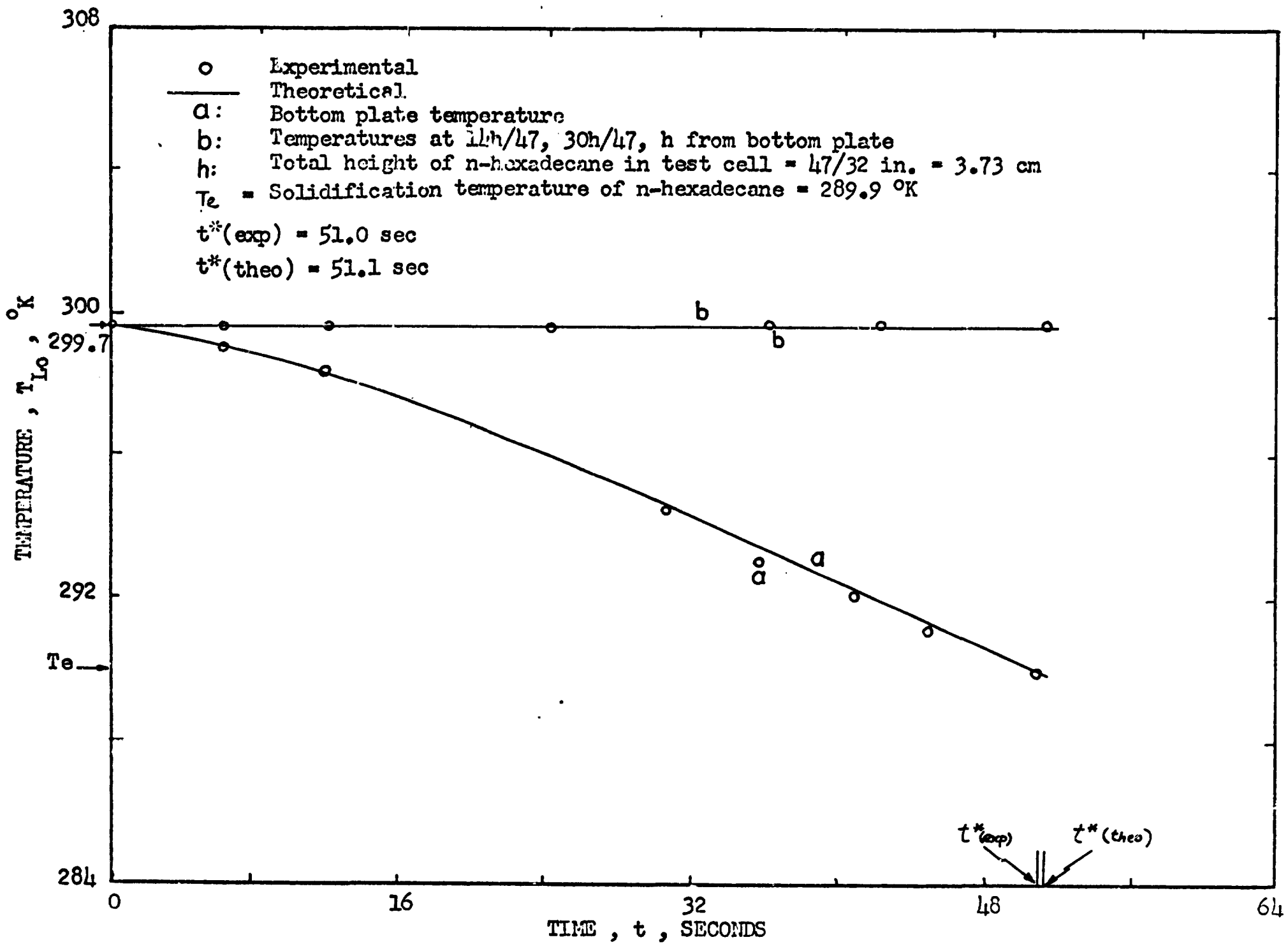
o Experimental
Theoretical
a: Bottom plate temperature
b: Temperatures at 1h/47, 30h/47, h from bottom plate
h: Total height of n-hexadecane in test cell = 47/32 in. = 3.73 cm
Te = Solidification temperature of n-hexadecane = 289.9 °K
t*(exp) = 51.0 sec
t*(theo) = 51.1 sec
308
300
299.7
292
Te
284
TEMPERATURE , T_Lo , °K
0
16
32
48
64
TIME , t , SECONDS
a
b
t*(exp)
t*(theo)

Run 1 (cont.)

Figure 17. Temperature profiles (experimental and theoretical) for the combined pre-solidification and post-solidification problems: Run 1.

——— Theoretical

Experimental	Theoretical	
o	1	Bottom-plate thermocouple
+	2	Thermocouple at 14h/47 from bottom plate
Δ	3	Thermocouple at 30h/47 from bottom plate
□	4	Thermocouple at h from bottom plate

h = 47/32 in. = 3.73 cm.

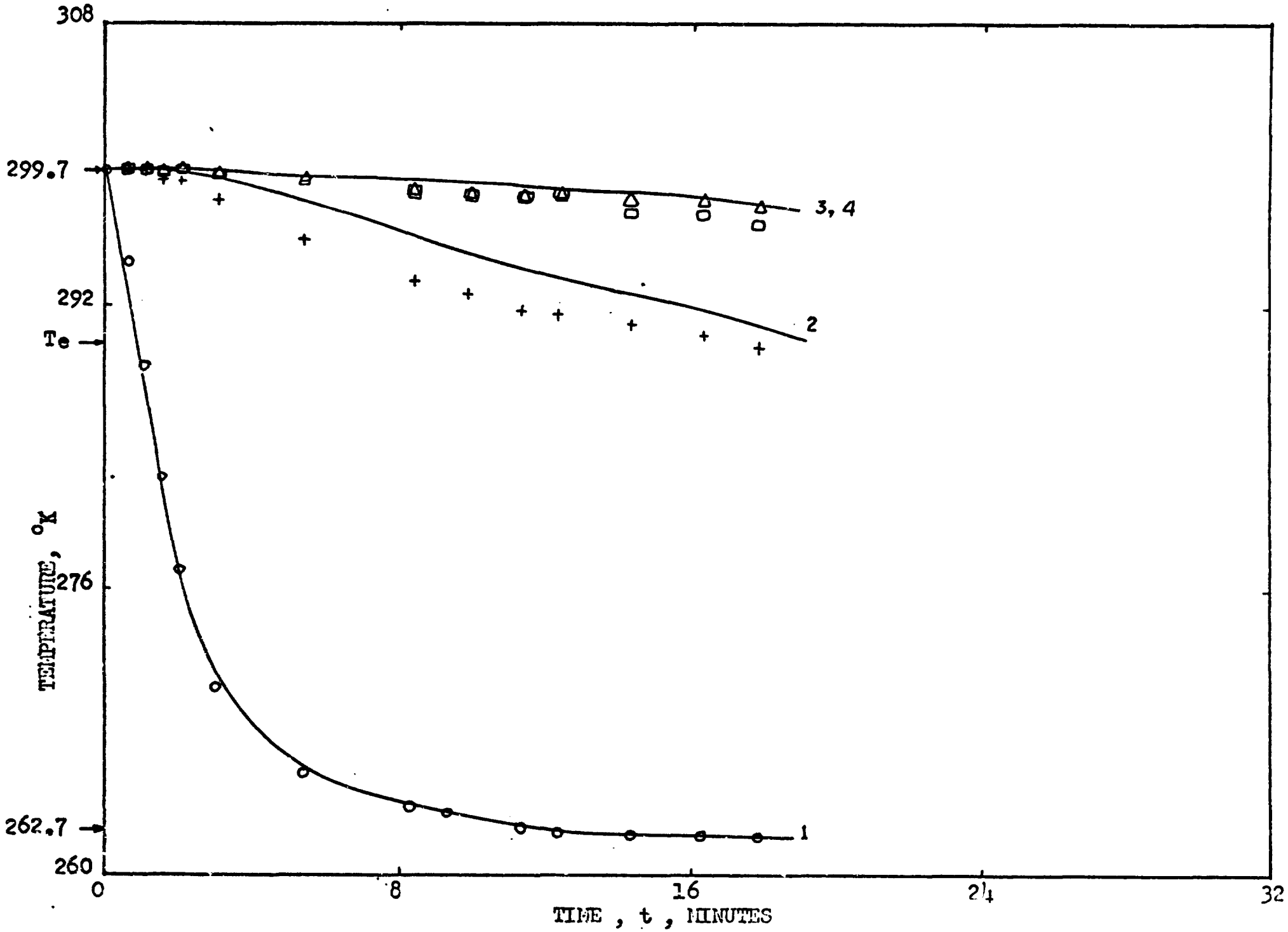
308
299.7
292
Te
276
262.7
260
TEMPERATURE, °K
0
8
16
24
32
TIME , t , MINUTES
3, 4
2
1

Run 1 (cont.)

Figure 18. Height of solid n-hexadecane as a function of time: Run 1.

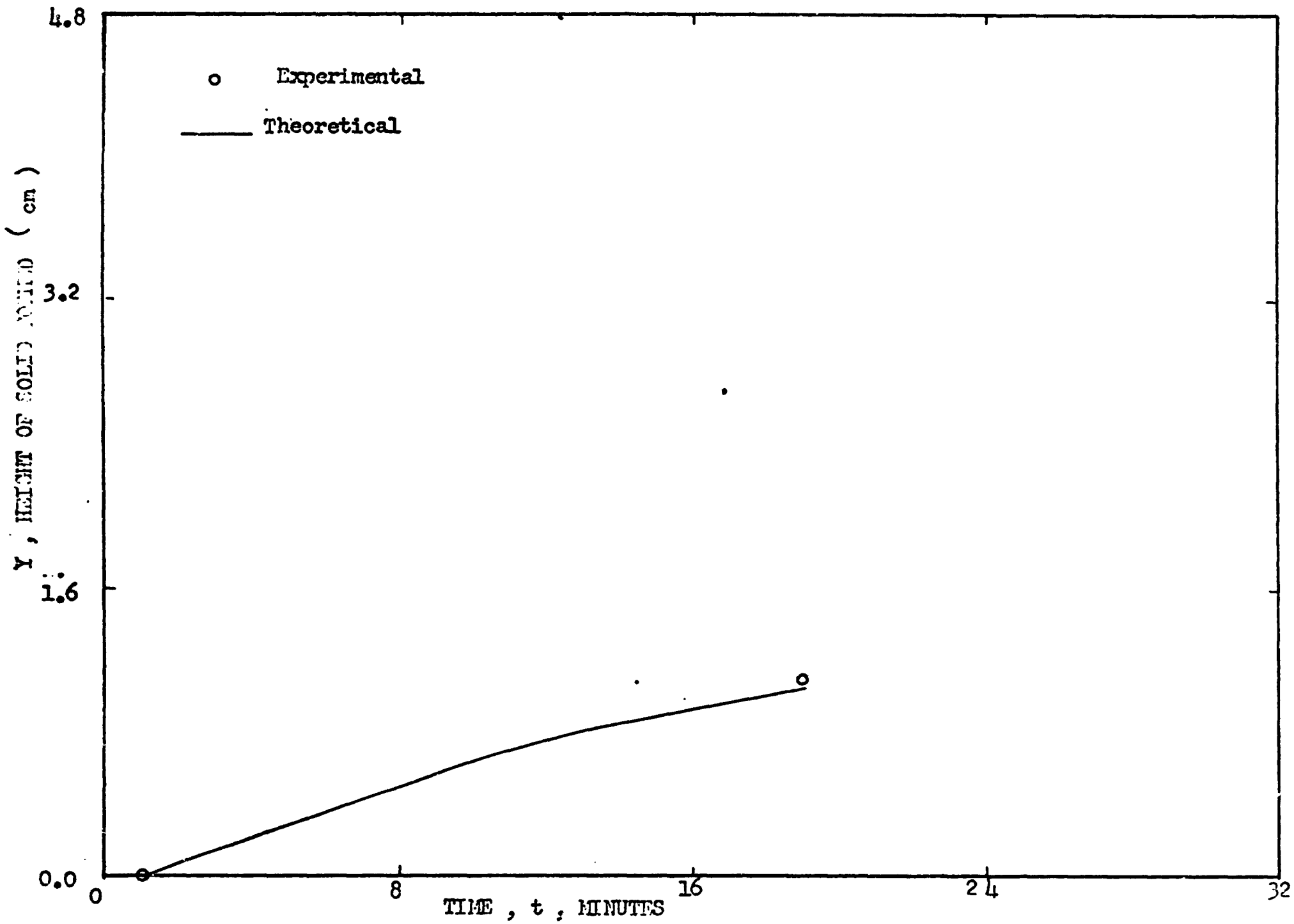
4.8
3.2
1.6
0.0
o Experimental
Theoretical
Y , HEIGHT OF SOLID ADDED (cm)
0
8
16
24
32
TIME , t , MINUTES

Run 2

Table 3

Least-squares fits, $f_1(t)$ and $f_2(t)$, to experimentally-measured temperatures of the bottom and top plates, respectively: Run 2.

T_a = Ambient temperature = $300.3^{\circ}K$

T_{cpf} = Final steady-state temperature of the bottom plate = $263.3^{\circ}K$

$$f_1(t) = 263.3 + 37.0e^{-c_1 t} \pm 0.5^{\circ}K$$

where $c_1 = 0.12787341 + 0.42746695t - 0.17143748t^2 + 3.0078475 \times 10^{-2}t^3 - 2.4362813 \times 10^{-3}t^4 + 7.3510422 \times 10^{-5}t^5$

and t is measured in minutes: $0.0 \leq t \leq 23.0$

$$f_2(t) = 263.3 + 27.0e^{-c_2 t} \pm 0.1^{\circ}K$$

where $c_2 = -4.7386052 \times 10^{-4} + 6.4491732 \times 10^{-4}t - 3.8541947 \times 10^{-5}t^2 + 8.3964074 \times 10^{-7}t^3$

and t is measured in minutes: $0.0 \leq t \leq 23.0$

Run 2 (cont.)

Figure 19. Temperature profiles (experimental and theoretical) for the pre-solidification problem: Run 2.

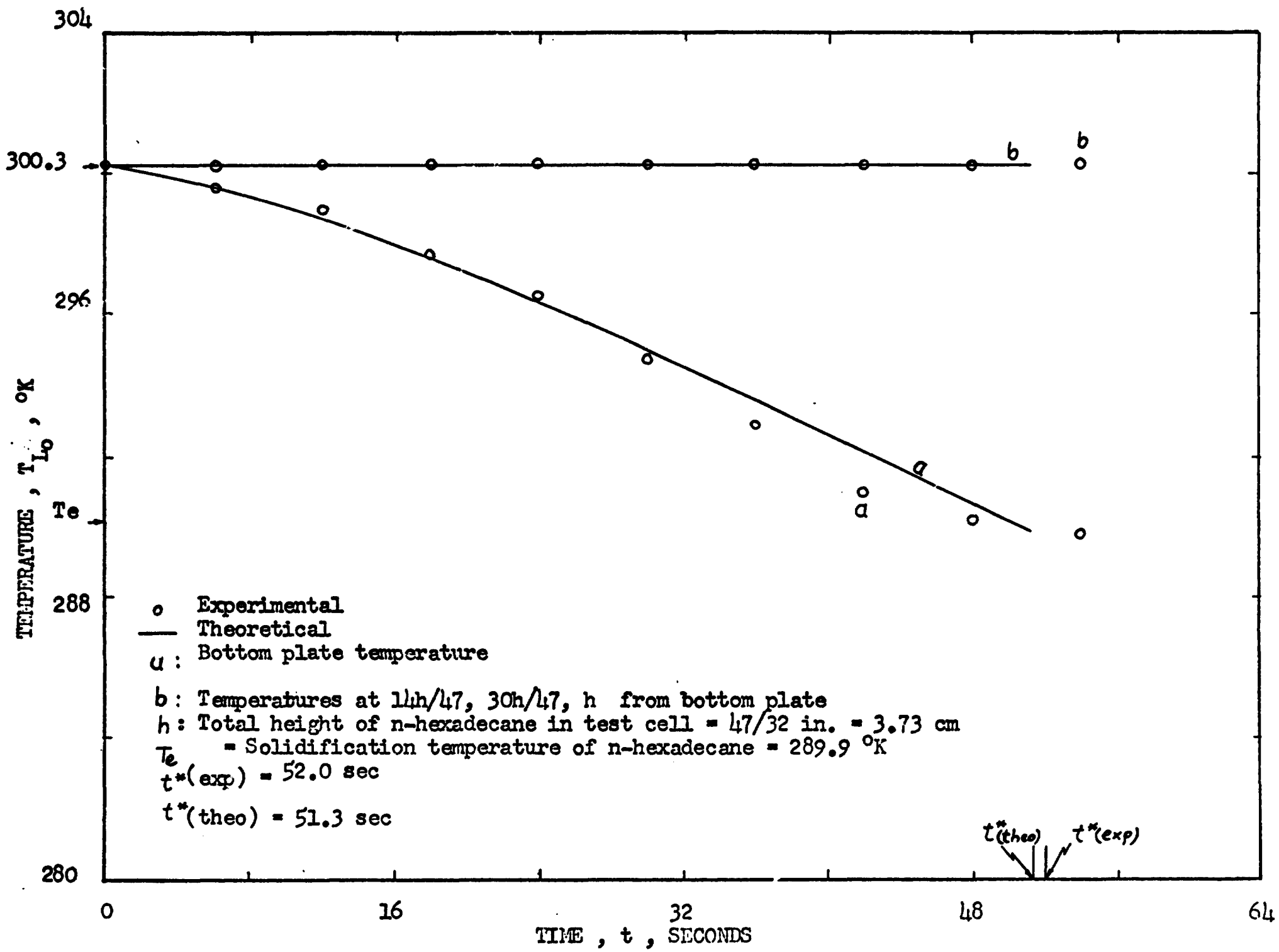
304
300.3
296
Te
288
280
TEMPERATURE , T_{L_0} , °K
0
16
32
48
64
TIME , t , SECONDS
a
b
o Experimental
—— Theoretical
a : Bottom plate temperature
b : Temperatures at 14h/47, 30h/47, h from bottom plate
h : Total height of n-hexadecane in test cell = 47/32 in. = 3.73 cm
T_e = Solidification temperature of n-hexadecane = 289.9 °K
t^*(exp) = 52.0 sec
t^*(theo) = 51.3 sec
$t^*_{(theo)}$
$t^*(exp)$

Run 2. (cont.)

Figure 20. Temperature profiles (experimental and theoretical) for the combined pre-solidification and post-solidification problems: Run 2.

——— Theoretical

Experimental	Theoretical	
o	1	Bottom-plate thermocouple
+	2	Thermocouple at 14h/47 from bottom plate
Δ	3	Thermocouple at 30h/47 from bottom plate
□	4	Thermocouple at h from bottom plate

h = 47/32 in. = 3.73 cm.

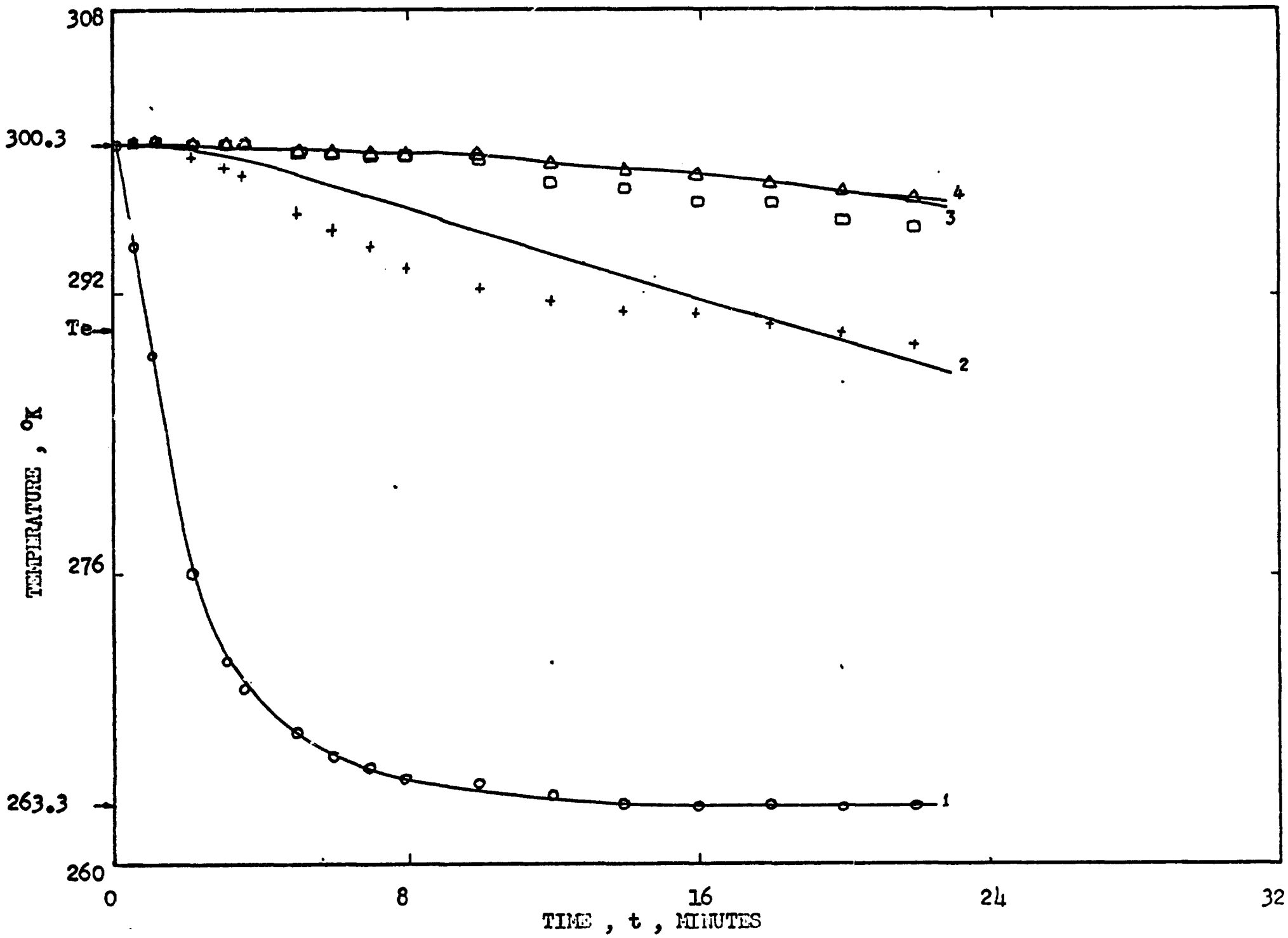
308
300.3
292
Te
276
263.3
260
TEMPERATURE , °K
0
8
16
24
32
TIME , t , MINUTES
1
2
3
4

Run 2 (cont.)

Figure 21. Height of solid n-hexadecane as a function of time: Run 2.

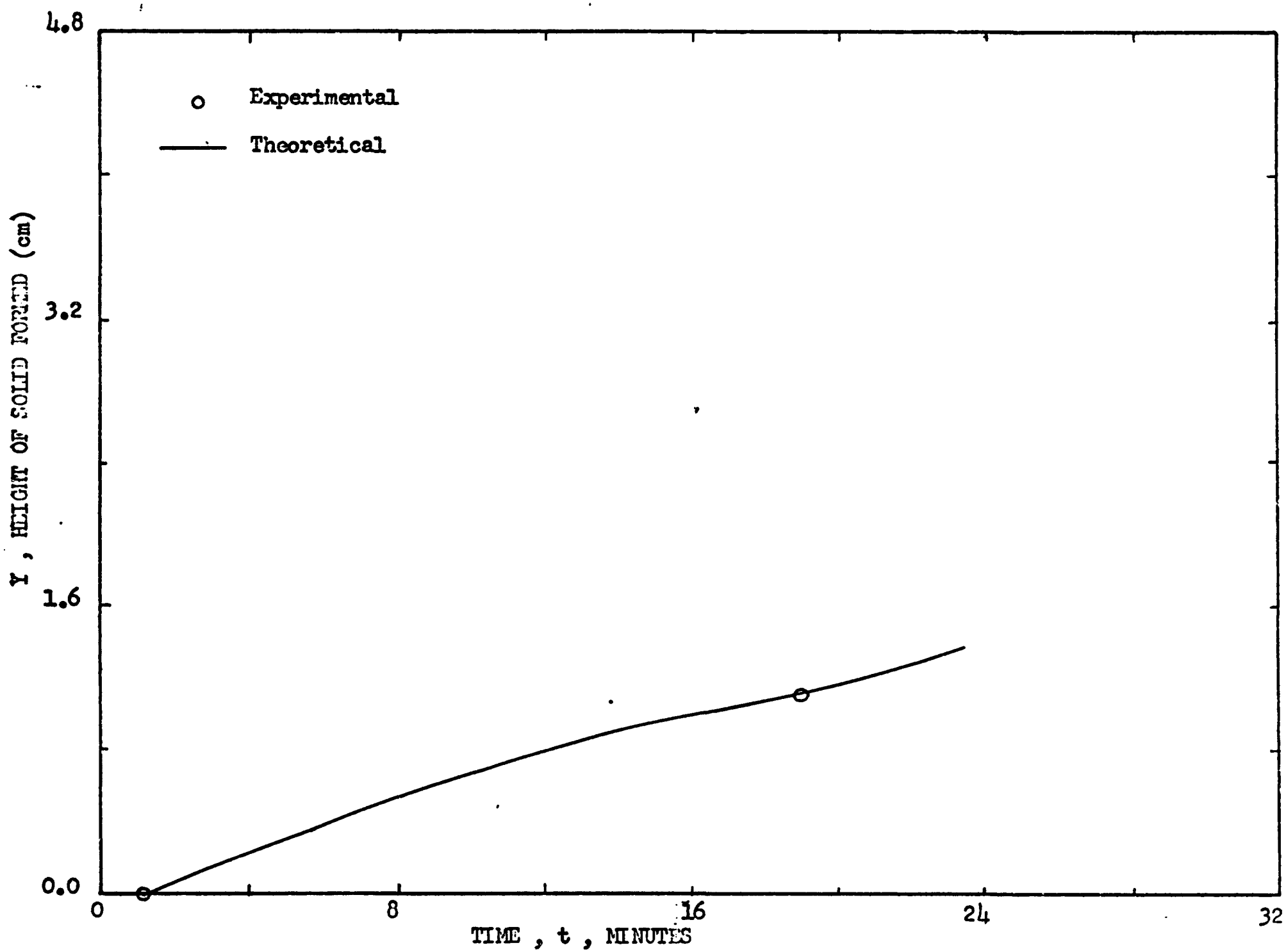
4.8
3.2
1.6
0.0
Y , HEIGHT OF SOLID FORMED (cm)
Experimental
Theoretical
0
8
16
24
32
TIME , t , MINUTES

Run 3

Table 4

Least-squares fits, $f_1(t)$ and $f_2(t)$, to experimentally-measured temperatures of the bottom and top plates, respectively: Run 3.

T_a = Ambient temperature = $301.5^{\circ}K$

T_{cpf} = Final steady-state temperature of the bottom plate = $265.3^{\circ}K$

$$f_1(t) = 265.3 + 36.2e^{-c_1 t} \pm 0.3^{\circ}K$$

where $c_1 = 0.24807854 + 0.19299560t - 5.7222949 \times 10^{-2} t^2 + 7.2362357 \times 10^{-3} t^3 - 4.2544939 \times 10^{-4} t^4 + 9.3636101 \times 10^{-6} t^5$

and t is measured in minutes: $0.0 \leq t \leq 34.3$

$$f_2(t) = 265.3 + 36.2e^{-c_2 t} \pm 0.3^{\circ}K$$

where $c_2 = -3.1603307 \times 10^{-4} + 4.2309680 \times 10^{-4} t - 2.8095101 \times 10^{-5} t^2 + 9.1612643 \times 10^{-7} t^3 - 1.0792678 \times 10^{-8} t^4$

and t is measured in minutes: $0.0 \leq t \leq 34.3$

Run 3 (cont.)

Figure 22. Temperature profiles (experimental and theoretical) for the pre-solidification problem: Run 3.

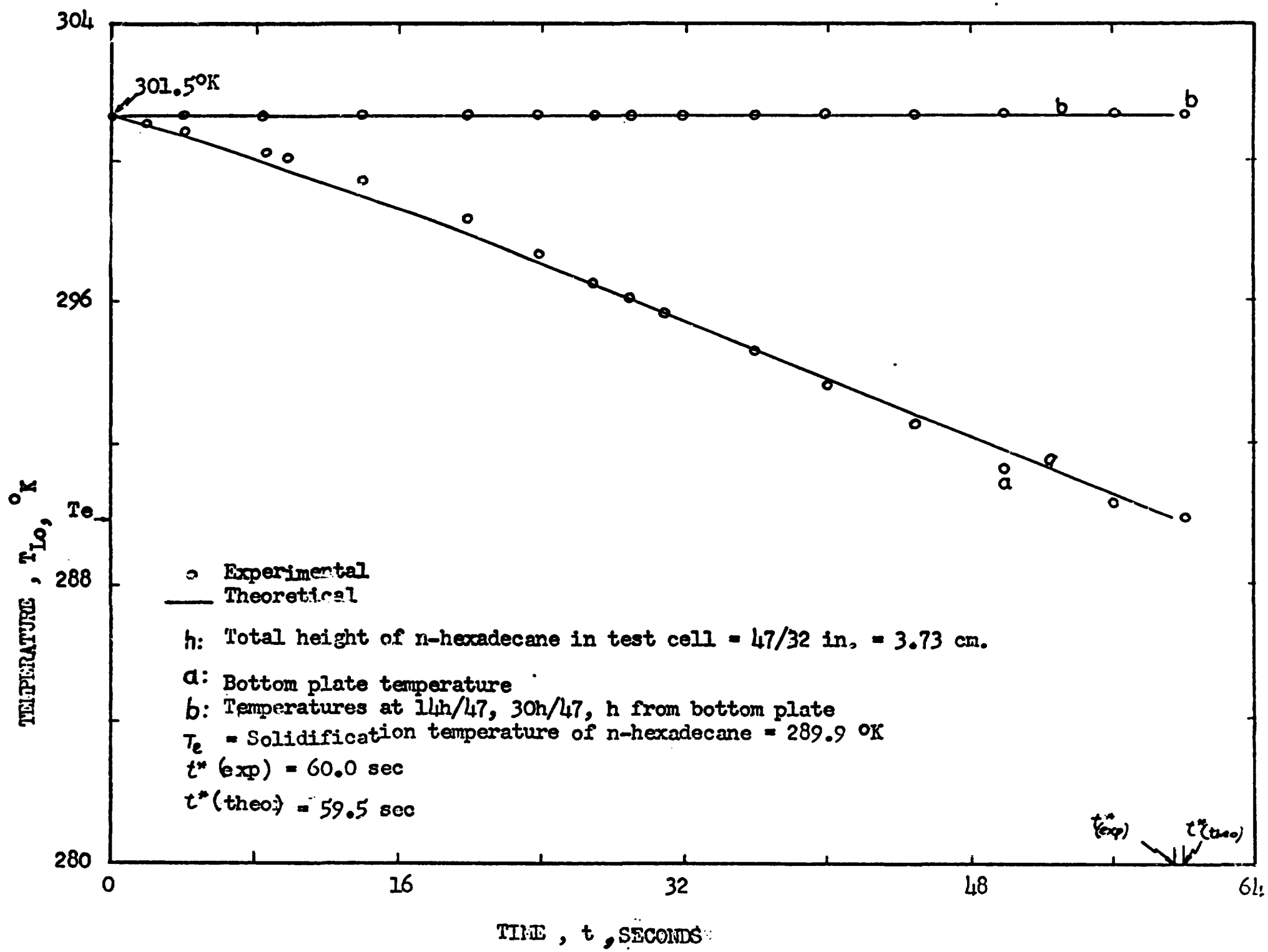
304
296
288
280
Te
301.5°K
b
b
a
a
TEMPERATURE , T_{Lo}, °K
0
16
32
48
64
TIME , t , SECONDS
t^*(exp)
t^*(theo)
Experimental
Theoretical
h: Total height of n-hexadecane in test cell = 47/32 in. = 3.73 cm.
a: Bottom plate temperature
b: Temperatures at 14h/47, 30h/47, h from bottom plate
T_e = Solidification temperature of n-hexadecane = 289.9 °K
t^* (exp) = 60.0 sec
t^*(theo) = 59.5 sec

Run 3 (cont.)

Figure 23. Temperature profiles (experimental and theoretical) for the combined pre-solidification and post-solidification problems: Run 3.

——— Theoretical

Experimental	Theoretical	
o	1	Bottom-plate thermocouple
+	2	Thermocouple at 14h/47 from bottom plate
Δ	3	Thermocouple at 30h/47 from bottom plate
□	4	Thermocouple at h from bottom plate

h = 47/32 in. = 3.73 cm.

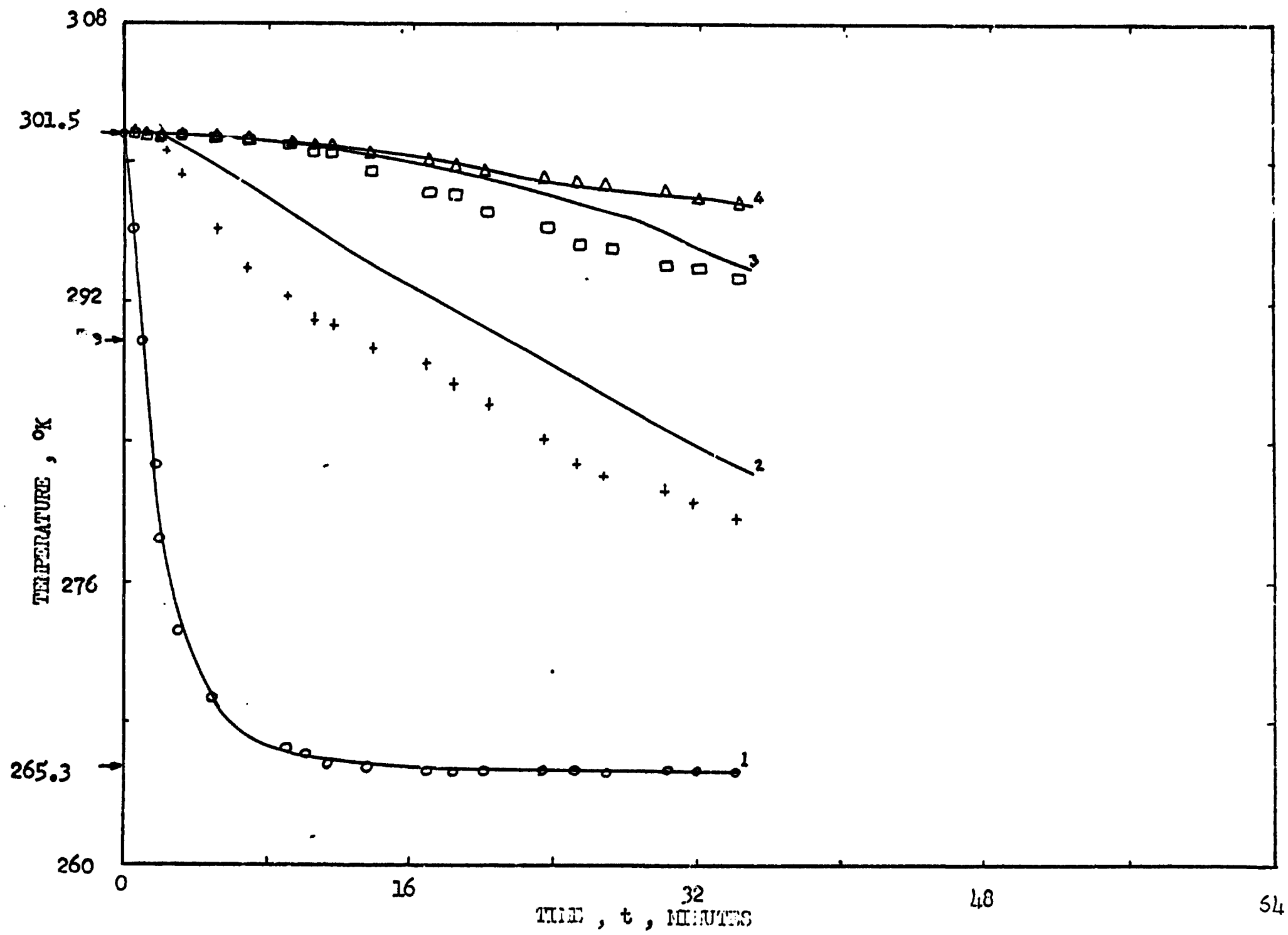
308
301.5
292
276
265.3
260
TEMPERATURE , °K
0
16
32
48
64
TIME , t , MINUTES
1
2
3
4

Run 3 (cont.)

Figure 24. Height of solid n-hexadecane as a function of time: Run 3.

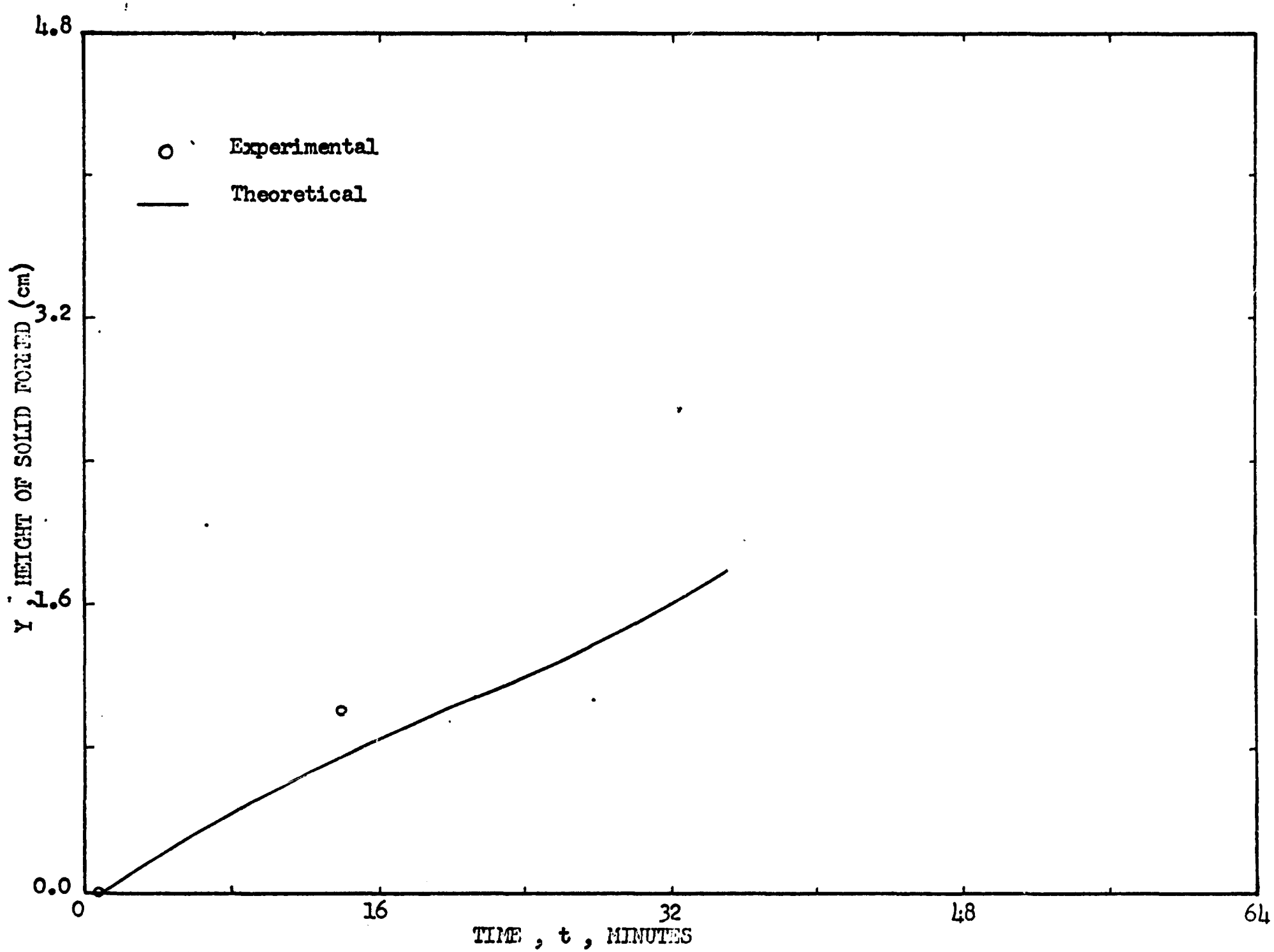
4.8
3.2
1.6
0.0
Y , HEIGHT OF SOLID FORMED (cm)
Experimental
Theoretical
0
16
32
48
64
TIME , t , MINUTES

Run 4

Table 5

Least-squares fits, $f_1(t)$ and $f_2(t)$, to experimentally-measured temperatures of the bottom and the top plates, respectively: Run 4.

T_a = Ambient temperature = 300.9°K

T_{cpf} = Final steady-state temperature of the bottom plate = 264.0°K

$$f_1(t) = 264.0 + 36.9e^{-c_1 t} \pm 0.5^{\circ}K$$

where $c_1 = 0.17001907 + 0.26454099t - 7.3114020 \times 10^{-2}t^2 + 7.9185015 \times 10^{-3}t^3 - 3.8016733 \times 10^{-4}t^4 + 6.6739894 \times 10^{-6}t^5$

and t is measured in minutes: $0.0 \leq t \leq 61.5$

$$f_2(t) = 264.0 + 36.9e^{-c_2 t} \pm 0.1^{\circ}K$$

where $c_2 = -3.3089768 \times 10^{-4} + 1.4827702 \times 10^{-4}t - 2.2737729 \times 10^{-6}t^2 + 1.0374753 \times 10^{-8}t^3$

and t is measured in minutes: $0.0 \leq t \leq 61.5$

Run 4 (cont.)

Figure 25. Temperature profiles (experimental and theoretical) for the pre-solidification problem: Run 4.

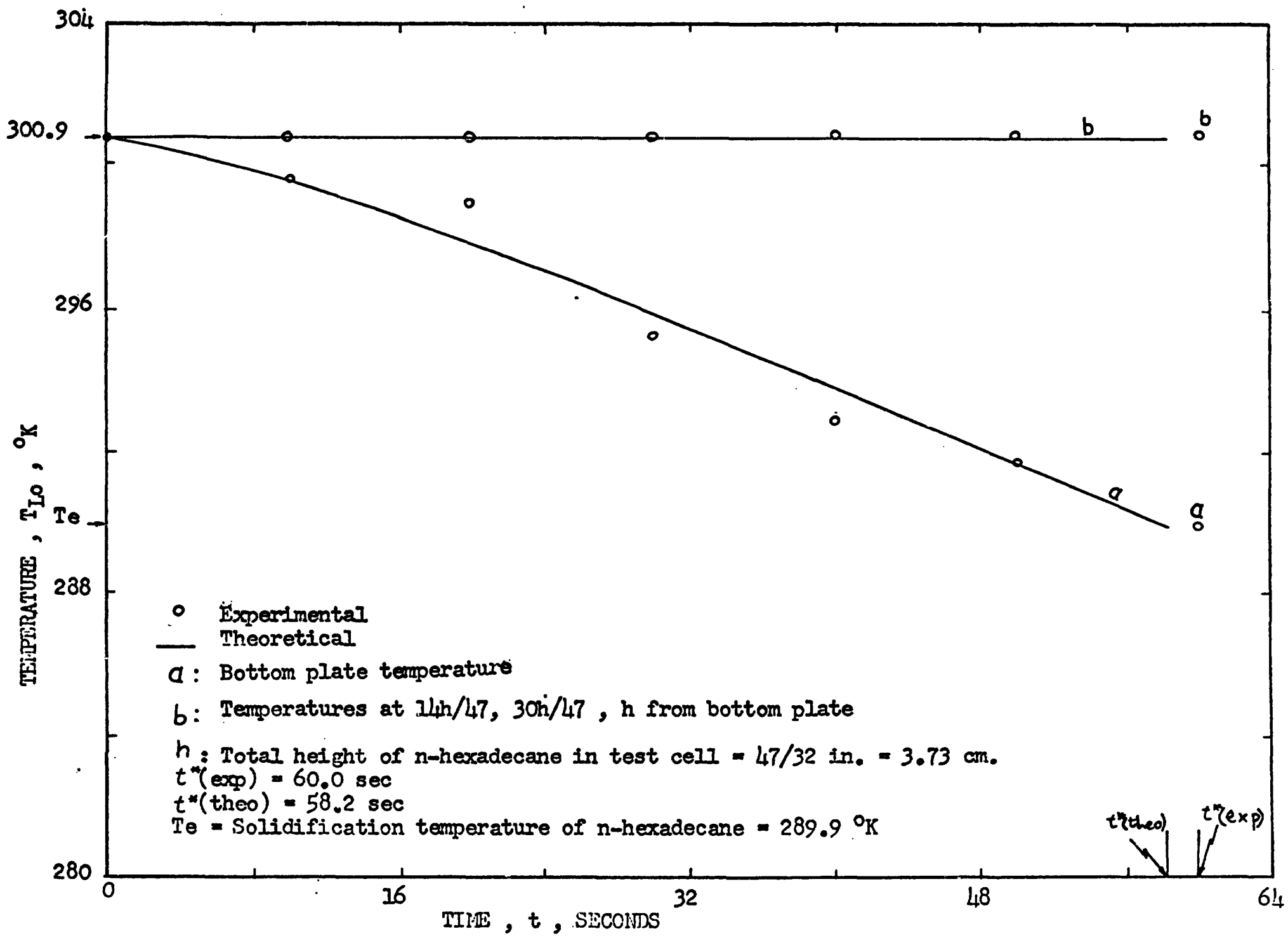
304
300.9
296
Te
288
280
TEMPERATURE , T_{Lo} , °K
0
16
32
48
64
TIME , t , SECONDS
b
b
a
a
t*(theo)
t*(exp)
Experimental
Theoretical
a : Bottom plate temperature
b : Temperatures at 14h/47, 30h/47 , h from bottom plate
h : Total height of n-hexadecane in test cell = 47/32 in. = 3.73 cm.
t*(exp) = 60.0 sec
t*(theo) = 58.2 sec
Te = Solidification temperature of n-hexadecane = 289.9 °K

Run 4 (cont.)

Figure 26. Temperature profiles (experimental and theoretical) for the combined pre-solidification and post-solidification problems: Run 4.

——— Theoretical

Experimental	Theoretical	
o	1	Bottom-plate thermocouple
+	2	Thermocouple at 14h/47 from bottom plate
Δ	3	Thermocouple at 30h/47 from bottom plate
□	4	Thermocouple at h from bottom plate

h = 47/32 in. = 3.73 cm.

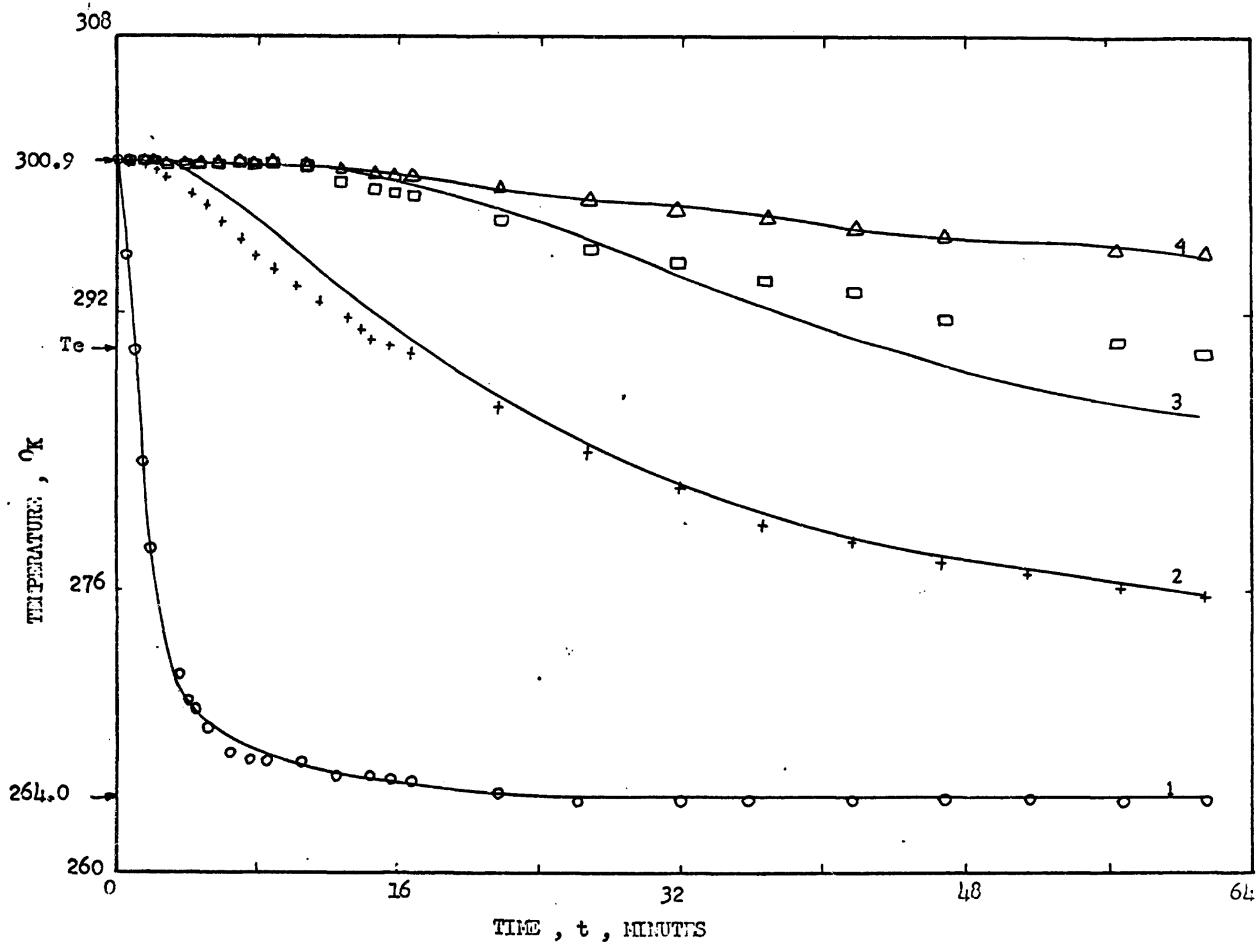
308
300.9
292
Te
276
264.0
260
0
16
32
48
64
TEMPERATURE , °K
TIME , t , MINUTES
1
2
3
4

Run 4 (cont.)

Figure 27. Height of solid n-hexadecane as a function of time: Run 4.

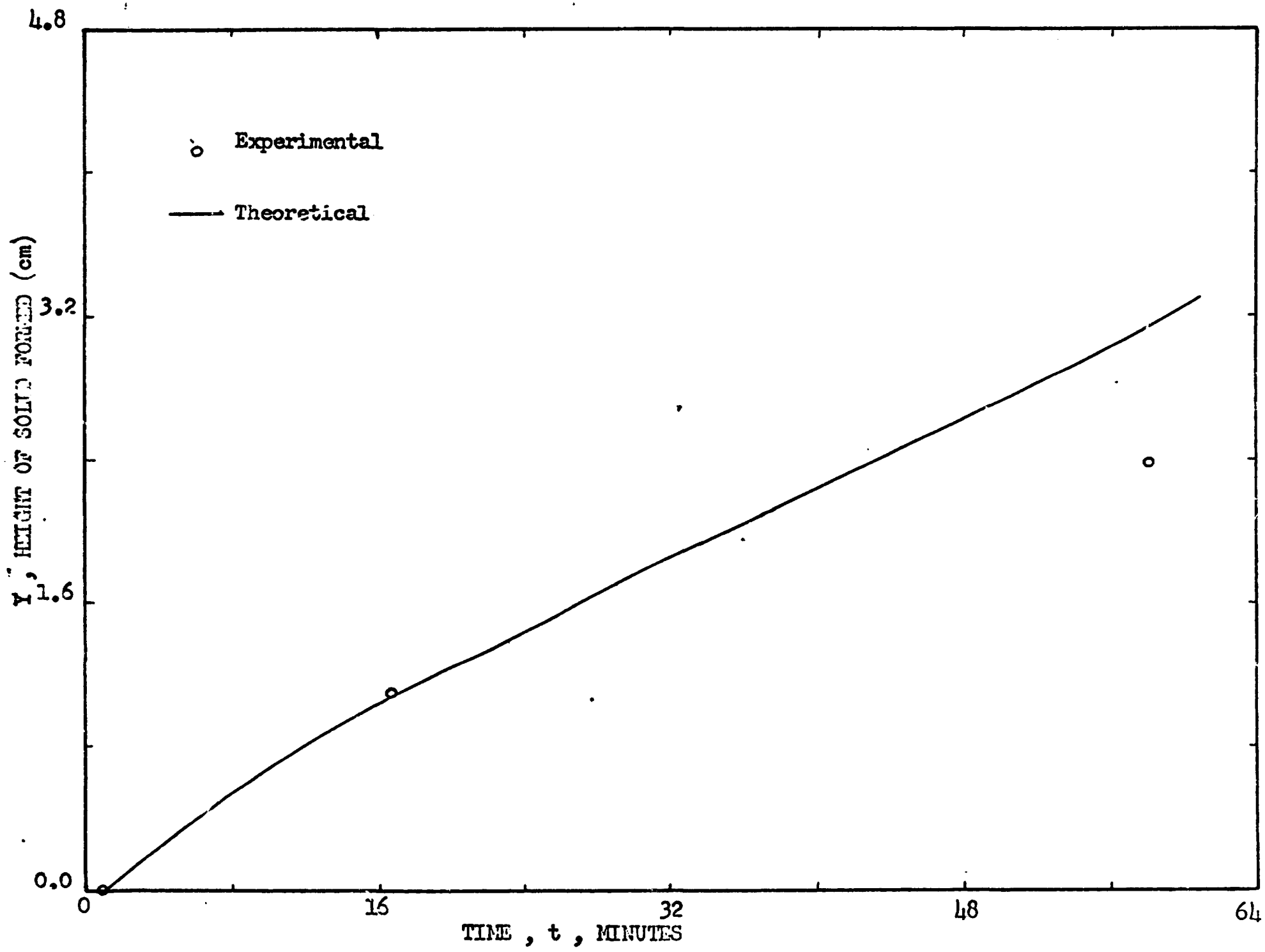
4.8
3.2
1.6
0.0
Y , HEIGHT OF SOLID FORMED (cm)
Experimental
Theoretical
0
16
32
48
64
TIME , t , MINUTES

Run 5

Table 6

Least-squares fits, $f_1(t)$ and $f_2(t)$, to experimentally-measured temperatures of the bottom and top plates, respectively: Run 5.

T_a = Ambient temperature = $297.8^{\circ}K$

T_{cpf} = Final steady-state temperature of the bottom plate = $262.7^{\circ}K$

$$f_1(t) = 262.7 + 35.1e^{-c_1 t} \pm 0.4^{\circ}K$$

where $c_1 = 6.5019191 \times 10^{-2} + 0.40147416t - 0.14185947t^2 + 2.2468639 \times 10^{-2}t^3 - 1.6686646 \times 10^{-3}t^4 + 4.7213390 \times 10^{-5}t^5$

and t is measured in minutes: $0.0 \leq t \leq 61.0$

$$f_2(t) = 262.7 + 35.1e^{-c_2 t} \pm 0.1^{\circ}K$$

where $c_2 = -3.3434403 \times 10^{-4} + 2.4737272 \times 10^{-4}t - 5.7413214 \times 10^{-6}t^2 + 5.2857290 \times 10^{-8}t^3 - 1.7660905 \times 10^{-10}t^4$

and t is measured in minutes: $0.0 \leq t \leq 61.0$

Run 5 (cont.)

Figure 28. Temperature profiles (experimental and theoretical) for the pre-solidification problem: Run 5.

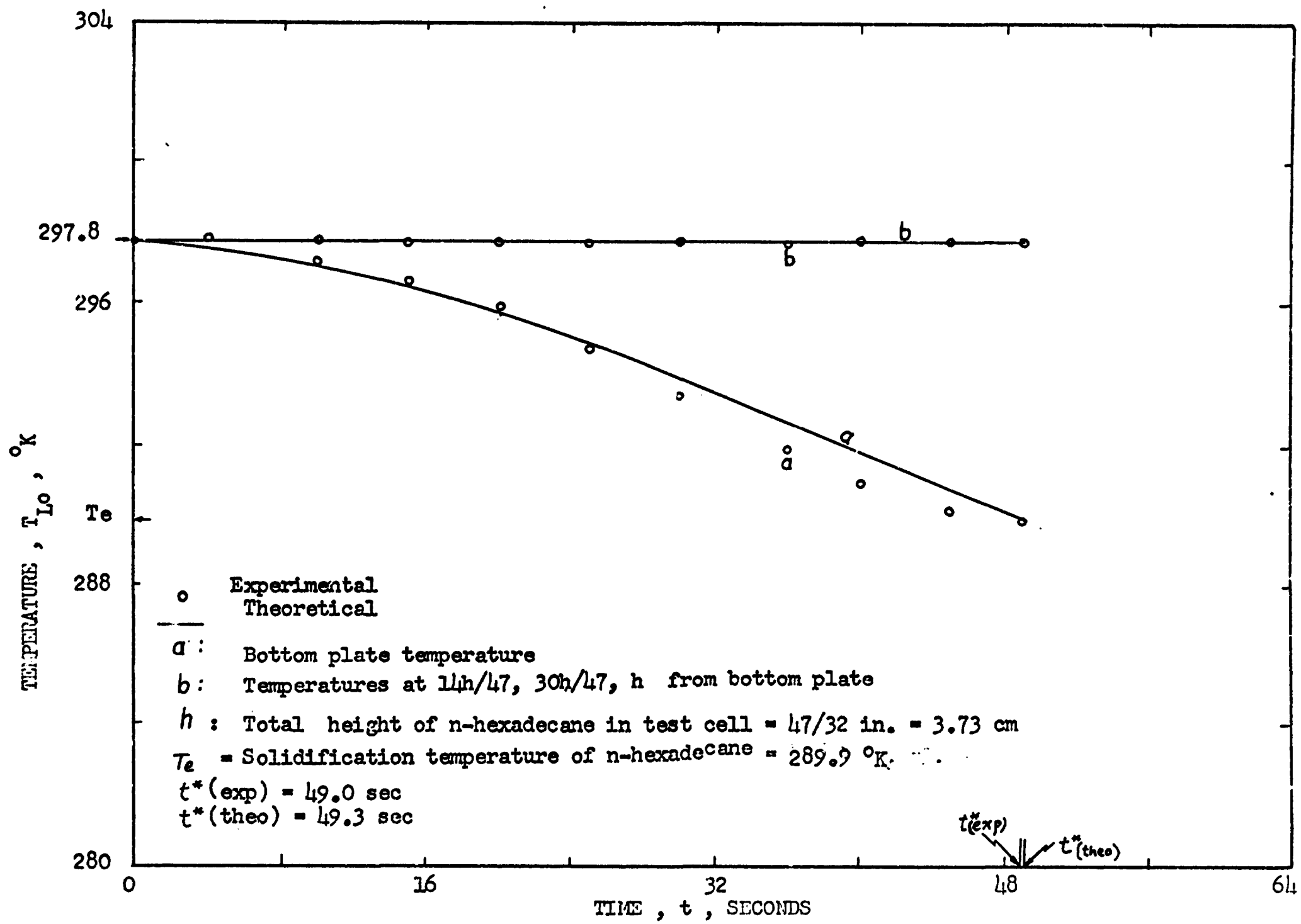
304
297.8
296
Te
288
280
TEMPERATURE , T_{Lo} , °K
0
16
32
48
64
TIME , t , SECONDS
b
b
a
a
$t^*_{(exp)}$
$t^*_{(theo)}$
o Experimental
Theoretical
a : Bottom plate temperature
b : Temperatures at 14h/47, 30h/47, h from bottom plate
h : Total height of n-hexadecane in test cell = 47/32 in. = 3.73 cm
T_e = Solidification temperature of n-hexadecane = 289.9 °K.
t^*(exp) = 49.0 sec
t^*(theo) = 49.3 sec

Run 5 (cont.)

Figure 29. Temperature profiles (experimental and theoretical) for the combined pre-solidification and post-solidification problems: Run 5.

——— Theoretical

Experimental	Theoretical	
o	1	Bottom-plate thermocouple
+	2	Thermocouple at 14h/47 from bottom plate
Δ	3	Thermocouple at 30h/47 from bottom plate
□	4	Thermocouple at h from bottom plate

h = 47/32 in. = 3.73 cm.

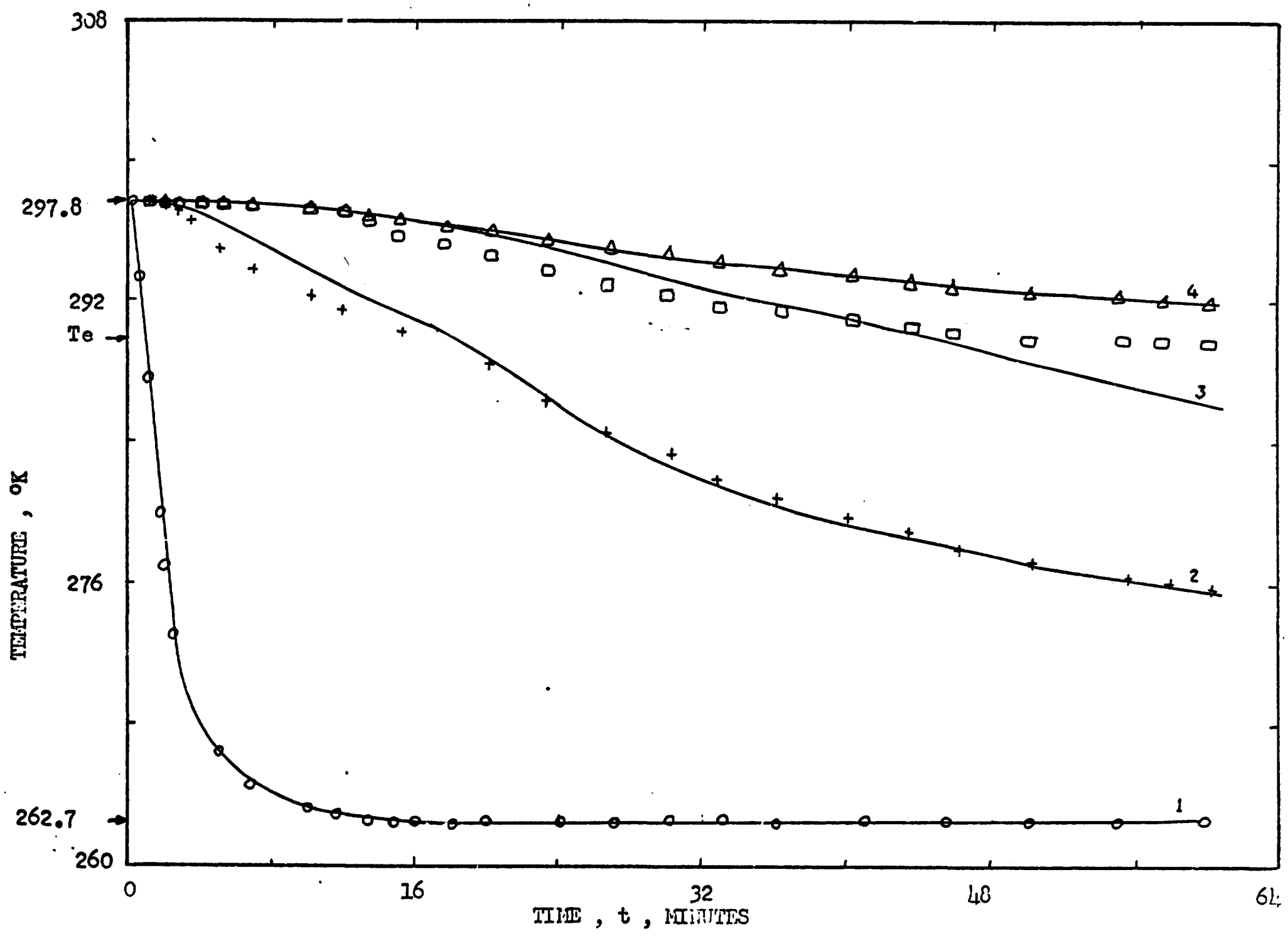
308
297.8
292
Te
276
262.7
260
TEMPERATURE , °K
0
16
32
48
64
TIME , t , MINUTES
1
2
3
4

Run 5 (cont.)

Figure 30. Height of solid n-hexadecane as a function of time: Run 5.

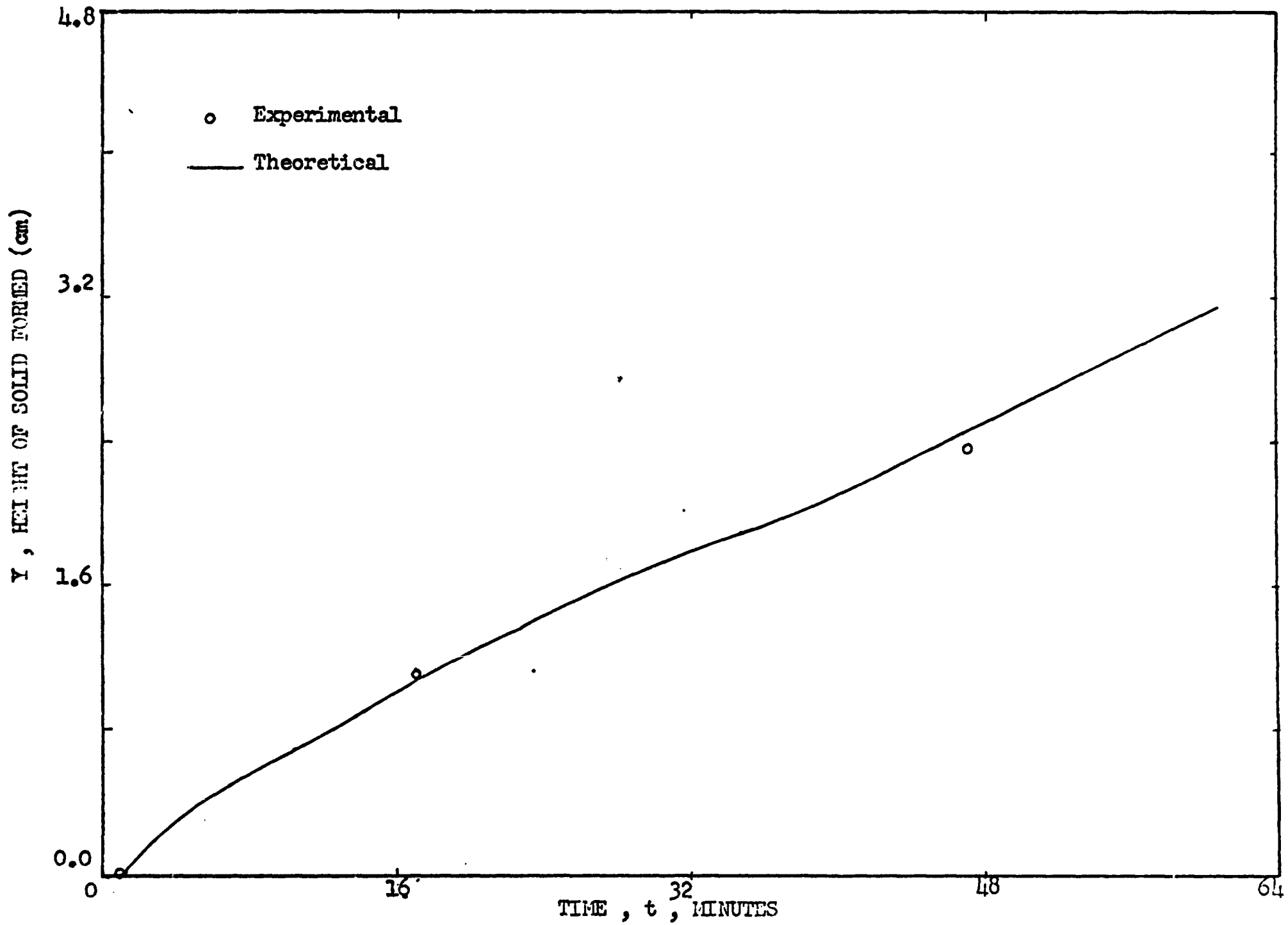
4.8
3.2
1.6
0.0
Y , HEIGHT OF SOLID FORMED (cm)
Experimental
Theoretical
0
16
32
48
64
TIME , t , MINUTES

Run 6

Table 7

Least-squares fits, $f_1(t)$ and $f_2(t)$, to experimentally-measured temperatures of the bottom and the top plates, respectively: Run 6.

T_a = Ambient temperature = 298.2°K

T_{cpf} = Final steady-state temperature of the bottom plate = 261.7

$$f_1(t) = 261.7 + 36.5e^{-c_1 t} \pm 0.5^{\circ}K$$

where $c_1 = 6.6373908 \times 10^{-2} + 3.6587915 \times 10^{-1}t - 1.1399978 \times 10^{-1}t^2 + 1.4684732 \times 10^{-2}t^3 - 8.4706573 \times 10^{-4}t^4 + 1.7879879 \times 10^{-5}t^5$

and t is measured in minutes: $0.0 \leq t \leq 62.0$

$$f_2(t) = 261.7 + 36.5e^{-c_2 t} \pm 0.3^{\circ}K$$

where $c_2 = -3.9221055 \times 10^{-4} + 3.7329234 \times 10^{-4}t - 1.0960065 \times 10^{-5}t^2 + 1.3965306 \times 10^{-7}t^3 - 8.2314786 \times 10^{-10}t^4 + 1.8183611 \times 10^{-12}t^5$

and t is measured in minutes: $0.0 \leq t \leq 62.0$

Run 6 (cont.)

Figure 31. Temperature profiles (experimental and theoretical) for the pre-solidification problem: Run 6.

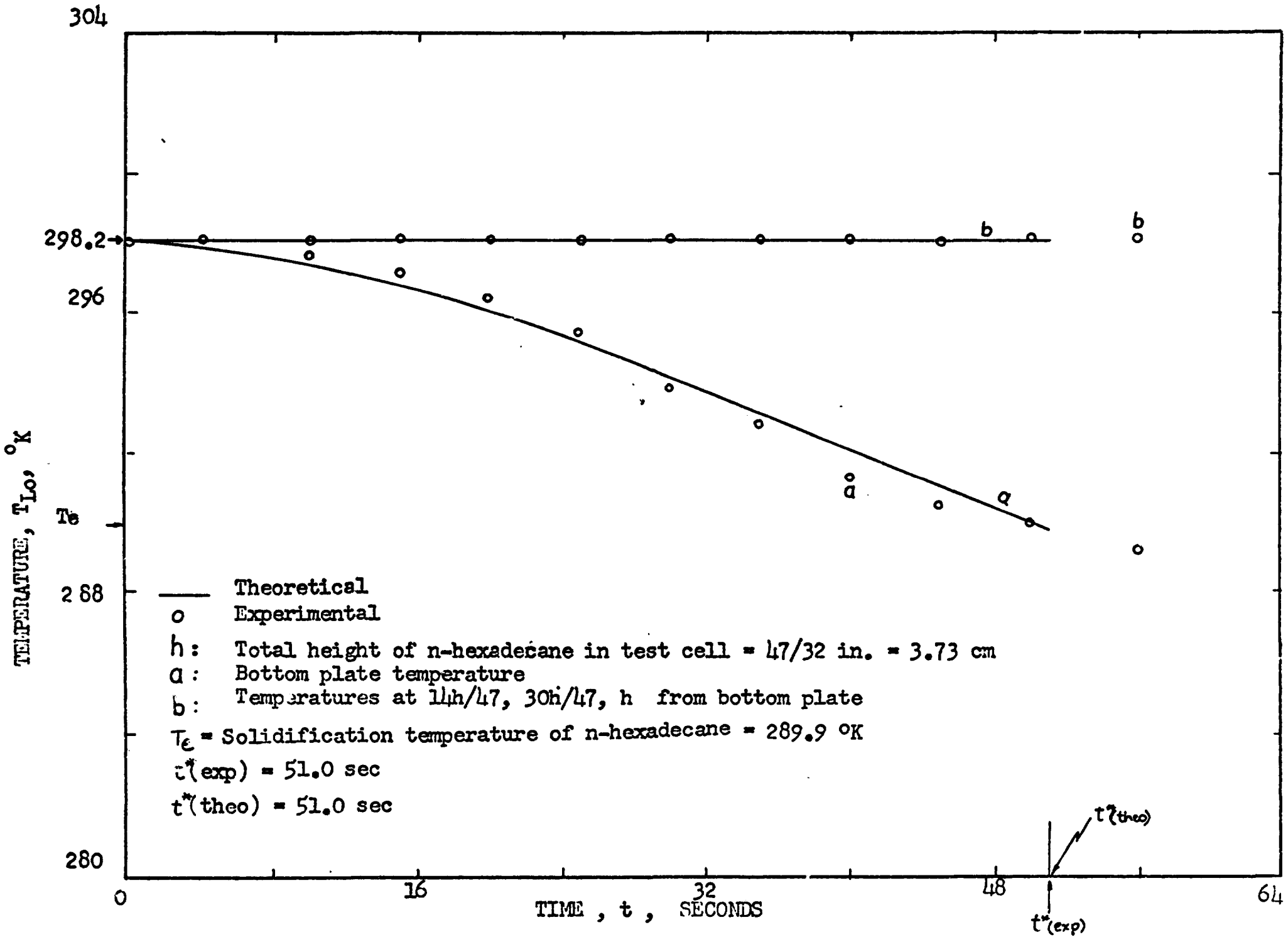
304
298.2
296
Te
288
280
TEMPERATURE, T_L, °K
0
16
32
48
64
TIME , t , SECONDS
b
b
a
a
Theoretical
Experimental
h : Total height of n-hexadecane in test cell = 47/32 in. = 3.73 cm
a : Bottom plate temperature
b : Temperatures at 14h/47, 30h/47, h from bottom plate
T_E = Solidification temperature of n-hexadecane = 289.9 °K
t*(exp) = 51.0 sec
t*(theo) = 51.0 sec
t*(theo)
t*(exp)

Run 6 (cont.)

Figure 32. Temperature profiles (experimental and theoretical) for the combined pre-solidification and post-solidification problems: Run 6.

——— Theoretical

Experimental	Theoretical	
o	1	Bottom-plate thermocouple
+	2	Thermocouple at 14h/47 from bottom plate
Δ	3	Thermocouple at 30h/47 from bottom plate
□	4	Thermocouple at h from bottom plate

h = 47/32 in. = 3.73 cm.

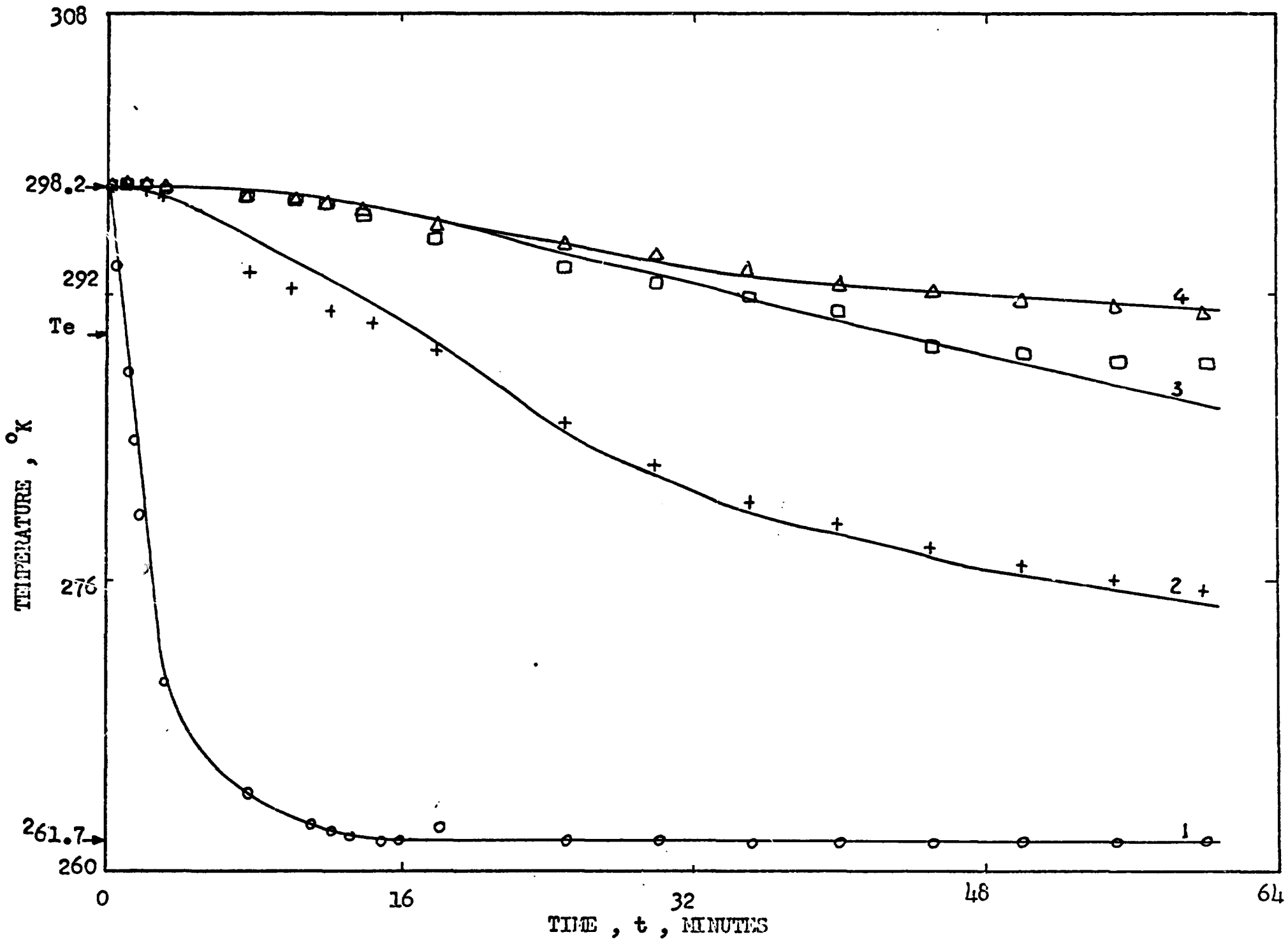
308
298.2
292
Te
276
261.7
260
TEMPERATURE , °K
0
16
32
48
64
TIME , t , MINUTES
1
2
3
4

Run 6 (cont.)

Figure 33. Height of solid n-hexadecane as a function of time: Run 6.

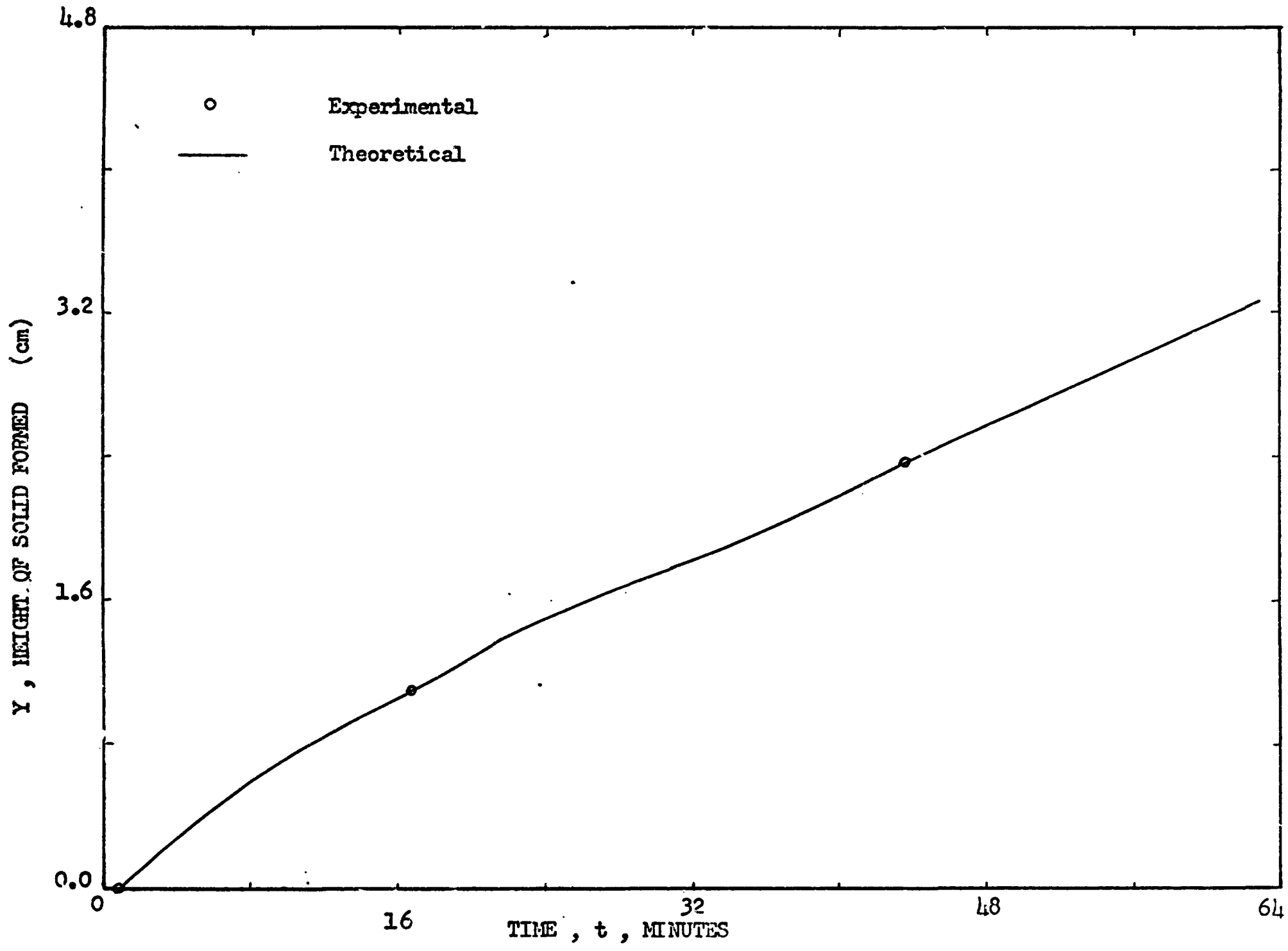
4.8
3.2
1.6
0.0
Y , HEIGHT OF SOLID FORMED (cm)
Experimental
Theoretical
0
16
32
48
64
TIME , t , MINUTES

CONCLUSIONS

In general, good agreement between experimental and theoretical results has been observed. Therefore, it seems obvious to conclude that the numerical analysis developed in this study has certain advantageous characteristics that make it extremely suitable for the study of problems involving unidimensional melting or freezing. However, it has some disadvantages, too.

The applicability of the numerical method developed here may be extended to cylindrical and spherical coordinates and for other geometric systems for which cross-sectional areas are functions of the distance from the origin only. The method also reduces the time and the memory bank used up by the computer program as compared to those used in explicit finite difference formulations. The use of polynomial fits of the temperatures of the boundaries, as has been done in this study, makes it unnecessary to calculate actual heat-transfer rates through the boundaries in order to solve similar problems with time-dependent boundary conditions.

However, one obvious disadvantage of the method used in this study, is that it is approximate. Heat gains or losses were neglected in all but one dimension. The boundary conditions which were used to solve the one-dimensional model

problem were only approximations of the actual boundary conditions or the experimentally-observed boundary conditions. Convection in the liquid phase was also neglected. Truncation errors in the formulation of the finite difference equations and the round-off errors in the computer programs which were used to calculate the theoretical results also contributed to the errors in the theoretical results. Average but different physical properties were used for the liquid and solid phases in the theoretical analysis whereas the actual physical properties of the two phases were temperature dependent. In addition to all these sources of error, there was some error in obtaining the experimental data, mainly due to built-in errors in the calibration of the experimental equipment and the judgement of this experimenter.

Although a good general agreement was obtained between experimental and theoretical results, it must be cautioned that the numerical treatment used in this study is rather involved and could hardly be applied to freezing or melting in systems with more than one coordinate dimension or in problems in which convective effects are being considered. In such cases, the assumption of partially-solidified elements should be eliminated and more conventional procedures (explicit finite difference formulations, "super-heat" method, "pseudo-specific heat" method, etc.) should be applied.

More accurate results and better theoretical models

would be obtained if heat gains, convective effects, interface area effects and other sources of error could be included in the theoretical analysis. Two or three-dimensional models should also be studied in order to obtain better theoretical results. It would also be extremely convenient to develop a more refined method of measuring heat inputs and losses and of establishing the actual time-dependent boundary conditions.

A study that included the study of convective effects as the test cell was tilted at various angles would be desirable, since convection definitely affects the solidification phenomena. In such a study it would no longer be necessary to minimize convection in the liquid phase by cooling the test cell from below. In the same category as a study of convective effects would be a study of the effects of mechanical shaking or vibrations on the solidification process. It is evident that the rate of heat transfer is the limiting factor for the practical applications of fusible materials as thermal controllers. Thus efforts should be made to increase the heat-transfer area and to improve the performance of the cell as a whole.

Nucleation was negligible in the present study, but it would be of interest to study the solidification of materials in which the effects of nucleation are appreciable.

Since outer space is virtually a vacuum, a study of the solidification process in situations in which the test cell

is kept in a vacuum could be useful in predicting the performance of the test material in outer space as a thermal controller. In such an experiment, care should be taken to prevent leaks from developing in the test cell. Radiation would be the main mode of free heat transfer between the test cell and its surroundings, besides the forced heat transfer due to the circulating coolant.

NOMENCLATURE

Text	Computer	
A	AO	Constant term in an exponential equation
A_i		Coefficient of $\theta_{i-1,j+1}$ in a tridiagonal matrix equation
α_L		Liquid-phase thermal diffusivity
α_s		Solid-phase thermal diffusivity
a_R		Fraction of a time step between the point (R, j+1) and the intersection of the interface with the Rth space grid line
B	A1	Constant in an exponential equation
B_i		Coefficient of $\theta_{i,j+1}$ in a tridiagonal matrix equation
b_i	SMALLB(I)	A term in the solution to a tridiagonal matrix equation for the ith space node
C_i		Coefficient of $\theta_{i+1,j+1}$ in a tridiagonal matrix equation
c(t)		Coefficient of the exponent in an exponential equation; a value obtained by a least-squares fit of c'(t)
c'(t)		Coefficient of the exponent in an exponential equation as calculated directly from experimentally-measured temperatures
$c_1(t)$	C(I)	Coefficient of the exponent in a least-squares exponential fit of the temperatures of the bottom plate
$c_2(t)$	C(I)	Coefficient of the exponent in a least-squares exponential fit of the temperatures of the top plate

Text	Computer	
c_{pL}		Liquid-phase specific heat
c_{ps}		Solid-phase specific heat
d_i	D(I)	Right-hand side of the ith tridiagonal matrix equation
$\Delta\tau, \Delta\tau_o$	AK	Dimensionless time increment
Δt		Time increment (sec)
Δz	AH	Dimensionless spatial increment
Δy		Spatial increment (cm)
$f_1(t)$	F11,F1, F(I,1)	Polynomial fit to experimentally-measured temperature profile of the bottom plate
$f_2(t)$	F21,F2, F(I,2)	Polynomial fit to experimentally-measured temperature profile of the top plate
H_f		Heat of solidification
h		Total height of n-hexadecane in a test cell at the start of an experiment
h_a	AH	Magnitude of finite dimensionless spatial step
J	AJ	Dimensionless constant
K_L		Liquid-phase thermal conductivity
K_s		Solid-phase thermal conductivity
^oK		Degree Kelvin
k_a	AK	Magnitude of finite dimensionless time step
L_o		Subscript referring to the liquid phase in the pre-solidification problem
L		Subscript referring to the liquid phase in the solidification problem

Text	Computer	
λ	GA	Dimensionless constant, α_s/α_L
M	AM	Dimensionless constant
N	N	Total number of spatial nodes, with the first node numbered '0'
$O(k_a)$		"Of the order of k_a"
p	P	k_a/h_a^2
q		Heat flow per unit area per unit time
q_i	Q(I)	A term in the solution to a tridiagonal matrix equation for the ith spatial node
R	R	Number of the spatial grid line (in the solid phase) which is on or next to the interface of solidification
ρ_L		Liquid-phase density
ρ_s		Solid-phase density
$S(\tau)$	BIGESS,S2, S3,S4	Dimensionless height of the solid phase which has been formed up to the dimensionless time, τ
s		Subscript referring to the solid phase in the solidification problem
T	T	Temperature
T_a	TA	Ambient temperature
T_{cpf}	AO	Final steady-state temperature of the bottom plate
T_{Lo}	TØ	Liquid-phase temperature in the pre-solidification problem
T_L	TØ	Liquid-phase temperature in the solidification problem

Text	Computer	
T_s	TS	Solid-phase temperature
Te	TE	Equilibrium temperature of solidification
t	TIME	Time (sec or min)
t*	TIMST	Time interval from the start of cooling to the start of solidification at the bottom plate (sec)
	TTP	Last experiment time at which a computer program should end
$\theta_{i,j}$		Dimensionless temperature for node located on spatial coordinate i and time coordinate j
θ_{Lo}	TETAZØ	Dimensionless liquid-phase temperature in the pre-solidification problem
θ_L	TZØ,TLØ	Dimensionless liquid-phase temperature for the solidification problem
θ_s	TSS,TS	Dimensionless solid-phase temperature
τ_o	TAUZRØ	Dimensionless time for the pre-solidification problem
τ_o^*	TAUOST	Dimensionless time interval from the start of cooling to the start of solidification at the bottom plate
τ	TAU	Dimensionless time for the solidification problem
x_{j+1}	X1	Fraction of a spatial element that has solidified by the (j+1)st time step
x_j	XØ	Fraction of a spatial element that has solidified by the jth time step
y	Y(I)	Spatial coordinate

Text	Computer	
$Y(t)$	Y1	Height of the solid phase formed up to time t
z	Z(I)	Dimensionless spatial coordinate
ε	OD	Maximum error in calculating the dimensionless height of the solid-phase during a dimensionless time step

Subindices	Subscripts	
i	I	Identifying number for finite spatial increment
j	J	Identifying number for finite time increment

LITERATURE CITED

1. Carslaw, H.S., and Jaeger, J.C., Conduction of heat in solids: Oxford Univ. Press, 2nd ed., p. 282-296 (1959).
2. Stefan, J., Uber die Theories der Eisbildung insbesondere über die Eisbildung in Polarmere: Annalen der Physik und Chemie, v. 42, p. 269 (1891).
3. Saito, S., On the distribution of temperature in steel ingots during cooling: Tohoku Imperial Univ. Science Reports, v. 10, p. 305 (1921).
4. Pekeris, C. L., and Slichter, L.B., Problem of ice formation: Jour. Applied Physics, v. 10, p. 135 (1939).
5. Danckwerts, P.V., Unsteady-state diffusion or heat conduction with moving boundary: Trans. Faraday Soc., v. 46, p. 701 (1950).
6. Booth, F., A note on the theory of surface diffusion reactions: Trans. Faraday Soc. (London), v. 44, p. 796 (1948).
7. Kreith, F., and Romie, F.E., A study of the thermal diffusion equation with boundary conditions corresponding to solidification or melting of materials initially at the fusion temperature: Proc. Phys. Soc., v. 68, p. 277 (1955).
8. Chambre, P.L., On the dynamics of phase growth: Quarterly Jour. of Mech. and Applied Math., v. 9, 224 (1956).

9. Chao, C.C., and Weiner, J.H., Heat conduction in semi-infinite solid in contact with linearly increasing mass of fluid: Quarterly of Applied Math., v. 14, p. 214 (1956).

10. Onsager, L., Reciprocal relations in irreversible processes: Physical Review, v. 37, p. 405 (1931).

11. Chambers, L.G., A variational principle for the conduction of heat: Quarterly Jour. of Mech. and Applied Math., v. 9, p. 234 (1956).

12. Biot, M. A., and Daughaday, H., Variational analysis of ablation: Jour. Aerospace Sciences, v. 29, p. 227 (1962).

13. Goodman, T.R., The heat-balance integral and its application to problems involving a change of phase: Trans. A.S.M.E., v. 80, p. 335 (1958).

14. Karman, T. von, and Pohlhausen, K., Zur naherungsweisen Integration der Differentialgleichungen der laminaren Grenzschicht: Zeitschrift fur Angewandte Math. und Mech., v. 1, p. 252 (1921).

15. Goodman, T.R., and Shea, J.J., The melting of finite slabs: Trans. A.S.M.E., Jour. Applied Mech., v. 27, p. 16 (1960).

16. Poots, G., An approximate treatment of a heat conduction problem involving a two-dimensional solidification front: Int. Jour. Heat and Mass Transfer, v. 5, p. 339 (1962).

17. Weiner, J.H., Transient heat conduction in multiphase media: Brit. Jour. Applied Physics, v. 6, p. 361 (1955).

18. Rubinshtein, L.I., On heat conduction in a multilayer medium with phase transitions: Doklady Akademiia Nauk Novaia Series, v. 79, p. 221 (1951).

19. Adams, C.M., Thermal considerations in freezing: Liquid metals and solidification: Am. Soc. for Metals, p. 187 (1958).

20. Dusinberre, G. M., Numerical methods for transient heat flow: Trans. A.S.M.E., v. 67, p. 703 (194[illegible]

21. Miller, M. L., Transient one-dimensional heat-conduction analysis for heterogeneous structures including an ablating surface: A.S.M.E. Paper No. 59-HT-22 (1959).

22. Ehrlich, L.W., A numerical method of solving a heat flow problem with moving boundary: Jour. Assoc. Computing Machinery, v. 5, no. 2, p. 161-176 (1958).

23. Pujado, P.R., Melting of a finite paraffin slab: Master of Science Thesis no. T-1215, Colorado School of Mines, Golden, Colorado (1968).

24. Shlosinger, A.P., and Bentilla, E.W., Thermal control by use of fusible materials: Interim Report, Northrop Corporation, NSL65-16, Contract NAS8-11163 (1965).

25. Bentilla, E.W., Sterrett, K.F., and Karre, L.E., Thermal control by use of fusible materials: Final report, Northrop Corporation, NSL65-16-1, Contract NAS8-11163 (1966).

26. Bannister, T.C., Space thermal control using phase change: NASA Tech. Memo., NASA TMX-53402 (1966).

27. Bannister, T.C., and Bentilla, E.W., Study on thermal control by use of fusible materials: Inst. Environmental Sci., Ann. Tech. Mtg. Proc., p. 593-607 (1966).

28. Sharma, O.P., Rotenberg, M., and Penner, S.S., Phase-change problems with variable surface temperatures: A.I.A.A. Jour., v. 5, no. 4, p. 677-682 (1967).

29. Grodzka, P.G., and Fan, C., Thermal control by freezing and melting: Interim report, Lockheed Missiles and Space Company, HREC-1123-1, LMSC/HRECA 791342, Contract NAS8-21123 (1968).

30. Muehlbauer, J.C., and Sunderland, J.E., Heat conduction with freezing and melting: Applied Mechanics Review, v. 18, no. 12, p. 951-959 (1965).

31. Sanborn Company, Sanborn low level preamplifier, Models 150-1500, 150-1500A instruction manual: Sanborn Company, Waltham 54, Massachusetts.

32. Chemical Rubber Company, CRC lab apparatus: The Chemical Rubber Co., Cleveland, Ohio, p. 20 (1969).

33. Brown, Jr., A.R., Subroutine Fit (X,Y,N,K,B,IP), Colorado School of Mines, January 1967.

APPENDIX

FORTRAN IV Computer Program for obtaining exponential fits to experimentally-measured temperatures of the bottom and the top plates.

The subroutine which was called in this program had been written by A.R. Brown, Jr.[33] for obtaining ordinary polynomial fits by the least-squares method. The subroutine was modified before being used in this particular program.

```
*FORTRAN      LISTING          5708      UKANWA,ANTHONY O.
C   LISTING OF THE FOLLOWING SUBROUTINE MAY BE OBTAINED BY REQUEST
      SUBROUTINE FIT (X,Y,N,K,B,IP)
C LEAST SQUARES POLYNOMIAL CURVE FIT
C         WRITTEN FOR CDC6400 TAPE FORTRAN BY A K BROWN, JR.
C         COMPUTING CENTER, COLORADO SCHOOL OF MINES
C         26 JANUARY 1967
C     THIS SUBROUTINE USES CONVENTIONAL METHODS FOR OBTAINING THE NORMAL
C     EQUATIONS FOR A LEAST SQUARES POLYNOMIAL CURVE FIT OF DEGREE K,
C     SOLVES THE EQUATIONS BY GAUSSIAN ELIMINATION,THEN OPTIONALLY MAY
C     PRINT COEFFICIENTS,RESIDUALS,AND SUM OF SQUARES OF RESIDUALS.
C
C  ----WARNING----DO NOT EXTEND TO POLYNOMIAL DEGREE GREATER THAN 5----
C  ---THIS METHOD HAS BAD ROUNDOFF CHARACTERISTICS FOR HIGHER DEGREE---
C
C     CALLING SEQUENCE
C         X=ARRAY OF OBSERVATIONS OF INDEPENDENT VARIABLE
C         Y=ARRAY OF CORRESPONDING OBSERVATIONS OF DEPENDENT VARIABLE
C         N=NUMBER OF OBSERVATIONS
C
C         K=DEGREE OF FITTED POLYNOMIAL (NO GREATER THAN FIVE)
C         B=(OUTPUT) ARRAY OF COEFFICIENTS OF FITTED POLYNOMIAL
                        DIMENSION X(1),Y(1),B(6)
C         IP=PRINT SIGNAL. PRINT IF IP=1 AND DON≠T PRINT IF IP=0
C
                        DIMENSION A(7,7)
   60 FORMAT(20X,20HDEGREE OF EQUATION =,I2//(3H B(,I2,3H) =,E16.8/))
   61 FORMAT(1X,4F15.6)
   62 FORMAT(6HSS = ,F15.8/)
   63 FORMAT(/5X,11HINDEPENDENT,6X,9HPREDICTED,7X,8HOBSERVED,7X,8HRESIDU
     1AL/)
C
C  COMPUTE COEFFICIENTS OF NORMAL EQUATIONS
      K1=K+1
      K2=K+2
      KK=K+K
      DO 50 M=1,KK
      SUM=0.0
      DO 51 I1=1,N
   51 SUM=SUM+X(I1)**M
      I1=1+(M+1)/2
      DO 50 I=1,I1
      J=M-I+2
      IF (J-6) 55,55,50
   55 A(I,J)=SUM
      A(J,I)=SUM
   50 CONTINUE
      DO 54 I=1,K
      SUM=0.0
      DO 52 I1=1,N
   52 SUM=SUM+Y(I1)*X(I1)**I
   54 A(I+1,K2)=SUM
      SUM=0.0
      DO 53 I1=1,N
   53 SUM=SUM+Y(I1)
      A(1,K2)=SUM
      A(1,1)=N
C
C  SOLVE SYSTEM OF NORMAL EQUATIONS
      DO 110 I=1,K
      I1=I+1
      DO 110 J=I1,K1
      KK=K2+1
      DO 110 M=J,K2
```

```
      KK=K2
      DO 120 J=1,K1
      M=KK
      KK=KK-1
      SUM=0.0
      DO 121 I=M,K2
      IF (K2-I) 120,120,121
  121 SUM=SUM+A(KK,I)*B(I)
  120 B(KK)=(A(KK,K2)-SUM)/A(KK,KK)
C
C     PRINT RESULTS
      IF(IP) 75,75,72
   72 PRINT 60,K,(J,B(J+1),J=0,K)
   74 PRINT 63
      A(7,1)=0.0
      DO 70 I1=1,N
      SUM=0.0
      DO 71 I=1,K1
      J=K1-I+1
   71 SUM=SUM*X(I1)+B(J)
      A(7,2)=SUM-Y(I1)
      A(7,1)=A(7,1)+A(7,2)*A(7,2)
   70 PRINT 61,X(I1),SUM,Y(I1),A(7,2)
      PRINT 62,A(7,1)
   75 RETURN
      END
C
C
C           PROGRAM TO OBTAIN EXPONENTIAL FITS TO OBSERVED TEMPERATURES
C           OF THE BOTTOM AND TOP PLATES OF THE CELL IN THE FORM
C           F=A0+A1*EXP(-C*T),WHERE A0,A1 ARE CONSTANTS. C IS A POLYNOMIA
C           IN T
C
C             M=NUMBER OF OBSERVATIONS
C
      DIMENSION T(42),F(42,2),C(42),D(42),FCAL(42,2),R(42),X(42),Y(42),
     2B(6)
    1 FORMAT(10X,I2)
    2 FORMAT(F6.1)
   20 FORMAT(6X,F6.2)
    5 FORMAT(10X,4HA0 =,F7.2,6H  A1 =,F7.2)
    8 FORMAT(10X,3H B(,I  3H) =,E16.10/)
   21 FORMAT(10X,3HW =,F5  )
   61 FORMAT(1X,5F15.6)
   62 FORMAT(8H0SUM1 = ,F15.5/)
   63 FORMAT(/5X,11HINDEPENDENT,6X,9HPREDICTED,7X,8HOBSERVED,7X,8HRESID
     1UAL,7X,8HEXP C(I)/)
      L=1
      READ 1,M
      DO 3 I=1,M
    3 READ 2,T(I)
   30 DO 4 I=1,M
    4 READ 20,F(I,L)
      A0=F(M,1)
      A1=F(1,1)-A0
      PRINT 5,A0,A1
      I=2
    6 D(I)=F(I,L)-A0
      IF(D(I))9,9,7
    7 I=I+1
      GO TO 6
    9 W=I-2.0
      N1=I-1
      N=N1-1
```

```
      PRINT 21,W
      DO 40 J=1,N
      X(J)=T(J+1)
   40 Y(J)=C(J+1)
      K=1
      IP=1
   12 CALL FIT(X,Y,N,K,B,IP)
      PRINT 8,(I,B(I+1),I=0,K)
      SUM1=0.0
      DO 13 I=1,M
      TOTAL=0.0
      DO 16 J=0,K
      KT=K-J+1
   16 TOTAL=TOTAL*T(I)+B(KT)
      C(I)=TOTAL
      FCAL(I,L)=A0+A1*EXPF(-C(I)*T(I))
      R(I)=FCAL(I,L)-F(I,L)
   13 SUM1=SUM1+R(I)**2
      PRINT 63
      DO 14 I=1,M
   14 PRINT 61,T(I),FCAL(I,L),F(I,L),R(I),C(I)
      PRINT 62,SUM1
      K=K+1
      IF(K-5)12,12,15
   15 L=L+1
      IF(L-2)30,30,26
   26 I=XEXIT(0)
      END
```

```
ERASABLE STORAGE      1 3154 TO 1 4556
        A0 = 263.26   A1 =  37.00
        W = 24.0
                    DEGREE OF EQUATION = 1

B( 0) =    .36456316E 00

B( 1) =    .62075666E-02
```

INDEPENDENT	PREDICTED	OBSERVED	RESIDUAL
.100000	.365184	.163491	.201693
.200000	.365805	.164850	.200955
.300000	.366425	.233195	.133231
.400000	.367046	.263401	.103646
.500000	.367667	.321861	.045806
.600000	.368288	.371906	-.003618
.700000	.368908	.413551	-.044642
.800000	.369529	.417217	-.047687
.900000	.370150	.370859	-.000709
1.000000	.370771	.384074	-.013303
1.100000	.371392	.393513	-.022121
1.600000	.374495	.464387	-.089892
2.100000	.377599	.494431	-.116832
2.600000	.380703	.507070	-.126368
3.100000	.383807	.494025	-.110218
3.600000	.386910	.478847	-.091936
4.100000	.390014	.473954	-.083940
4.600000	.393118	.483614	-.090496
5.100000	.396222	.436201	-.039979
6.100000	.402429	.429126	-.026696
7.100000	.408637	.410954	-.00231[illegible]

APPENDIX

FORTRAN IV Computer Program for solving the pre-solidification problem.

```
WFORTRAN      EISTANO
      DIMENSION TETAZO(48),Q(48),D(48),SMALLB(48),B(6,2),Z(48),TZO(48),
     1Y(48),TO(48)
    1 FORMAT(7X,2I1,I2)
    2 FORMAT(F6.2,F5.2)
    3 FORMAT(2E17.10)
    5 FORMAT(F6.2)
    6 FORMAT(//10X,14HTAU SUB ZERO =,E16.8,3X,6HTIME =,E16.8)
    7 FORMAT(/10X,1HZ,6X,13HTETA SUB ZERO,9X,1HY,11X,11HTEMPERATURE/)
    8 FORMAT(3X,F8.5,6X,F13.10,3X,F13.10,3X,F13.10)
   69 FORMAT(//10X,19HTAU SUB ZERO STAR =,E16.8,3X,11HTIME STAR =,E16.8
     1)
      READ 1,K1,K2,N
      READ 2,A0,A1
      KK=K1+1
      DO 12 I=1,6
   12 READ 3,B(I,1),B(I,2)
      READ 5,TA
      TE=289.86
      AK=1./15300.
      AH=1./47.
      P=AK/(AH**2)
      N1=N+1
      TAUZRO=0.0
      TIM=0.0
      DO 10 I=1,N1
      TETAZO(I)=TA/TE
      TO(I)=TE*TETAZO(I)
      W1=I-1.0
      Z(I)=W1*AH
   10 Y(I)=(Z(I)*47.*2.54)/32.
   19 PRINT 6,TAUZRO,TIM
      PRINT 7
      DO 11 I=1,N,2
   11 PRINT 8,Z(I),TETAZO(I),Y(I),TO(I)
      PRINT 8,Z(N1),TETAZO(N1),Y(N1),TO(N1)
      T1=255.0*TAUZRO
      T=T1+255.0*AK
      TAUZRO=TAUZRO+AK
      TIM=TAUZRO*15300.0
      SU1=0.0
      TOT1=0.0
      KT=K2+1
      DO 13 I=0,K1
      KR=KK-I
   13 SU1=SU1*T+B(KR,1)
      DO 14 I=0,K2
      KP=KT-I
   14 TOT1=TOT1*T+B(KP,2)
      F11=A0+A1*EXPF(-SU1*T)
      F21=A0+A1*EXPF(-TOT1*T)
            TZO(1)=F11/TE
            TZO(N1)=F21/TE
      D(1)=TZO(1)
      D(N1)=TZO(N1)
      SMALLB(1)=0.0
      Q(1)=D(1)
      DO 15 I=2,N
      D(I)=((+P/2.)*TETAZO(I-1))+((1-P)*TETAZO(I))+((P/2.)*TETAZO(I+1))
      SMALLB(I)=(-P/2.)/(1.+P+((P/2.)*SMALLB(I-1)))
   15 Q(I)=(D(I)+((P/2.)*Q(I-1)))/(1.+P+((P/2.)*SMALLB(I-1)))
      Q(N1)=D(N1)
      TZO(N1)=Q(N1)
       DO 30 K3=1,N
```

```
20    DO 21 I=1,N1
      TETAZO(I)=TZO(I)
21    TO(I)=TE*TETAZO(I)
      GO TO 19
22    V=(TETAZO(1)-1.)/(TETAZO(1)-TZO(1))
      V1=V*P
      TZO(1)=1.0
      DO 23 I=2,N
23    TZO(I)=(V1*TETAZO(I-1))+((1.-2.*V1)*TETAZO(I))+(V1*TETAZO(I+1))
      TAU0ST= TAUZR0-(1.-V)*AK
      TIMST=15300.0*TAU0ST
      S=0.0
      DO 17 I=0,K2
      K4=KT-1
17    S=S*TAU0ST+B(K4,2)
      TZO(N1)=(A0+A1*EXPF(-S*TAU0ST))/TE
      DO 50 I=1,N1
50    TO(I)=TE*TZO(I)
      PRINT 69,TAU0ST,TIMST
      PRINT 7
      DO 18 I=1,N,2
18    PRINT 8,Z(I),TZO(I),Y(I),TO(I)
      PRINT 8,Z(N1),TZO(N1),Y(N1),TO(N1)
      I=XEXITF(0)
      END
```

ERASABLE STORAGE 1 2200 TO 1 5143

TAU SUB ZERO = .00000000E 00 TIME = .00000000E 00

Z	TETA SUB ZERO	Y	TEMPERATURE
.00000	1.0362243876	.0000000000	.3003600E 03
.04255	1.0362243876	.1587499984	.3003600E 03
.08511	1.0362243876	.3174999975	.3003600E 03
.12766	1.0362243876	.4762500018	.3003600E 03
.17021	1.0362243876	.6349999949	.3003600E 03
.21277	1.0362243876	.7937499993	.3003600E 03
.25532	1.0362243876	.9524999931	.3003600E 03
.29787	1.0362243876	1.1112499908	.3003600E 03
.34043	1.0362243876	1.2699999884	.3003600E 03
.38298	1.0362243876	1.4287499860	.3003600E 03
.42553	1.0362243876	1.5874999985	.3003600E 03
.46809	1.0362243876	1.7462499812	.3003600E 03
.51064	1.0362243876	1.9050000086	.3003600E 03
.55319	1.0362243876	2.0637499839	.3003600E 03
.59574	1.0362243876	2.2224999815	.3003600E 03
.63830	1.0362243876	2.3812499791	.3003600E 03
.68085	1.0362243876	2.5399999768	.3003600E 03
.72340	1.0362243876	2.6987500042	.3003600E 03
.76596	1.0362243876	2.8574999720	.3003600E 03
.80851	1.0362243876	3.0162499771	.3003600E 03
.85106	1.0362243876	3.1750000045	.3003600E 03
.89362	1.0362243876	3.3337499723	.3003600E 03
.93617	1.0362243876	3.4924999699	.3003600E 03
.97872	1.0362243876	3.6512499675	.3003600E 03
1.00000	1.0362243876	3.7306249663	.3003600E 03

TAU SUB ZERO = .65359477E-04 TIME = .10000000E 01

APPENDIX

FORTRAN IV Computer Program for solving the solidification problem.

```
.JKANEA,69049,1,C 791,TONY3,                    FORTRAN SOURCE LIST
      ISN        SOURCE STATEMENT

    0 $FTRAN TONY3   LIST
      C
      C        PHASE CHANGE THERMAL CONTROL - SOLIDIFICATION OF N-HEXADECANE
      C
      C        POST-SOLIDIFICATION PROBLEM
      C
      C
    1          DIMENSION TETAZD(48),Q(48),D(48),SMALLB(48),B(6,2),Z(48),TZD(48
              1Y(48),TD(48),TLD(48),TS(48),TSS(48),TETAES(48)
    2        1 FORMAT(7X,2I1,I2)
    3        2 FORMAT(F6.2,F5.2)
    4        3 FORMAT(2F17.10)
    5        5 FORMAT(F6.2)
    6        9 FORMAT(//10X,5HTAU =,E16.8,3X,11HTIME(SEC) =,E16.8)
    7       15 FORMAT(3X,F8.5,3X,F7.3,2(3X,F11.5,3X,F7.2))
   10       24 FORMAT(10X,3HS =,E16.8,3X,3HH =,E16.8)
   11       25 FORMAT(10X,13HSOLID LIQ,CM =,E16.8,3X,20HGROWTH RATE,CM/SEC =,E1
              18//)
   12       26 FORMAT(/5X,1HZ,9X,5HY(CM),4X,10HTETA SUB L,1X,8HLIQ TEMP,5X,10-
              21HA SUB S,3X,8HSOL TEMP)
   13      130 FORMAT(7X,9HX(N+1) = ,E16.8,2X,9HR(N+1) = ,I3,3X,5HAN = ,E16.8)
   14      102 FORMAT(//3X,4HNG =,F4.1,3X,4HIK =,I20)
   15      106 FORMAT(//3X,4HNGG =,F4.1,3X,4HIR =,I20)
   16      113 FORMAT(//3X,4HAG =,F4.1,3X,4HX1 =,E16.8)
   17        6 FORMAT(6X,E11.4)
   20          READ 1,K1,K2,N
   24          READ 2,A0,A1
   25          READ 6,TTP
   26          KK=K1+1
   27          DO 12 I=1,6
   30       12 READ 3,B(I,1),B(I,2)
   32          READ 5,TA
   33          TE=289.86
   34          AK=2./15300.
   35          AH=1./47.
   36          P=AK/(AH**2)
   37          N1=N+1
   40          TAUZRD=0.0
   41          TIM=0.0
   42          DO 10 I=1,N1
   43          TETAZD(I)=TA/TE
   44          TD(I)=TE*TETAZD(I)
   45          QR=I
   46          W1=QR-1.0
   47          Z(I)=W1*AH
   50       10 Y(I)=(Z(I)*47.*2.54)/32.
   52       19 T1=255.0*TAUZRD
   53          T=T1+255.0*AK
   54          TAUZRD=TAUZRD+AK
   55          TIM=TAUZRD*15300.0
   56          SD1=0.0
   57          TDT1=0.0
   60          KT=K2+1
   61          DO 13 I=0,K1
   62          KR=KT-I
```

```
63      13  SQ1=SQ1*T+B(KB,1)
65          DO 14 I=0,K2
66          KP=KT-I
67      14  TOT1=TOT1*T+B(KP,2)
71          F1=A0+A1*EXP(-SQ1*T)
72          F2=A0+A1*EXP(-TOT1*T)
73                  TZU(1)=F1/TE
74                  TZU(N1)=F2/TE
75          D(1)=TZU(1)
76          D(N1)=TZU(N1)
77          SMALLB(1)=0.0
100         Q(1)=D(1)
101         DO 15 I=2,N
102         D(I)=((P/2.)*TETAZU(I-1))+((1.-P)*TETAZU(I))+((P/2.)*TETAZU(I+1
103         SMALLB(I)=(-P/2.)/(1.+P+((P/2.)*SMALLB(I-1)))
104     15  Q(I)=(D(I)+((P/2.)*Q(I-1)))/(1.+P+((P/2.)*SMALLB(I-1)))
106         Q(N1)=D(N1)
107         TZU(N1)=D(N1)
110         DO 30 K3=1,N
111         I=N1-K3
112     30  TZU(I)=Q(I)-SMALLB(I)*TZU(I+1)
114         IF(TZU(1)-1.)22,20,20
115     20  DO 21 I=1,N1
116         TETAZU(I)=TZU(I)
117     21  TU(I)=TE*TETAZU(I)
121         GO TO 19
122     22  V=(TETAZU(1)-1.)/(TETAZU(1)-TZU(1))
123         V1=V*P
124         TZU(1)=1.0
125         DO 23 I=2,N
126     23  TZU(I)=(V1*TETAZU(I-1))+((1.-2.*V1)*TETAZU(I))+(V1*TETAZU(I+1))
130         TAUOST= TAUZRU-(1.-7)*AK
131         TIMST=15300.0*TAUOST
132         S=0.0
133         DO 17 I=0,K2
134         K4=KT-I
135     17  S=S*TAUOST+B(K4,2)
137         TZU(N1)=(A0+A1*EXP(-S*TAUOST))/TE
140         DO 4 I=1,N1
141      4  TU(I)=TE*TZU(I)
143         BIGESS=0.0
144         U=0.0
145         U1=0.0
146         Y1=0.0
147         TAU=0.0
150         YU=0.0
151         TIME=TIMST
152         IRU=0
153         TS(1)=TZU(1)
154         TETAS(1)=TS(1)*TE
155         DO 31 I=2,N1
156         TS(I)=0.0
157     31  TETAS(I)=TS(I)*TE
161         AN=0.0
162         DP=P
```

```
ISN        SOURCE STATEMENT

163            AKK=AK
164            AH=2.463
165            AJ=2.367
166            PRINT 130,XU,IRU,AN
167            PRINT 9,TAU,TIME
170            PRINT 26
171            DO 126 I=1,N1
172      126   PRINT 16,Z(I),Y(I),TZU(I),TU(I),TS(I),TETAFS(I)
174            PRINT 24,BIGESS,U
175            PRINT 25,Y1,U1
176            LM=1
177            MN=8
200            JK=1
201       64   TAUI=TAU+AK
202            BM=LM
203            TADI=BM*60.0
204            M=1
205            TIME=15300.0*(TAUI+TAUOST)
206            T=255.0*(TAUI+TAUOST)
207            SUM=0.0
210            TUT=0.0
211            DO 33 I=0,K1
212            KR=KK-I
213       33   SUM=SUM*T+B(KK,1)
215            DO 34 I=0,K2
216            KP=KT-I
217       34   TUT=TUT*T+B(KP,2)
221            IF(JK.EQ.1)GO TO 213
224            GO TO 217
225      213   CD=EXP(-SUM*T)
226            IF(CD-0.10E-12)203,203,202
227      203   JK=4
230            GO TO 217
231      202   F1=A0+A1*CD
232            GO TO 204
233      217   F1=A0
234      204   F2=A0+A1*EXP(-TUT*T)
235            TSS(1)=F1/TE
236            TLD(N1)=F2/TE
237            D(1)=TSS(1)
240            D(N1)=TLD(N1)
241            D(N1)=D(N1)
242            D(1)=D(1)
243            SMALLB(1)=0.0
244            IF(TAU)100,214,218
245      214   S3=AH/2.0
246            GO TO 35
247      218   S3=BIGESS+DSI
250       35   AN=S3/AH
251      110   IR=AN
252            R=IR
253            Y1=AN-R
254      227   I1=IR+1
255            I2=I1+1
256            I3=I2+1
```

```
 ISN        SOURCE STATEMENT

 257        N3=N-1
 260        N2=N-2
 261        N4=N-3
 262        D(I2)=((2.0-X1)*(1.0-X1)*TZU(I2))+(2.0*P)
 263        C=-((2.0*P)*(1.0-X1))
 264        DRI=(2.0-X1)*(1.0-X1+(2.0*P))
 265        IF(IP-N2)36,39,40
 266   36   SMALLB(I2)=C/DRI
 267        Q(I2)=D(I2)/DRI
 270        DO 37 I=I3,N
 271        SMALLB(I)=(-P/2.)/(1.+P+((P/2.)*SMALLB(I-1)))
 272        D(I)=((P/2.)*TZU(I-1))+((1.-P)*TZU(I))+((P/2.)*TZU(I+1))
 273   37   Q(I)=(D(I)+((P/2.)*Q(I-1)))/(1.+P+((P/2.)*SMALLB(I-1)))
 275        J=N1-I2
 276        DO 38 K=1,J
 277        I=N1-K
 300   38   TLD(I)=Q(I)-SMALLB(I)*TLD(I+1)
 302        GO TO 40
 303   39   TLD(I2)=(D(I2)-(C*TLD(I3)))/DRI
 304   40   IF(IP-N)120,120,100
 305  120   GA=0.9627
 306        PA=P*GA
 307        DO 41 I=1,I1
 310   41   TLD(I)=0.0
 312        IK=IP-IRD
 313        IF(IK)101,42,50
 314  101   WG=1.1
 315        PRINT 102,WG,IK
 316        GO TO 100
 317   42   IF(IP-1)43,44,44
 320   43   TSS(I1)=D(1)
 321        GO TO 65
 322   44   AR=-(2.0*PA*X1)/(1.+X1)
 323        BR=(2.*PA)+X1
 324        D(I1)=(X1*TS(I1))+((2.*PA)/(1.+X1))
 325        IF(IP-2)45,46,46
 326   45   TSS(I1)=(D(I1)-(AR*TSS(IR)))/BR
 327        GO TO 65
 330   46   DO 47 I=2,IR
 331        SMALLB(I)=(-PA/2.0)/(1.+PA+((PA/2.)*SMALLB(I-1)))
 332        D(I)=((PA/2.)*TS(I-1))+((1.-PA)*TS(I))+((PA/2.)*TS(I+1))
 333   47   Q(I)=(D(I)+((PA/2.)*Q(I-1)))/(1.+PA+((PA/2.)*SMALLB(I-1)
 335   48   Q(I1)=(Q(I1)-(AR*Q(IR)))/(BR-(AR*SMALLB(IR)))
 336        TSS(I1)=Q(I1)
 337        DO 49 KN=1,IR
 340        I=I1-KN
 341   49   TSS(I)=Q(I)-SMALLB(I)*TSS(I+1)
 343        GO TO 65
 344   50   IF(IK-1)104,51,57
 345  104   WG=2.2
 346        PRINT 102,WG,IK
 347        GO TO 100
 350   51   ARMI=-PA
 351        BRMI=1.+(2.*PA)
 352        CMI=-PA
```

```
ISN        SOURCE STATEMENT

353            AR=-(2.*PA*X1)/(1.+X1)
354            BR=(2.*PA)+1.-X0+X1
355            D(IR)=TS(IR)
356            D(I1)=((2.*PA)/(1.+X1))+1.-X0+X1
357            IF(IR-1)105,45,52
360      105   GG=1.0
361            PRINT 106,GG,IR
362            GO TO 100
363       52   IF(IR-2)107,53,54
364      107   GG=2.0
365            PRINT 106,GG,IR
366            GO TO 100
367       53   SMALLB(IR)=CMI/(BRMI-(ARMI*SMALLB(IR-1)))
370            Q(IR)=(D(IR)-(ARMI*Q(IR-1)))/(BRMI-(ARMI*SMALLB(IR-1)))
371            GO TO 48
372       54   IK1=I1-2
373       55   DO 56 I=2,IK1
374            SMALLB(I)=(-PA/2.0)/(1.+PA+((PA/2.)*SMALLB(I-1)))
375            D(I)=((PA/2.)*TS(I-1))+((1.-PA)*TS(I))+((PA/2.)*TS(I+1))
376       56   D(I)=(D(I)+((PA/2.)*Q(I-1)))/(1.+PA+((PA/2.)*SMALLB(I-1))
400            GO TO 53
401       57   IF(IR-2)108,58,63
402      108   GG=3.3
403            PRINT 102,GG,IR
404            GO TO 100
405       58   ARM2=-PA
406            ARMI=-PA*((1.+X1)/(2.-X0+X1))
407            BRM2=1.+(2.*PA)
410            AR=-(2.*PA*X1)/(1.+X1)
411            BRMI=((2.*PA)*((1.+X1)/(2.-X0+X1)))+1.
412            BR=(2.*PA)+(2.-X0+X1)
413            CM2=ARM2
414            CMI=ARMI
415            D(I1)=(2.-X0+X1)+((2.*PA)/(1.+X1))
416            D(IR)=1.
417            IK2=I1-2
420            D(IK2)=TS(IK2)
421            IF(IR-2)109,53,59
422      109   GG=3.0
423            PRINT 106,GG,IR
424            GO TO 100
425       59   IF(IR-3)112,60,61
426      112   GG=4.0
427            PRINT 106,GG,IR
430            GO TO 100
431       60   SMALLB(IK2)=CM2/(BRM2-(ARM2*SMALLB(IK2-1)))
432            Q(IK2)=(D(IK2)-(ARM2*Q(IK2-1)))/(BRM2-(ARM2*SMALLB(IK2-1
433            GO TO 53
434       61   IK1=I1-3
435            DO 62 I=2,IK1
436            SMALLB(I)=(-PA/2.0)/(1.+PA+((PA/2.)*SMALLB(I-1)))
437            D(I)=((PA/2.)*TS(I-1))+((1.-PA)*TS(I))+((PA/2.)*TS(I+1))
440       62   D(I)=(D(I)+((PA/2.)*Q(I-1)))/(1.+PA+((PA/2.)*SMALLB(I-1)
442            GO TO 53
443       63   PSI=PSI/2.
```

```
ISN        SOURCE STATEMENT

444          P=P/2.
445          AH=AH/2.
446          GO TO 64
447     65   DO 111 I=I2,N1
450    111   TSS(I)=0.0
452          IF(NP.EQ.1)GO TO 631
455          IF(IR-N4)417,417,418
456    417   SIGPS=-((2.5-X1)*TLO(I2))+((4.-(2.*X1))*TLO(I3))-((1.5-X1)*TL
            1+1))
457    418   IF(IR-2)421,420,420
460    420   SIGPS=((0.5+X1)*TSS(IR-1))-((2.+(2.*X1))*TSS(IR))+((3.+(2.*X1
            2SS(I1))
461    421   IF(X1.LE.0.25)GO TO 66
464          GO TO 79
465     66   IF(IR-N2)425,425,426
466    425   SIGL=(((2.-X1)/(1.-X1))*TLO(I2))-(((1.-X1)/(2.-X1))*TLO(I3))-
            4-(2.*X1))/((1.-X1)*(2.-X1)))
467    426   IF(IP.EQ.0)GO TO 68
472          GO TO 69
473     68   S2=BIGESS+(P*AH)*(((4.0*AH)*(1.0-TSS(1)))-(AJ*SIGL))
474          GO TO 90
475     69   IF(IP.EQ.1)GO TO 70
500          GO TO 71
501     70   S2=BIGESS+(P*AH)*((AM*((1.0-TSS(1))/(1.+X1)))-(AJ*SIGL))
502          GO TO 90
503     71   IF(IR.LE.N4)GO TO 72
506          GO TO 73
507     72   S2=BIGESS+(P*AH)*((AM*SIGPS)-(AJ*SIGL))
510          GO TO 90
511     73   IF(IR.EQ.N2)GO TO 74
514          GO TO 75
515     74   S2=BIGESS+(P*AH)*((AM*SIGPS)-(AJ*((TLO(N1)-1.)/(2.-X1))))
516          GO TO 90
517     75   IF(IR.EQ.N3)GO TO 76
522          GO TO 77
523     76   S2=BIGESS+(P*AH)*((AM*SIGPS)-(AJ*((TLO(N1)-1.)/(1.-X1))))
524          GO TO 90
525     77   IF(IR.EQ.N)GO TO 78
530          GG=5.0
531          PRINT 106,GG,IR
532          GO TO 100
533     78   S2=1.
534          GO TO 90
535     79   IF(X1.LE.0.75)GO TO 80
540          GO TO 87
541     80   IF(IP.EQ.0)GO TO 477
544          GO TO 476
545    476   SIGS=((X1/(1.+X1))*TSS(IR))-(((1.+X1)/X1)*TSS(I1))+((1.+(2.*X
            3(X1+(X1**2)))
546    477   IF(IR-N2)478,478,500
547    478   SIGL=(((2.-X1)/(1.-X1))*TLO(I2))-(((1.-X1)/(2.-X1))*TLO(I3))-
            6-(2.*X1))/((1.-X1)*(2.-X1)))
550    500   IF(IP.EQ.0)GO TO 81
553          GO TO 82
554     81   S2=BIGESS+(AH*P)*(((AM/X1)*(1.-TSS(1)))-(SIGL*AJ))
```

```
 ISN        SOURCE STATEMENT

 555            GO TO 90
 556      82    IF(IP.LE.N2)GO TO 83
 561            GO TO 84
 562      83    S2=BIGESS+(P*AH)*((AM*SIGS)-(AJ*SIGL))
 563            GO TO 90
 564      84    IF(IP.EQ.N3)GO TO 85
 567            GO TO 86
 570      85    S2=BIGESS+(AM*P)*((AM*SIGS)-(AJ*((TLO(N1)-1.)/(1.-X1))))
 571            GO TO 90
 572      86    IF(IP.EQ.N)GO TO 78
 575            GG=0.0
 576            PRINT 106,GG,IP
 577            GO TO 100
 600      87    IF(X1.LE.1.)GO TO 88
 603            AG=1.0
 604            PRINT 113,AG,X1
 605            GO TO 100
 606      88    IF(IP.EQ.0)GO TO 533
 611            GO TO 532
 612     532    SIGS=((X1/(1.+X1))*TSS(IP))-(((1.+X1)/X1)*TSS(I1))+((1.+(2.*X1)
               3(X1+(X1**2)))
 613     533    IF(IP.EQ.0)GO TO 89
 616            GO TO 300
 617      89    S2=BIGESS+(AM*P)*(((AM/X1)*(1.-TSS(1)))-(SIGPL*AJ))
 620            GO TO 90
 621     300    IF(IP.EQ.1)GO TO 301
 624            GO TO 302
 625     301    S2=BIGESS+(P*AH)*((AM*((1.0-TSS(1))/(1.+X1)))-(AJ*SIGPL))
 626            GO TO 90
 627     302    IF(IP.LE.N4)GO TO 303
 632            GO TO 304
 633     303    S2=BIGESS+(P*AH)*((AM*SIGS)-(AJ*SIGPL))
 634            GO TO 90
 635     304    IF(IP.EQ.N2)GO TO 305
 640            GO TO 306
 641     305    S2=BIGESS+(P*AH)*((AM*SIGS)-(AJ*(TLO(N1)-1.)/(2.-X1)))
 642            GO TO 90
 643     306    IF(IP.EQ.N3)GO TO 307
 646            GO TO 308
 647     307    S2=BIGESS+(P*AH)*((AM*SIGS)-((AJ*4.)*(TLO(N1)-1.)))
 650            GO TO 90
 651     308    IF(IP.EQ.N)GO TO 78
 654            AG=2.0
 655            PRINT 113,AG,X1
 656            GO TO 100
 657      90    D0=0.0004
 660            S4=S3
 661            ATDM=ABS(S3-S2)
 662            S3=0.5*(S3+S2)
 663     612    IF(ATDM-D0)91,91,610
 664     610    IF(G.LT.20)GO TO 95
 667            GO TO 91
 670      95    N=N+1
 671            GO TO 35
 672      91    PH=(47.0*2.54)/32.0
```

```
ISN        SOURCE STATEMENT

673            S2=S4
674            IF(S2.LE.BIGESS)GO TO 615
677            GO TO 616
700      615   S2=BIGESS
701            U=0.0
702            U1=0.0
703            MN=1
704            DSI=AH
705            GO TO 630
706      616   DSI=S2-BIGESS
707            U=(S2-BIGESS)/AK
710            U1=(U*BH)/15300.0
711      630   IF(S2.LE.0.10E-12)GO TO 400
714            GO TO 401
715      400   AWD=0.0
716            S2=0.0
717            IR=0
720            R=0.0
721            X1=0.0
722            GO TO 650
723      401   AWD=S2/AH
724      402   IR=AWD
725            R=IR
726            X1=AWD-R
727      650   IF(X1.LT.0.99)GO TO 634
732            MN=1
733            IR=IR+1
734            R=R+1.0
735            X1=0.01
736            S2=(R+X1)*AH
737            GO TO 616
740      634   AW=AWD
741            IF(MN.EQ.1)GO TO 237
744      631   BIGESS=S2
745            IF(BIGESS.EQ.0.0)GO TO 663
750            GO TO 664
751      663   Y1=0.0
752            AWD=0.0
753            BIGESS=0.0
754            GO TO 665
755      664   AWD=R+X1
756            BIGESS=AWD*AH
757            Y1=BIGESS*BH
760      665   IRD=IR
761            RD=R
762            XD=X1
763            TAU=TAUI
764            TAD=TAU*15300.0
765            DO 92 I=1,N1
766            TZD(I)=TLS(I)
767       92   TS(I)=TSS(I)
771            DO 97 I=1,I1
772            TD(I)=0.0
773       97   TETAS(I)=TS(I)*TE
775            DO 97 I=I2,N1
```

```
 ISN        SOURCE STATEMENT

  776            TETAES(I)=0.0
  777      98    TU(I)=TEMP(ZU(I)
 1001     481    TS=AK
 1002     482    AK=APK
 1003            P=PP
 1004            PSI=(DSI*AK)/AS
 1005     475    DRT=TAD-TADI
 1006            IF(ABS(DRT)-0.01)160,160,161
 1007     160    LK=1
 1010            GO TO 162
 1011     161    LK=3
 1012     162    IF(LK.EQ.1) GO TO 93
 1015            GO TO 64
 1016      93    PRINT 130,XJ,IPU,AWU
 1017            PRINT 9,TAU,TIME
 1020            PRINT 26
 1021            DO 32 I=1,N1
 1022      32    PRINT 16,Z(I),Y(I),TZU(I),TU(I),TS(I),TETAES(I)
 1024            PRINT 24,BIGESS,U
 1025            PRINT 25,Y1,U1
 1026            KN=5
 1027            LM=LK+1
 1030            IF(TIME-TTP)64,64,525
 1031     525    PRINT 526.
 1032     526    FORMAT(//16HTHE DEED IS DONE)
 1033     100    STOP
 1034            END
```